Waste and Biomass Valorization (2022) 13:1385–1429
https://doi.org/10.1007/s12649-021-01577-w

ORIGINAL PAPER

A Review of Graphene: Material Synthesis from Biomass Sources

Jhantu Kumar Saha[1] · **Animesh Dutta**[1]

Received: 6 December 2020 / Accepted: 8 September 2021 / Published online: 17 September 2021

Abstract

Single-atom-thick graphene is a particularly interesting material in basic research and applications owing to its remarkable electronic, mechanical, chemical, thermal, and optical properties. This leads to its potential use in a multitude of applications for improved energy storage (capacitors, batteries, and fuel cells), energy generation, biomedical, sensors or even as an advanced membrane material for separations. This paper provided an overview of research in graphene, in the area of synthesis from various sources specially from biomass, advanced characterization techniques, properties, and application. Finally, some challenges and future perspectives of graphene are also discussed.

Graphic Abstract

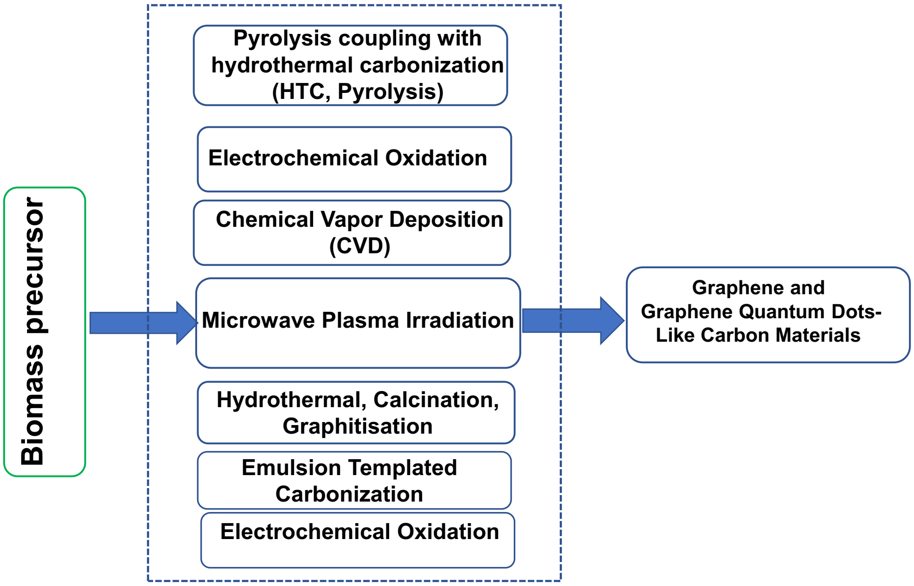

Keywords Graphene · Energy generation · Solar cells · Energy storage · Capacitors · Batteries · Fuel cells · Biomedical · Sensors · Membrane · COVID-19

Statement of Novelty

Reduction from graphene oxide is one of the most promising ways and is probably the most widely accepted method in graphene synthesis. Unfortunately, very few commercial technologies involving graphene-based materials have emerged, in large part due to the difficulty in processing these 2D sheets into useful, 3D materials with predicable

---

✉ Jhantu Kumar Saha
jsaha@uoguelph.ca

[1] School of Engineering, University of Guelph, Guelph, Canada

structure and thus function. Our proposed novel graphene synthesis from biomass sources will provide an alternative, inexpensive, and more versatile approach to make large area graphene. The application of our graphene from biomass sources and with many polymer composites will lead to the revolution in many sectors including biomedical, energy sectors. Continued development and successful implementation of graphene from biomass sources that could lead to new jobs and a potentially huge source of revenue to fuel the future economy.

Introduction

Single-atom-thick graphene is a particularly interesting material in basic research and applications owing to its remarkable electronic, mechanical, chemical, thermal, and optical properties [1]. For a given surface area, it is the lightest weight electronic conductor of any material and can be produced relatively inexpensively, and in large volume, from natural graphite resource. This leads to its potential use in a multitude of applications for improved energy storage (capacitors, batteries, and fuel cells), energy generation (solar cells), biomedical, sensors or even as an advanced membrane material for separations.

A lot of effort had been devoted for creating high-quality large-area graphene. The earliest method, mechanical exfoliation of graphene from highly oriented pyrolytic graphite using scotch tape, yields good quality but µm-sized graphene [2]. In addition, it is uncontrollable and not scalable. Other formation techniques, such as epitaxial graphene from a single crystalline SiC substrate [3–8] or transition metals [9–14], can yield larger graphene domains. However, they encounter difficulty for large-scale production due to the high cost of the substrates, the requirement of ultrahigh vacuum, and limited scalability. Recently, high-quality monolayer or bilayer graphene was obtained via the chemical vapor deposition (CVD) of CH_4 or C_2H_2 gases on copper or nickel substrates [15–20]. Commercial wafer-scale and 30-in. (76.2 cm) graphene films have been reported [20, 21]. Currently, CVD technique is widely employed and has great potential for the large-scale production of high quality films [22–29]. However, since the CVD growth of high quality graphene requires a nearly oxygen-free environment or high-vacuum (10^{-6} Torr) base pressure, a long pumping and/or purge time is needed to evacuate the air in the chamber [30–35]. In addition, some of the gaseous raw materials are hazardous. These disadvantages limit its use in some applications and are a concern for large-scale production. Recently, much simpler, less expensive, and less hazardous techniques for growing graphene have been demonstrated [36–42]. These techniques use solid carbon sources (e.g., polymers, SiC, and amorphous carbon). For a Ni catalyst, carbon atoms diffuse into the Ni film during a high-temperature annealing process. Some of the C atoms segregate from the bulk to the Ni surface due to lower solid solubility at lower temperature [43]. A graphene layer forms with a specific and well-controlled cooling rate in a high-vacuum environment [44, 45]. A nearly oxygen-free environment is required in the graphene growth process not only to prevent the precipitated carbon from reacting with oxygen but also to avoid catalyst surface oxidation at high temperature. If graphene can be grown in a non-vacuum environment could open new applications. Many recent works [29, 37, 46] have shown that graphene can be grown at the interface of silicon dioxide and metal catalysts and Pt-based catalyst approach is also useful and was discussed in reference [47]. Moreover, a very important catalyst-free approach was also presented in reference [48]. Presently, there are several synthesis routes of graphene such as mechanical, chemical exfoliation, chemical vapor deposition, pyrolysis, epitaxial methods for obtaining graphene films [49]. A scheme depicting various conventional synthesis methods of graphene along with their important features, and their current and prospective applications are discussed in reference [50].

Unfortunately, very few commercial technologies involving graphene-based materials have emerged, in large part due to the difficulty in processing these 2D sheets into useful, 3D materials with predicable structure and thus function. To address this challenge, this research aims to develop new sources, tools, and processes to create a platform of graphene-based materials whose structure can be manipulated and fine-tuned at the nanoscale. Among these methods, reduction from graphene oxide is one of the most promising ways and is probably the most widely accepted method in large scale preparation. Considering both the scalability of this method and the purity of the final product, reduction of graphene oxide is better than other techniques. Nevertheless, industrialization with low cost is one of the major challenges in graphene field. With such consideration, the mechanical exfoliation and reduction of graphene oxide are the two possible methods for bulk production of graphene. On the other hand, pyrolysis and other chemical etching and gasification have been common techniques to synthesize graphene on metal surfaces from different carbon sources or other activated carbons [36, 51–57]. These also can be achieved by developing processes capable of depositing large-area monolayer graphene films onto a variety of substrates from biomass sources. However, the preparation of graphene by surface growth is limited in yield.

To develop devices based on graphene based materials from various sources, several synthetic schemes for the preparation of graphene including 3D graphene-based materials, and their properties, advanced characterization techniques, properties and their application for energy generation and storage, sensing, biomedical areas. Finally, analysis and challenges along with their future perspectives have been reviewed in discussion section:

Materials and Methods

This section firstly presents an overview various synthesis technique that is used for the development of graphene from various sources including graphite, non-graphite sources followed by graphene synthesis from bio-mass sources.

Synthesis from Graphite Sources

Micromechanical Cleavage-the Scotch Tape Method

Graphene can be extracted from the high-quality of graphite using mechanical exfoliation, which is a simple peeling process. Mechanical exfoliation of graphite using scotch tape is obtained from a commercially available highly oriented pyrolytic graphite (HOPG) sheet by dry etching in oxygen plasma. These thin flakes are composed of monolayer or a few layers of graphene [58]. Optical microscope image of multilayer graphene using Micromechanical cleavage-the scotch tape method as shown in Fig. 1.

Chemical Cleavage and Exfoliation

The two-step process to obtain graphene from graphite oxide requires first exfoliating the bulk material and then reducing the individual sheets back to graphene as shown in Fig. 2. Exfoliation is usually achieved by sonicating graphite oxide in water, followed by centrifugation. The supernatant from this procedure is colloidal and contains few- and single-layer sheets of graphene oxide. This liquid can be left as is or drop-cast onto a substrate for further processing.

Synthesis from Non-graphitic Sources

Epitaxial Growth from Silicon Carbide

Among the many graphene synthesis methods, the epitaxial growth approach from silicon carbide could help large-size and single-domain graphene production in a controlled manner. Supporting substrate is very important to access the intrinsic electronic properties of graphene. This lack of suitable substrate has so far been a major hurdle for the epitaxial growth of graphene using PECVD [61].

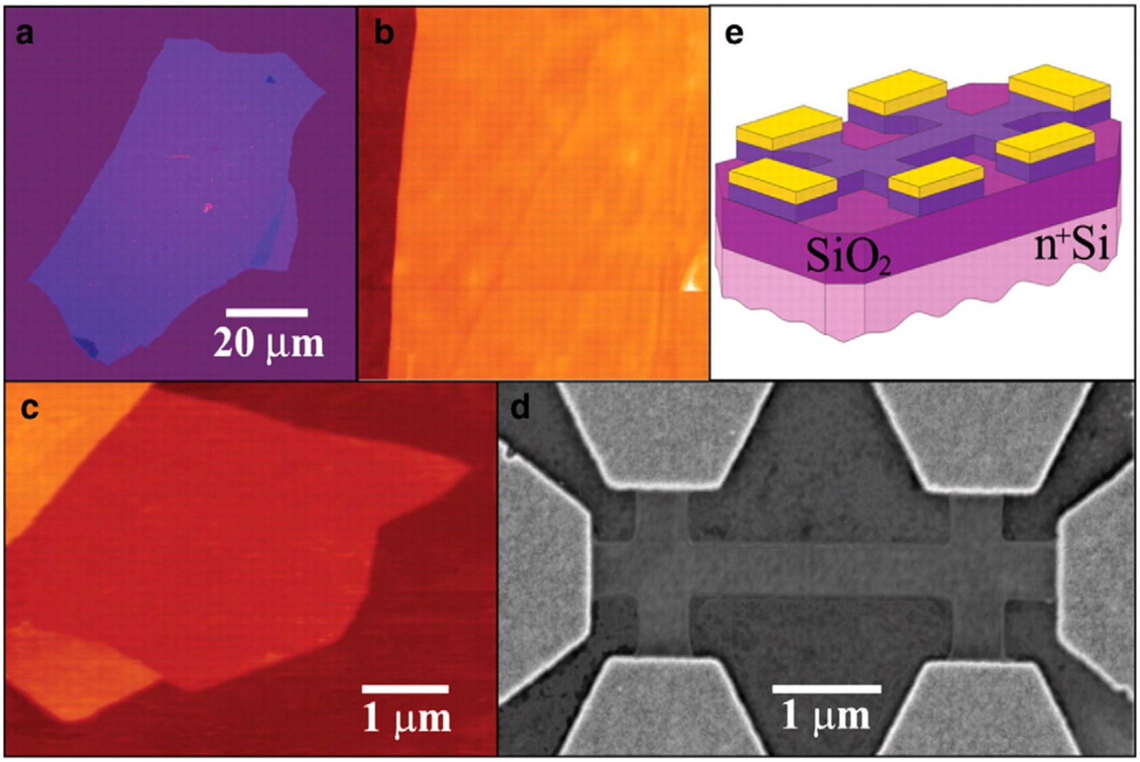

Fig. 1 **a** Optical microscope image of multilayer graphene cleaved from bulk graphite using the "scotch tape method". **b** AFM image of an edge of the flake. **c** AFM image of few-layer graphene. **d** SEM of a device used by Geim and Novoselov for their studies of the electric field effect in graphene. **e** Schematic of device in d. (Reprinted with permission from Ref. [1, 2])

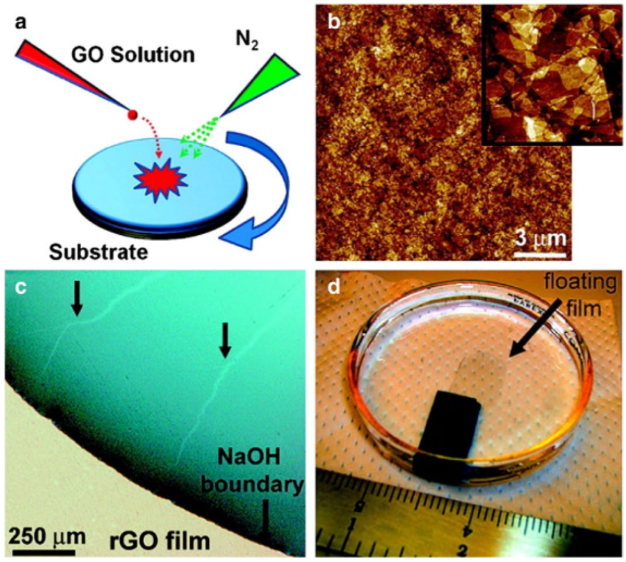

Fig. 2 Spin-coating technique employed in the deposition of graphene oxide on a surface. **b** AFM image of thin film spin-coated graphene oxide. **c** Optical microscope image of the delamination of rGO film from its substrate. **d** Floating rGO film ready for transfer onto an arbitrary substrate. (Reprinted with permission from Refs. [59, 60])

Physical Vapor Deposition

Multiplayer graphene carbon films can be produced using simplified filtered cathodic vacuum arc (FCVA) deposition system. Carbon films were deposited using a FCVA system equipped with a double bend magnetic filter to minimize the deposition of macroparticles [61]. These macroparticle can be ejected from the carbon cathode as shown in Fig. 3.

The schematic in Fig. 4 shows the steps involved in synthesis of the carbon films.

Chemical Vapor Deposition from CH_4

Graphene single crystals can be grown using low-pressure chemical vapor deposition in copper-foil enclosures using methane as a precursor. The dimensions of graphene crystal could be up to 0.5 mm on a side (Fig. 5).

The CVD growth of graphene occurs on Cu grows by a surface adsorption process whereas the CVD growth of graphene on Ni occurs by a C segregation or precipitation process [64].

Conversion of Carbon Dioxide to Graphene

The methodology produces few-layer graphene captured directly from CO_2 by burning Mg in it. The combustion of magnesium metal in carbon dioxide to form few-layer graphene is unprecedented and provides further incentives for exploration of several environmentally friendly ways for capturing carbon dioxide [36, 65]. The burning magnesium metal in a CO_2 environment produces carbon materials as shown in Eq. (1).

$$Mg(S) + 2CO_2 \rightarrow MgO(S) + C(S) \tag{1}$$

Growth of Graphene from Solid Carbon Sources

Chemical Vapor Deposition (CVD) technique is limited to the use of gaseous raw materials, making it difficult to apply the technology to a wider variety of potential

Fig. 3 Schematic diagram (not to scale) of the Filtered Cathode Vacuum Arc (FCVA) coating technology system. (Reprinted with permission from Ref. [62])

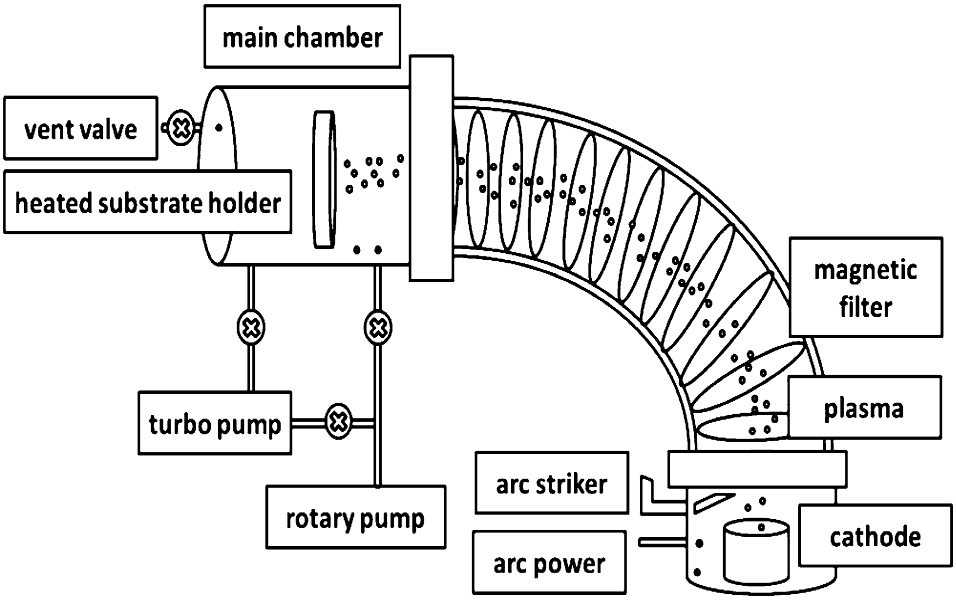

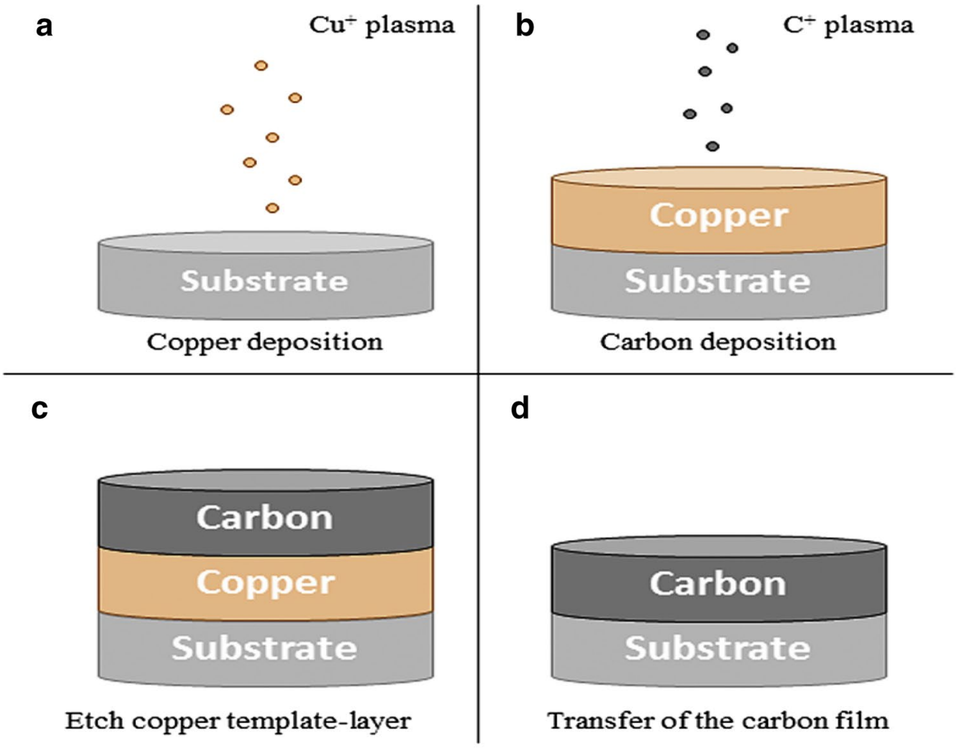

Fig. 4 Schematic showing the growth sequence and transfer process employed to fabricate carbon films on silicon/silica substrates (Reprinted with permission from Ref. [63])

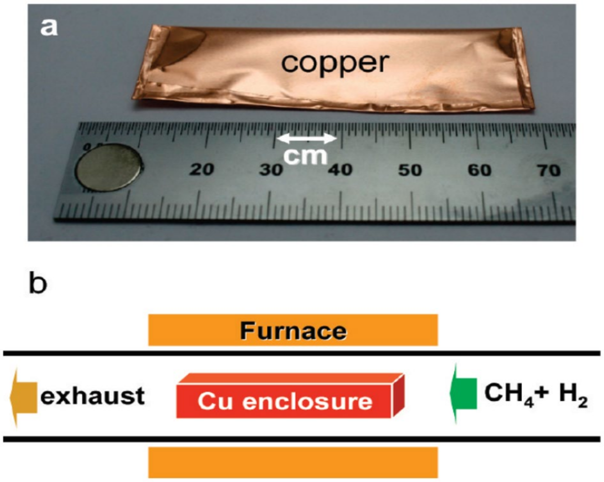

Fig. 5 **a** Copper foil enclosure prior to insertion in the furnace. **b** Schematic of the CVD system for graphene on copper (Reprinted with permission from Ref. [19])

feedstocks. The large area, high quality graphene with controllable thickness can be grown from different solid carbon sources[poly(methyl methacrylate) (PMMA), high impact polystyrene (HIPS), or acrylonitrile butadiene-styrene (ABS)] —such as polymer films or small molecules—deposited on a metal catalyst substrate at temperatures as low as 800 °C. Both pristine graphene and doped graphene were grown with this one-step process using the same experimental set-up [36].

Figure 6 illustrates the procedure for the growth of bilayer graphene directly on the SiO_2 substrate. The SiO_2 substrate was cleaned with oxygen-plasma and Piranha solution (4:1 sulfuric acid/hydrogen peroxide), and then a 400 nm thick nickel film was thermally evaporated onto the top of the SiO_2 substrate used as the metal catalyst. Either solid polymers (PMMA, HIPS, or ABS) or gas-phase methane was used as a carbon source for the transfer-free growth of bilayer graphene.

The two mechanisms of graphene growth on Ni and Cu can be understood from the C-metal binary phase diagram. The binary phase diagrams of C-Ni and C-Cu are similar in that C has a limited solubility in the metal without the presence of a metal-carbide line compound. The only significant difference is that the solubility of C in Cu is much lower than that in Ni. Since only a small amount of carbon can be dissolved in Cu, the source for graphene formation is mainly from the CH_4 that is catalytically decomposed on the Cu surface with minimal carbon diffusion into the Cu. Once the surface is fully covered with graphene growth terminates because of the absence of a catalyst to decompose CH_4 [19, 36, 63–66]

In contrast, Ni can dissolve more carbon atoms and hence it is difficult to get uniform graphene films due to precipitation of extra C during the cool-down. The C precipitation process is a nonequilibrium process, which should

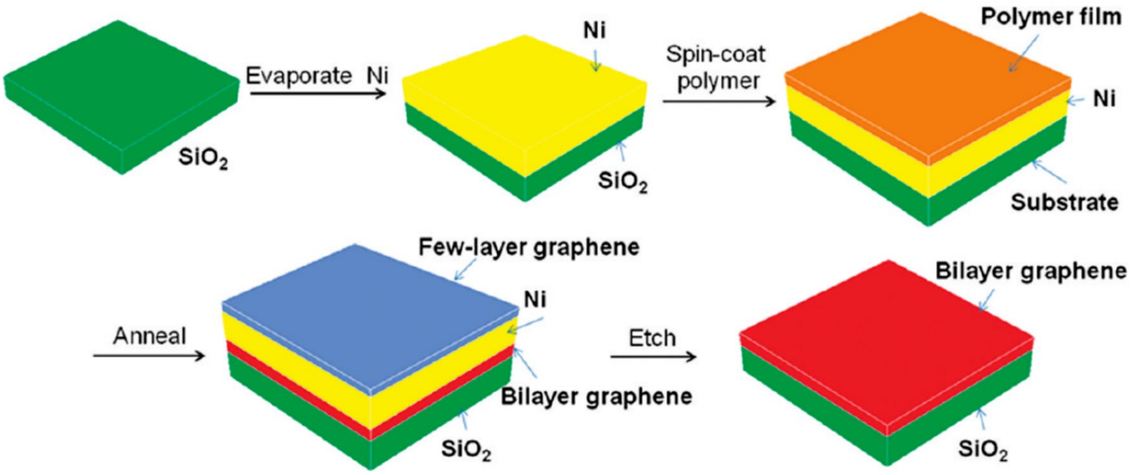

Fig. 6 Schematics of the growth of bilayer graphene from a solid carbon source. A 400 nm nickel film was thermally evaporated onto SiO_2 substrate, followed by the spin-coating of polymers on the nickel. After annealing samples at 100 °C under a reductive Ar/H_2 pressure for ~ 10 min and then etching away the nickel, bilayer graphene is obtained directly on SiO_2. The polymer film formation can be replaced by exposure to methane during the annealing step (Reprinted with permission from Ref. [66])

be suppressed if one aims to achieve monolayer graphene growth, for example, by using a controlled thin Ni film and/or high cooling rate. However, because of microstructural defects, predominantly grain boundaries, it is very difficult to fully eliminate the effect of precipitation for metals with high carbon solubility. Hence, metals with low C solubility such as Cu offer a possible path to large-area growth of graphene. Discrete regions of isotopically labelled graphene for growth on Cu may also yield novel devices and transport physics in future studies [19, 36, 63–66, 77–80]).

Moreover, a carbon diffusion mechanism through Ni layer is proposed for the growth mechanism of bilayer graphene on SiO_2 substrates [66].

Graphene Ssynthesis from Polymers

Graphene films can be formed directly on a SiO_2/Si substrate from solution-processed common polymers. Patterned graphene layers can also be directly formed on active electronic devices without any physical transfer process as shown Fig. 7. The metal capping layer is used to prevent of vaporization of dissociated molecules and catalysis of graphene formation.

Facile Synthesis of Graphene from Plastic by Pyrolysis of Poly(methyl ethacrylate), PMMA

Figure 8 illustrates the preparation procedures of graphene by pyrolyzing PMMA composite. When the composite is heated at1000°C, PMMA is immediately decomposed into various carbon derivatives (Cn).

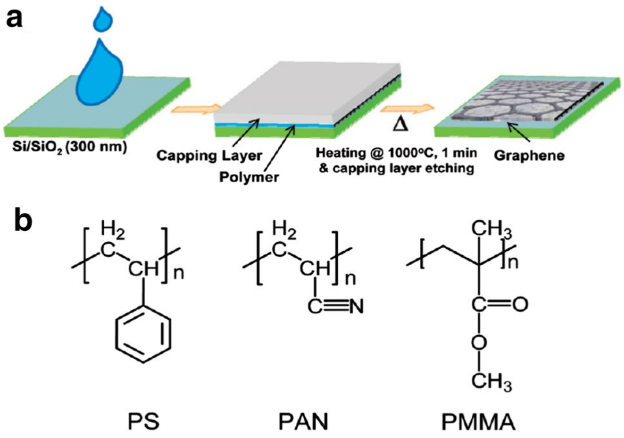

Fig. 7 **a** Graphene growth process and **b** chemical structure of polymers used as graphene precursors (reproduced with permission from Ref [67].)

Based on the reported works, a summary and comparison of these preparation methods were listed in Table 1. Some of the groundbreaking efforts in synthesizing graphene are summarized for graphene production in Ref. [69]. Among these methods, mechanical exfoliation and CVD can produce good-quality graphene. However, the practical application of graphene is blocked by the high price and insufficient supply.

Synthesis of graphene refers to any method for fabricating or isolating graphene from carbonaceous precursor. Numerous methods have been established to synthesis graphene with their merits and challenges of the specific product as listed in Table 1.

Recently, many researchers have suggested to develop green production methods for synthesizing graphene using

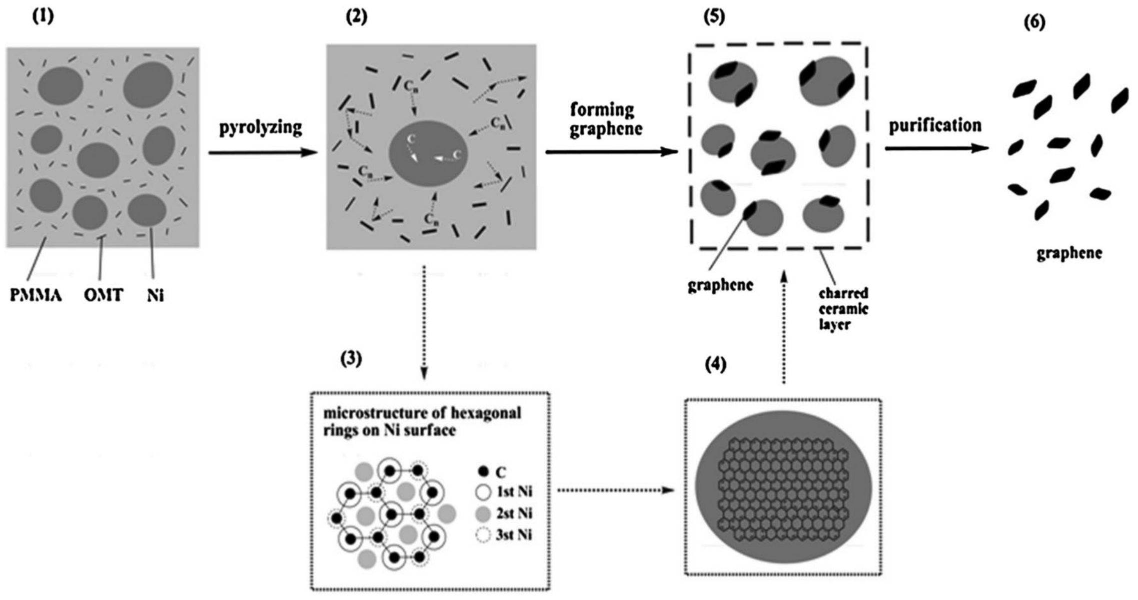

Fig. 8 Illustration of the procedure for growth of the graphene on nickel particles by pyrolysis of PMMA composite: PMMA/OMT/Ni composite; (2) pyrolytic state in a specific microzone; (3) microstructure of hexagonal rings on Ni surface (4) continuous growth of graphene on Ni surface; (5) the graphene hybrid containing clay and catalyst; and (6) final purified graphene (Reprinted with permission from Ref. [68])

Table 1 Summary of current approaches to produce graphene using various synthesis techniques

Method	Source materials	Merits	Challenges	References
Mechanical cleave	Graphite	Pristine graphene	Low production	[2, 58]
Direct sanitation	Graphite	Pristine graphene	Low production	[59, 60]
Thermal treatment	Graphite oxide	High production	Slow process Low bulk density Hard to transport Safety issue	[43, 59, 60]
Colloidal dispersion & chemical treatment	Graphite oxide	High production Bulk density	Hazard chemicals Slow process Uncontrollable & Not scalable	[59, 60]
Physical vapor deposition/sputtering (PVD)	Single crystalline SiC substrate Transition metals	Epitaxial graphene can yield larger graphene domains	Encounter difficulty for large-scale production due to the high cost of the substrates, the requirement of ultrahigh vacuum, and limited scalability	[62]
Chemical vapor deposition (CVD)	CH_4 and C_2H_2 Gases	High-quality monolayer or bilayer graphene	Requires a nearly oxygen-free environment or high-vacuum (10^{-6} Torr) base pressure, a long pumping and/or purge time is needed to evacuate the air in the chamber Some of the gaseous raw materials are hazardous. These disadvantages limit its use in some applications and are a concern for large-scale production	[15–20, 64]
Pyrolysis	Different carbon sources Other activated carbons	Large-area monolayer graphene films onto a variety of substrates	The preparation of graphene by surface growth is limited in yield	[36, 51–57]

environmentally friendly biomass resources such as sugar, chitosan, and alfalfa plants as discussed below.

Synthesis of Graphene from Biomass Sources

High-quality graphene can be formed using catalyst metal foil. The cost-effective, mass production of graphene can be formed using the biomass resource and waster materials.

The usage of biomass resource and waste materials as carbon sources is a promising method that results in a cost-effective, mass production of graphene. However, it is difficult to synthesize large amounts of graphene using a catalyst. Additionally, when plants and waste materials are used as a carbon source without using a catalyst, problems such as low quality and high defects might exist.

Thermochemical conversion of biomass has been a topic of intensive research and several techniques, such as pyrolysis, gasification, liquefaction, and hydrothermal carbonization (HTC). These techniques have been implemented to convert biomass into different products. Figure 9 shows the schematic representation of pyrolysis process and its product (biochar) applications from biomass sources.

The HTC method leaves the biomass precursor "partially" carbonized, which can be upgraded into desired graphene-like carbon materials by subsequent activation/carbonization process (Fig. 10). Various chemicals can be added in the HTC or the pyrolysis step to realize graphene-like carbon formation. The fundamental investigation of the effects of different chemicals on the hydrothermal treatment and carbonization have been highlighted below [72].

Synthesis of Monolayer-Patched Graphene from Glucose via Pyrolysis

The synthesis process of Monolayer-Patched Graphene from Glucose and dicyandiamide (DCDA) via pyrolysis is discussed in Ref. [72]. A typical layered graphic carbon nitride, g-C_3N_4 can be formed by calcination of dicyandiamide (DCDA), urea, and melamine in the temperature range of 500–600 °C. Then it undergoes decomposition at above 750 °C by forming NH_3, C_2N_2+, C_3N_2+, and C_3N_3+ species. Thus, g-C_3N_4 can be served as a sacrificial template for layered graphene-like carbon material synthesis. This method allows the nitrogen doping in the resultant carbon nanosheet with content about 3–5 at.% even at a high temperature pyrolysis of 1000 °C. By using this method, monolayer and two-layer graphene can be formed when using glucose or HMF (Hydroxymethylfurfural) as precursors.

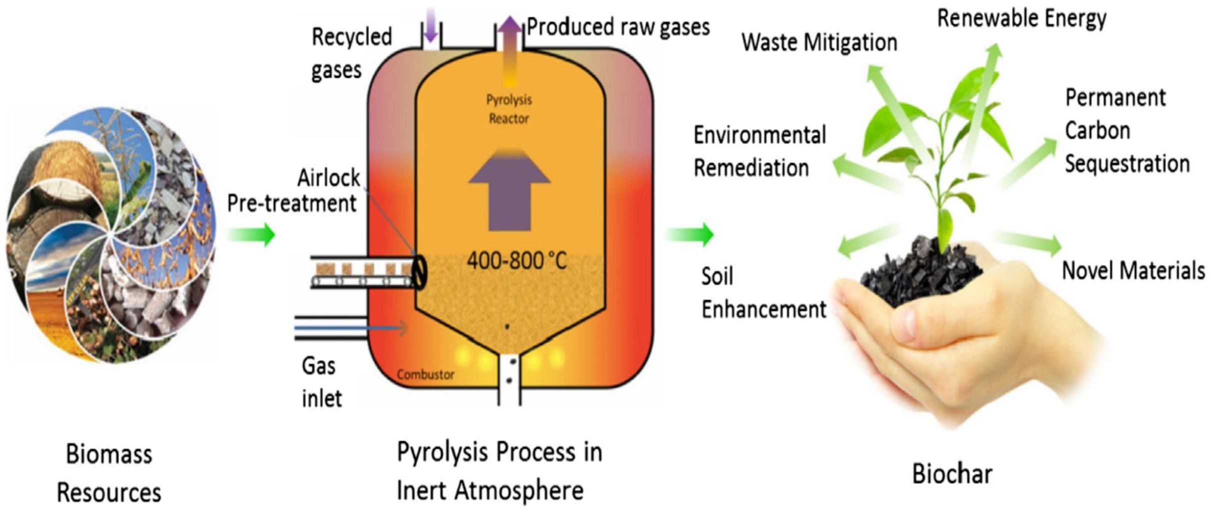

Fig. 9 The pyrolysis process of the biochar obtained (Reprinted with the permission from Ref. [70])

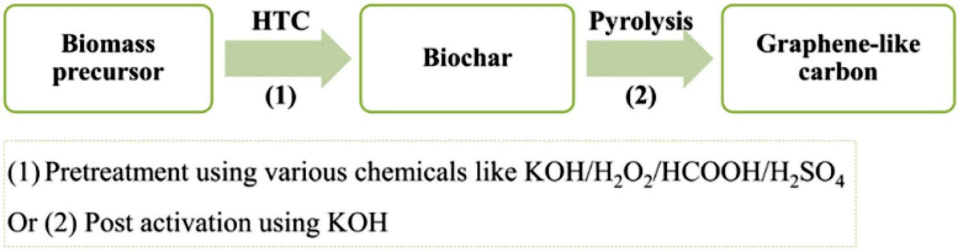

Fig. 10 Graphene-like carbon synthesis by coupling HTC with pyrolysis (Reprinted with the permission from Ref. [71])

Synthesis of Graphene from Fungus via Pyrolysis Coupling with Hydrothermal Carbonization Pretreatment

The hydrothermal pretreatment from fungus with the addition of KOH can yield graphene-like materials with subsequent carbonization [73]. A hydrothermal reaction of fungus (Auricularia) was conducted at temperature of 120 °C as shown in Fig. 11. The obtained samples were freeze-dried and activated using KOH under N_2 at 800 °C. Finally, graphene-like carbon materials with the densely porous structure were synthesized, with 10 nm in thickness. Ban et al. [74] also found that the hydrothermal pretreatment of reed membranes using KOH before pyrolysis generates carbon materials with higher surface area, compared with traditional post-KOH activation method.

Synthesis of Graphene via Green Chemistry Approach

A simple, eco-friendly, and scalable method using one-step pyrolysis from dead camphor leaves (Cinnamomum Camphora) graphene can be produced as shown in Fig. 12.

In this pyrolysis process, dead camphor leaves were heated to 1200 °C at 10 °C/min in nitrogen atmosphere. After heating in nitrogen atmosphere, leaves were cooled down to room temperature without any external disturbances. Few layers graphene (FLG) can be separated from the final pyrolytic components, with the help of π–π interaction with D-Tyrosine and centrifugation [75].

Porous 3D Graphene-Based Bulk Materials

The desired property including specific surface area (SSA) and conductivity of graphene can be achieved using a simple and green but very efficient and industrially scalable approach as shown in Fig. 13. Two standard industrial steps are used. Those steps are: (1) in-situ hydrothermal polymerization/carbonization of the mixture of cheap biomass or industry carbon sources with graphene oxide (GO) to firstly get the 3D hybrid precursor materials and then (2) a chemical activation is a step to achieve the desired SSA and conductivity. Both steps are very industrially scalable and efficient to make truly large quantity of products. Various structural and morphology analysis demonstrate that these materials consist of almost entirely defected/wrinkled single layer graphene sheets in the dimensional size of a few nanometers, with ultrahigh SSA (up to 3523 m^2/g) and excellent bulk conductivity (up to 303 S/m). The pore size of these materials mainly distributes in the mesopore size range, significantly different from the conventional materials. These combined outstanding properties make them superior candidate materials for various applications, the best supercapacitor performance as demonstrated.

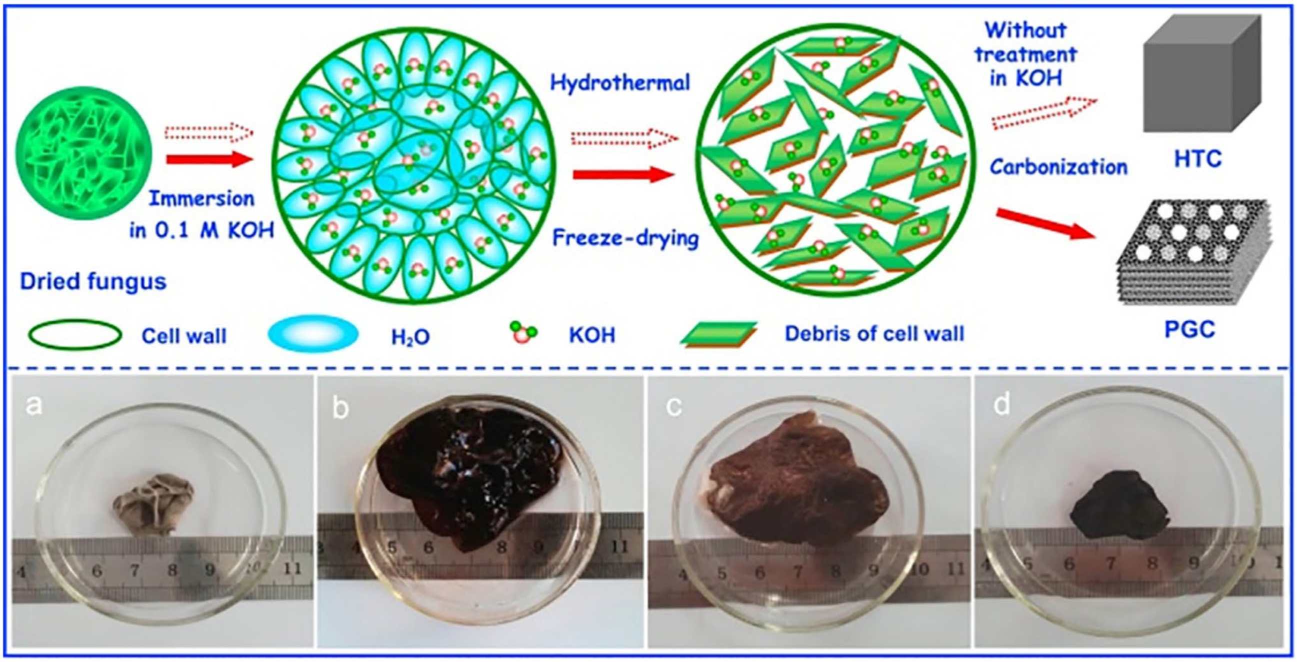

Fig. 11 Schematic illustration of the formation of carbon with (porous graphene-like carbon, PGC) and without (HTC) treatment of KOH. **a** The optical figure of the originally dried fungus; **b** Swelled fungus after hydrothermal treatment in 0.1 M KOH solution; **c** Freeze-dried fungus; **d** The as-prepared carbon materials by pyrolysis of freeze-dried fungus (Reprinted with the permission from Ref. [73])

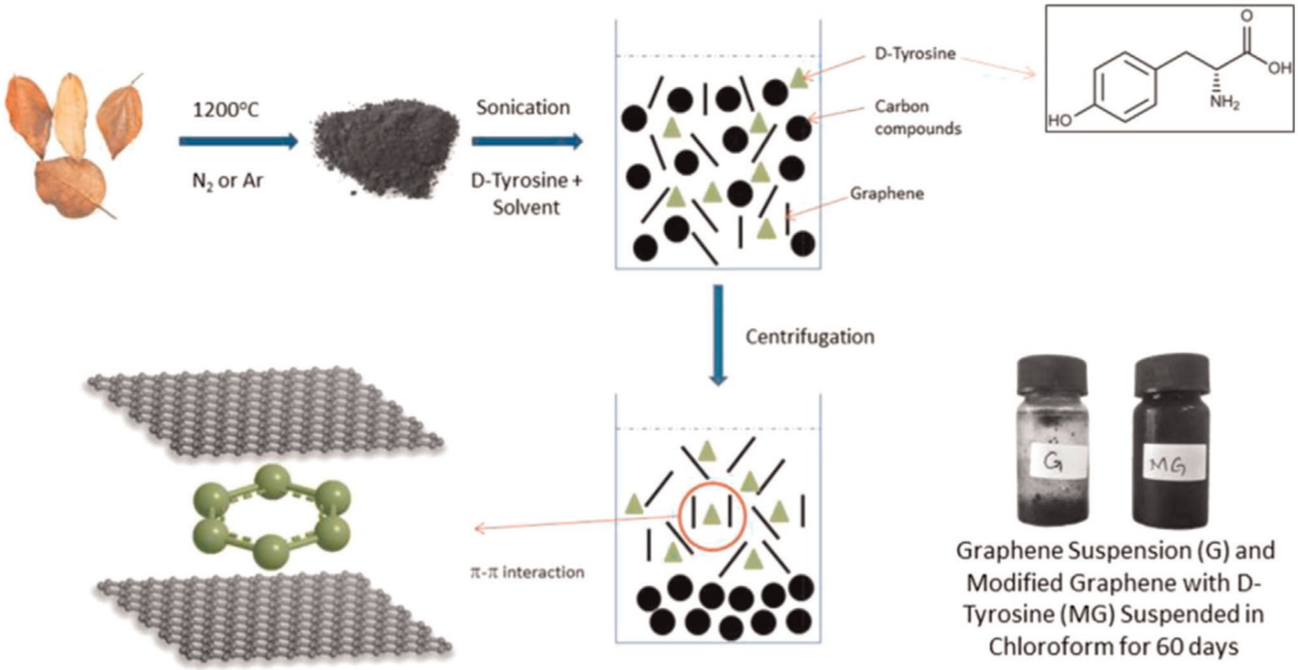

Fig. 12 Synthetic scheme for the preparation of graphene (Reprinted with the permission from Ref. [75])

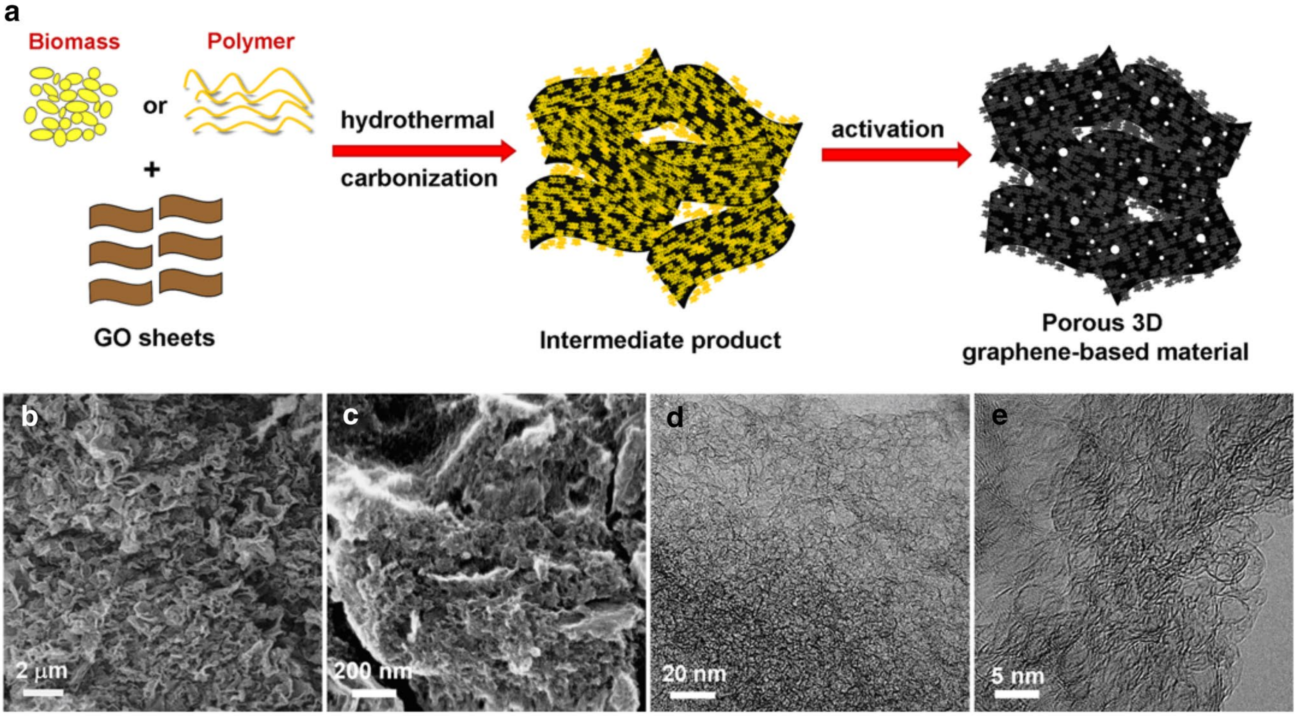

Fig. 13 **a** A schematic show of the simple and green process of synthesizing porous 3D graphene-based materials. **b** Low magnification and **c** high-resolution scanning electron microscopy (SEM) images of products from the mixtures of PF [the simple mixture of phenol (P) and formaldehyde (F) as the carbon source (denoted as ''PF'')] and GO with optimized ratios, which exhibited sponge-like morphology and porous structure. **d** Low magnification and **e** high-resolution transmission electron microscopy (TEM) images of products from the mixtures of PF and GO with optimized ratios, which also showed a dense 3D pore structure with highly curved or wrinkled surface (Reprinted with the permission from Ref. [76])

Growth of Graphene from Food, Insects, and Waste

High-quality monolayer graphene can be produced directly on the surface of Cu foils under a H_2/Ar flowing atmosphere from inexpensive carbon sources including food, insects, and waste (cookies, chocolate, grass, plastics, roaches, and dog feces) without purification as shown in Fig. 14 [77].

On the left, the Cu foil with the carbon source contained in a quartz boat is placed at the hot zone of a tube furnace. The growth is performed at 1050˚C under low pressure with a H_2/Ar gas flow. On the right is a cross view that represents the formation of pristine graphene on the backside of the Cu substrate. (B) Growth of graphene from a cockroach leg. (a) One roach leg on top of the Cu foil. (b) Roach leg under vacuum. (c) Residue from the roach leg after annealing at 1050 °C for 15 min. The pristine graphene grew on the bottom side of the Cu film (not shown) (Reprinted with the permission from Ref. [77]).

Graphene from Rice Husk (RH) by Microwave Plasma Irradiation (MPI)

Figure 15a shows a schematic diagram of microwave plasma irradiation (MPI) technique for the RH-derived nanocarbons [78–80]. Firstly, 1 g rich husk (RH) powders, located in a home-made nickel case, were placed on the stage. The experimental setup and procedure are like the methods employed to fabricate graphene nanosheets from solid carbon [78] and Kapton polyimide [79] except for the pressure. Using this method, not only graphene but also CNTs and g-CNTs can produce. The pressure plays a critical role to synthesize diverse nanocarbons from RHS. After the plasma processing, the nickel cases were covered by soot-like appearance as shown in Fig. 15b.

A possible growth model has been proposed for converting the rice husks into nanocarbons including graphene, CNTs, and g-CNTS as shown in Fig. 16.

As shown in Fig. 16, the nickel foil was irradiated to produce the nickel atoms, which tend to aggregate with each other by reducing surface energy, resulting in formation of nickel clusters. The resulting nickel clusters with irregular shapes in usual 30–150 nm size can initiate and accelerate the graphitization process by assembling carbon radicals into graphene surrounding the nickel clusters. At high pressure conditions, the graphene structures can wrap into tube-like structures to further reduce the surface energy. In this stage, the herringbone CNTs were formed at relatively lower growth temperatures, the bamboo-like CNTs at higher growth temperatures due to the different surface diffusion rates of carbon radicals on the surface of nickel particles [80].

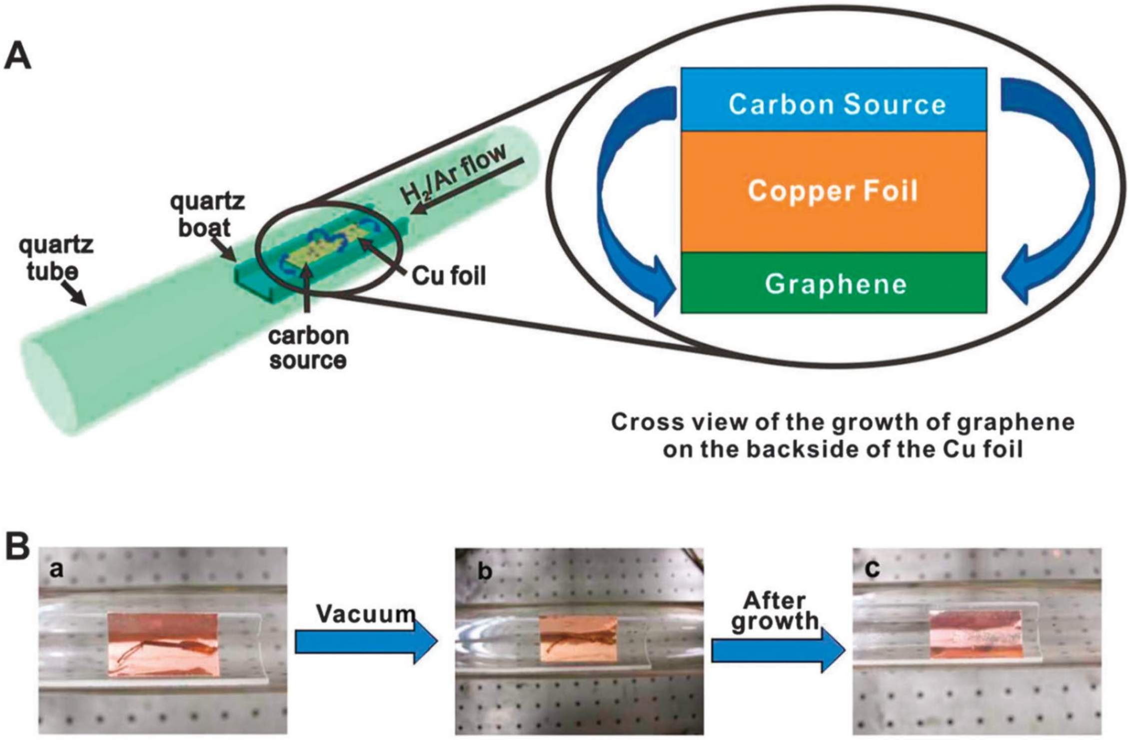

Fig. 14 Diagram of the experimental apparatus for the growth of graphene from food, insects, or waste in a tube furnace (Reproduced with permission from Ref. [77])

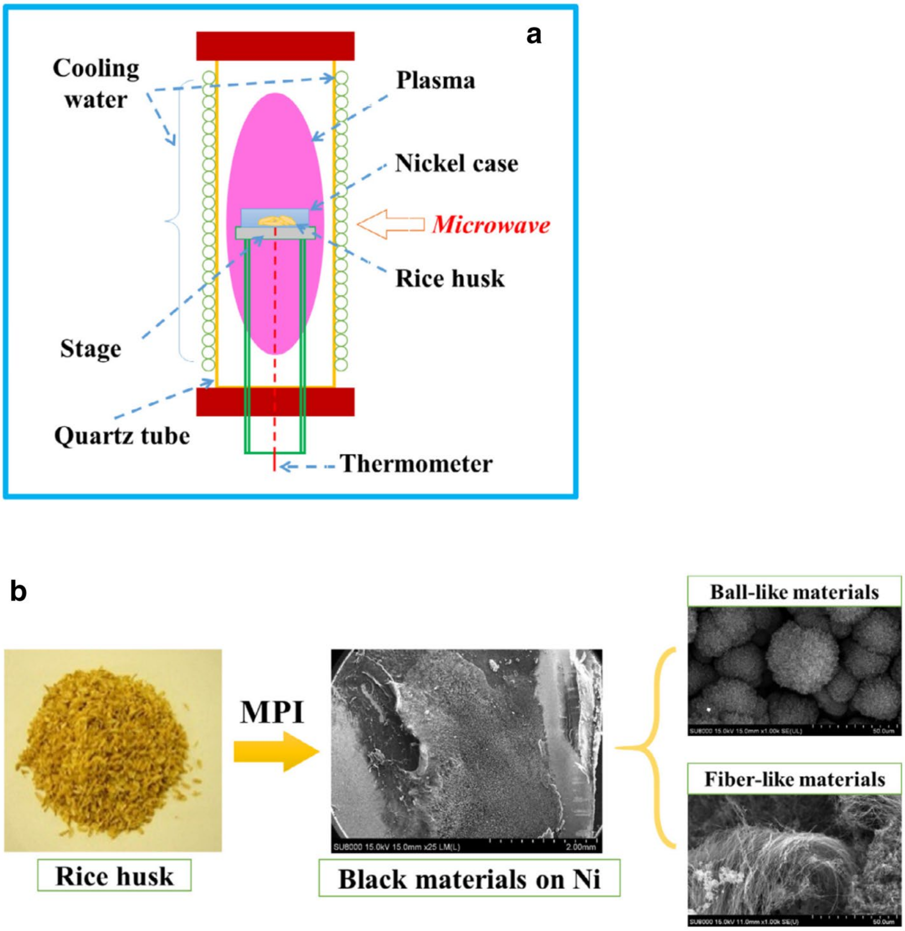

Fig. 15 **a** A schematic diagram of MPI technique for nanocarbon growth from RHs. **b** The conversion process of RHs into soot-like materials on the nickel surface, which include ball- and fiber-like structures (Reprinted with the permission from Ref. [79])

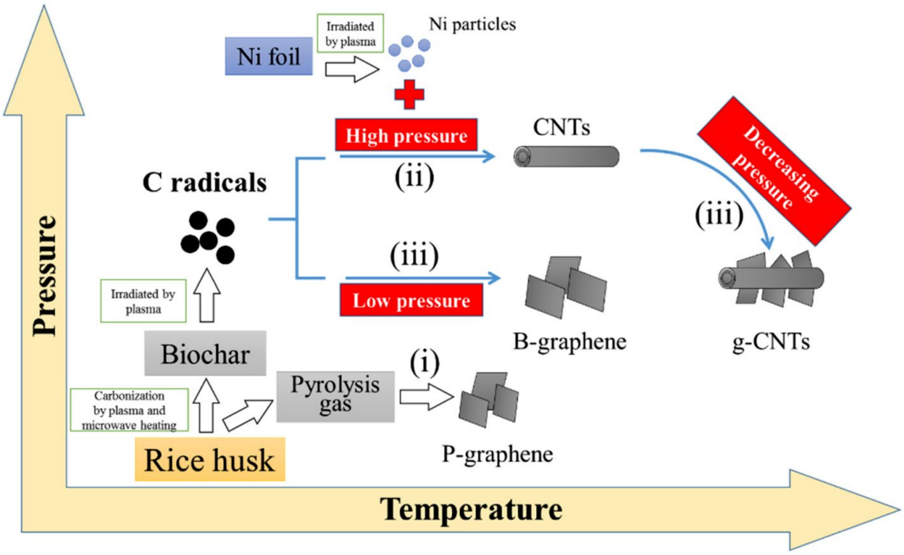

Fig. 16 A possible growth model for graphene, CNTs, and g-CNTs from RHs by MPI technique (Reprinted with the permission from Ref. [79])

Facile Synthesis of Few-Layer Graphene from Bbiomass Waste

A less expensive method has been developed to synthesize high-quality graphene sheets from wheat straw via a combined hydrothermal and graphitization approach for the first time [81]. The resulting graphene sheets show favorable features such as ultrathin nanosheet frameworks (2–10 atomic layers), high graphitization (up to 90.7%), graphite-like interlayer spacing (0.3362 nm), and the mesoporous structure. Figure 17 illustrates the overall evolution of synthetic processes.

Catalyst-Free Plasma Enhanced Growth of Graphene from Sustainable Sources

High quality graphene films were grown using *Melaleuca alternifolia*, a volatile natural extract from tea tree plant as the precursor without aid of catalyst as shown in Fig. 18.

Green Synthesis of Chemical Converted Graphene Sheets Derived from Pulping Black Liquor

Graphene sheets can be derived from black liquor and it is abbreviated as BL-G. These graphene sheets can be manufactured into flexible transparent conductive films (TCFs) through spin coating method on flexible PET substrate which exhibit good conductivity, high transparency and low sheet resistance as shown in Fig. 19.

Large Area Few-Layer Graphene with Scalable Preparation from Waste Biomass

Peanut shell-derived few layer graphene (PS-FLG) was prepared by a simple activation (by KOH) followed by mechanical exfoliation method (Fig. 20). Figure 18 shows the schematic pathway used for the synthesis of PS-FLG from precursor PS-P and its subsequent integration into a solid-state device [84].

The methods used to produce few layers graphene material compared to other methods for producing graphene-like carbon from biomass is shown in Table 2.

The summary of various synthesis techniques which can be used to develop graphene quantum dots from many biomass sources are shown in Fig. 21.

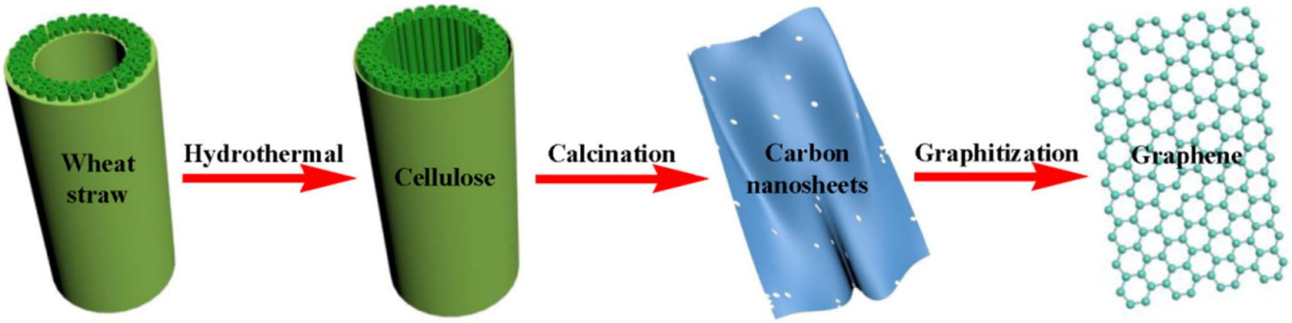

Fig. 17 Schematic diagram displaying the overall evolution of wheat straw into few-layer graphene (Reprinted with the permission from Ref. [81])

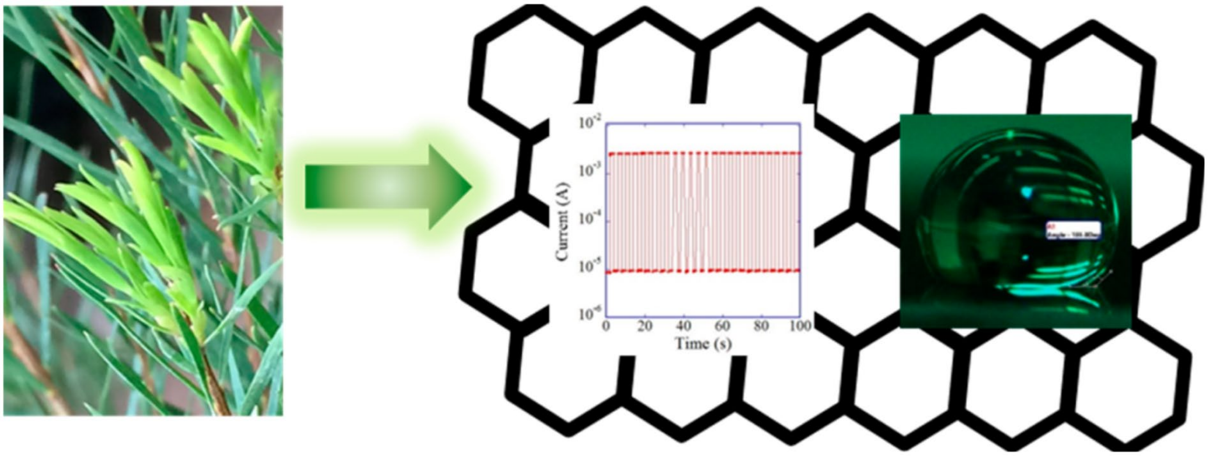

Fig. 18 As-fabricated graphene films yielded a stable contact angle of 135°, indicating their potential application in very high hydrophobic coatings (Reprinted with the permission from Ref. [82])

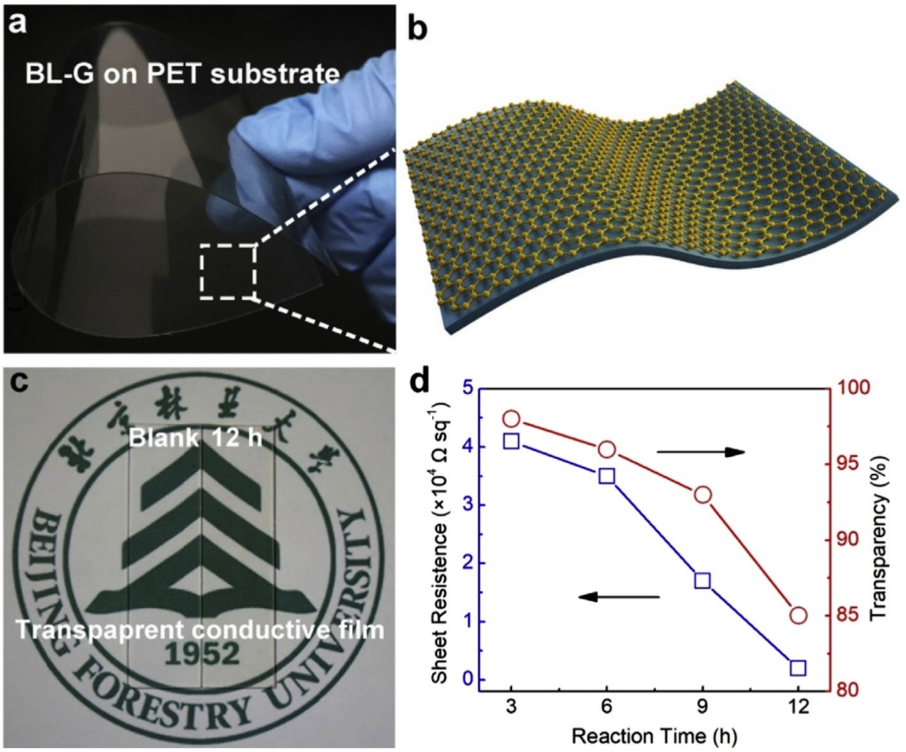

Fig. 19 **a** Digital photography and **b** scheme of BL-G after spin-coating on transparent and flexible PET substrate. **c** Left: blank PET, right: TCF fabricated with BL-G sheets in reaction time of 12 h. **d** Sheet resistance (left vertical axis in blue color) and transparency for 550 nm light (right vertical axis in red color) of BL-G-based TCFs changing with reaction time of 3 h, 6 h, 9 h and 12 h. (Reprinted with the permission from Ref. [83])

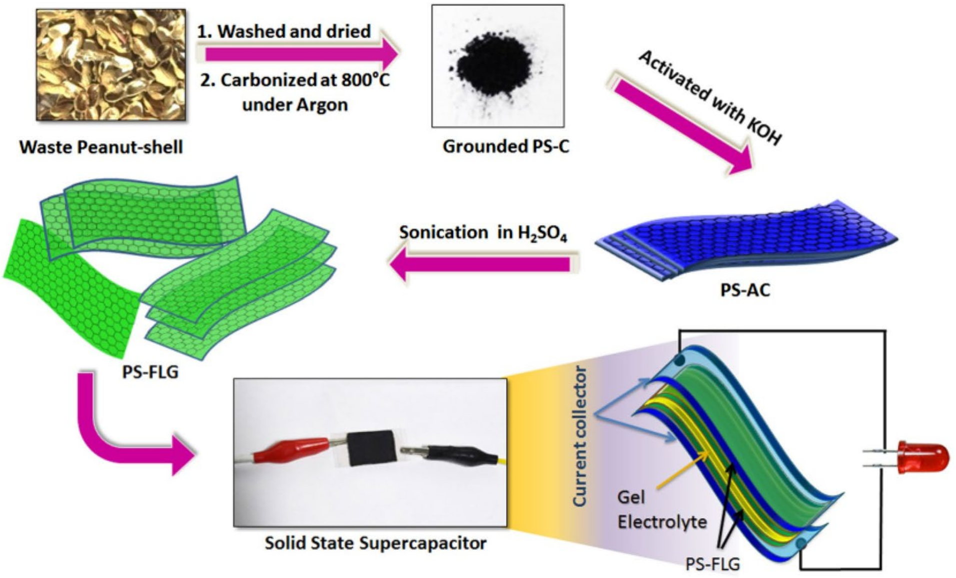

Fig. 20 Schematic representation for the synthesis of PS-FLG active material and its subsequent integration into a solid-state device (Reprinted with the permission from Ref. [84])

Biomass-Waste Derived Graphene Quantum Dots

Quantum dots (QDs) are man-made nanoscale crystals that that can transport electrons. When UV light hits these semiconducting nanoparticles, they can emit light of various colours. These artificial semiconductor nanoparticles that have found applications including composites, solar cells, and fluorescent biological label.

Graphene, which basically is an unrolled, planar form of a carbon nanotube therefore has become an extremely interesting candidate material for nanoscale electronics. Researchers have shown that it is possible to carve out nanoscale transistors from a single graphene crystal (i.e., graphene quantum dots). Unlike all other known materials, graphene remains highly stable and conductive even when it is cut into devices one nanometer wide.

Table 2 Comparison of different graphene-based materials synthesized from waste biomass as a carbon source and their applications (Reprinted with the permission from Ref. [85])

Waste source	Synthetic name		BET surface area (m^2 g^{-1})	Application	References
	Activating agent	Graphitization process (graphitic catalyst precursor)			
Peanut shell	KOH	-	2070	Supercapacitor	[85]
Coconut shell	$ZnCl_2$	$FeCl_3$	1874	Supercapacitor	[86]
Soybean shell	KOH	Thermal treatment with NH_3 injection for N-doped graphene	1152	Oxygen reduction reaction	[87]
Wheat Straw	KOH	Thermal treatment in graphite furnace	35.5	Li-ion battery	[88]
Tea tree plant	Plasma enhanced chemical vapor deposition			Hydrophobic coating	[82]
Auricularia + GO	KOH	Hydrothermal carbonization with GO	1723	Supercapacitor	[89]
Waster paper (Co decorated porous graphene)	-	Graphitization & $Co(acac)_2$ + 1,10 phenanthroline	542	Oxygen reduction reaction	[90]

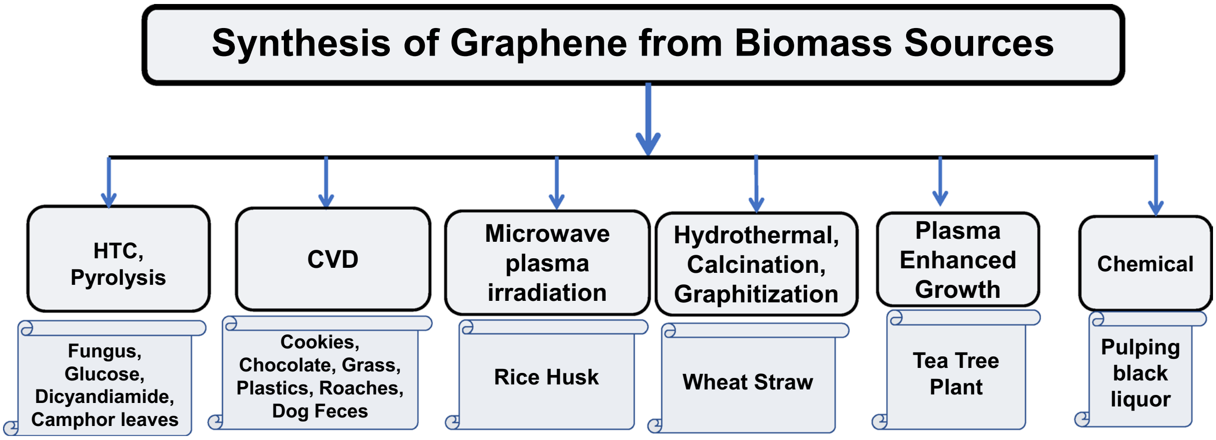

Fig. 21 Synthesis techniques of graphene from biomass sources

Vertically Aligned Graphene Nanosheet Arrays (VAGNA) from Biomass Wastes

Vertically aligned graphene nanosheet arrays (VAGNA) can be synthesized from biomass wastes. Figure 22 illustrates the overall synthesis process and mechanism of 3D VAGNAs derived from spruce bark [91, 92]. This process is a catalyst-free synthetic strategy towards high-quality graphene for electrochemical energy storage.

Figure 23f gives the FESEM image of the as prepared VAGNA-900, revealing that the KOH activation resulted in curved nanosheets growing vertically on the surface of bulk carbon particles, and connected to each other to form the 3D interconnect framework. Obviously, in this case, the formation of 3D VAGNAs is due to the dual function of KOH: the penetrating behavior of molten KOH into layers of the as-obtained carbonized precursor and activation agent to induce porosity in carbon materials [91].

Table 3 shows the lists of biomass resources for Graphene Quantum Dots, GQDs synthesis via different techniques.

Graphene quantum dots can be developed from wide range of synthesis techniques using various biomass sources is shown in Fig. 24. Each synthesis process has its own distinctive attributes that can be used for different types biomass sources to graphene development. In the next section, different advanced characterization techniques used to find out the properties for the specific purposes/application as discussed.

Results

In previous section II, the wide range of synthesis techniques of Graphene from various sources including biomass sources have been explored. The higher speed, larger capacity, and smaller size are required for advanced electronic devices

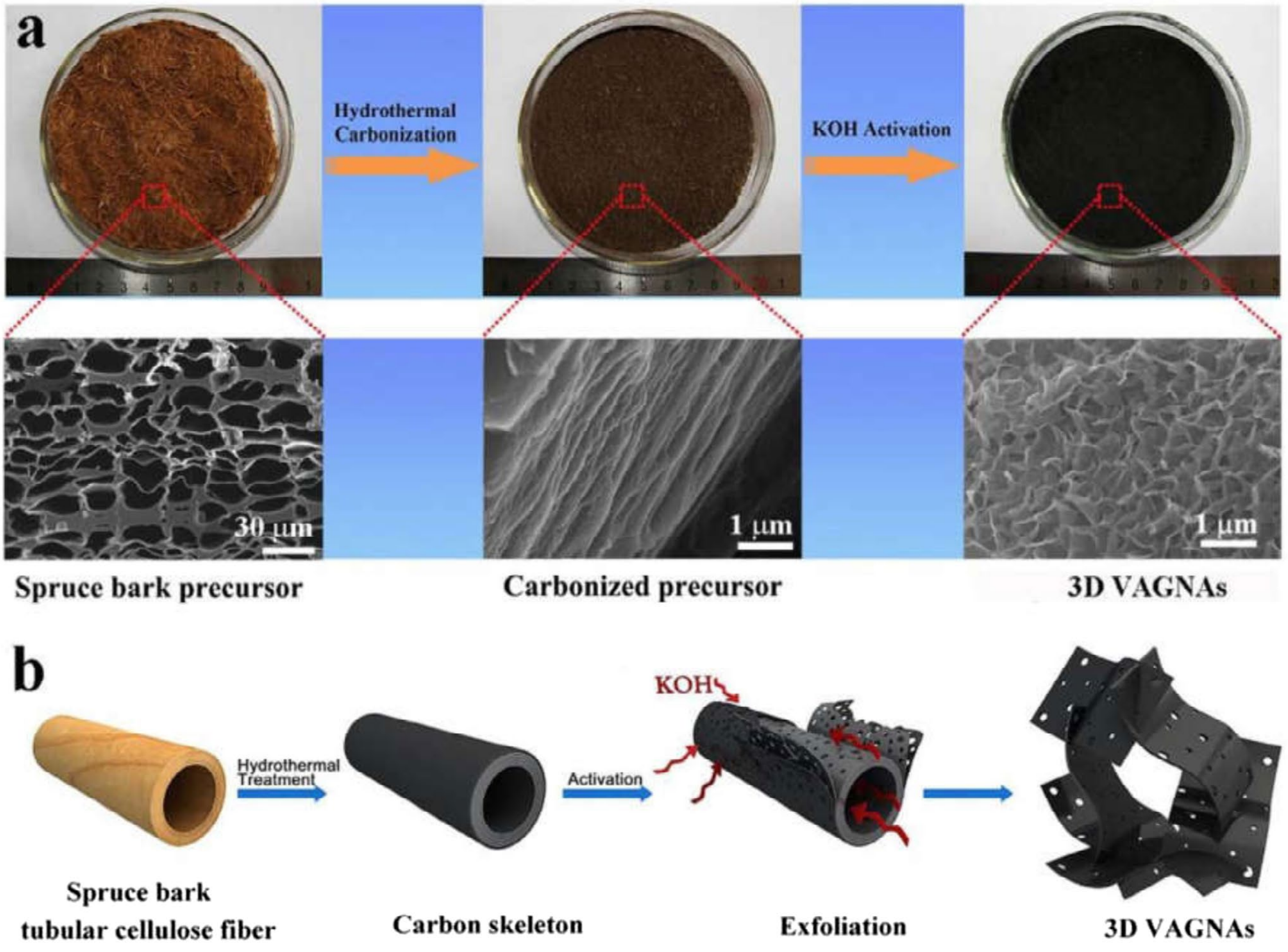

Fig. 22 Schematic illustrations of **a** overall formation process and **b** the synthetic mechanism of 3D VAGNAs (Reprinted with the permission from Ref. [92])

during last few decades. Moreover, flexible, foldable, or even wearable properties are required for more comfortable electronics devices to attract the peoples. Thus, the paradigm of electronics is shifting from technology-oriented to user-oriented devices with various types of human interfaces. Figure 25 shows possible applications of flexible transparent electrodes for corresponding sheet resistance ranges [99]. In general sense, material characterization denotes a systematic analysis, measurement, testing, modeling, and simulation procedure that yield both qualitative and quantitative data of the specific attributed of specific purposes/applications. Therefore, it is imperative to find their various properties using advanced material characterization techniques.

The advanced material analysis and characterization techniques of graphene include UV–VIS Absorption Spectroscopy, Thermogravimetric Analysis (TGA), X-ray Photoelectron Spectroscopy (XPS), Optical Microscope, Atomic Force Microscopy (AFM), Scanning Electron Microscopy (SEM), High-Resolution Transmission Electron Microscopy (TEM), X-ray Diffraction (XRD), Scan Electron Microscopy (SEM), Spectroscopic ellipsometry (SE) are discussed to understand the structural, surface, optical, electrical, microwave.behaviors of Graphene. Moreover, electrical, thermal, parameters (conductivity, stability, etc.), microwave properties (scattering parameters i.e. complex permittivity, attenuation, dielectric loss, and reflection loss in the gigahertz range) are also discussed. Figure 25 demonstrates that the advanced characterization techniques are required for graphene used to wide range of applications. In the following sections, the techniques are described in detail.

Ultraviolet–Visible (UV–VIS) Absorption Spectroscopy UV–visible (UV–VIS) absorption spectroscopy is necessary to understand the graphene oxide dispersions of known concentrations. Moreover, stability critically depends on the amount of reducing agent employed in relation to the mass of graphene oxide present in the dispersion. Figure 26 (inset) shows a digital picture of 0.1 mg mL^{-1} graphene oxide dispersion in water (left), together with its chemically reduced counterpart (right). The yellow brown color characteristic of

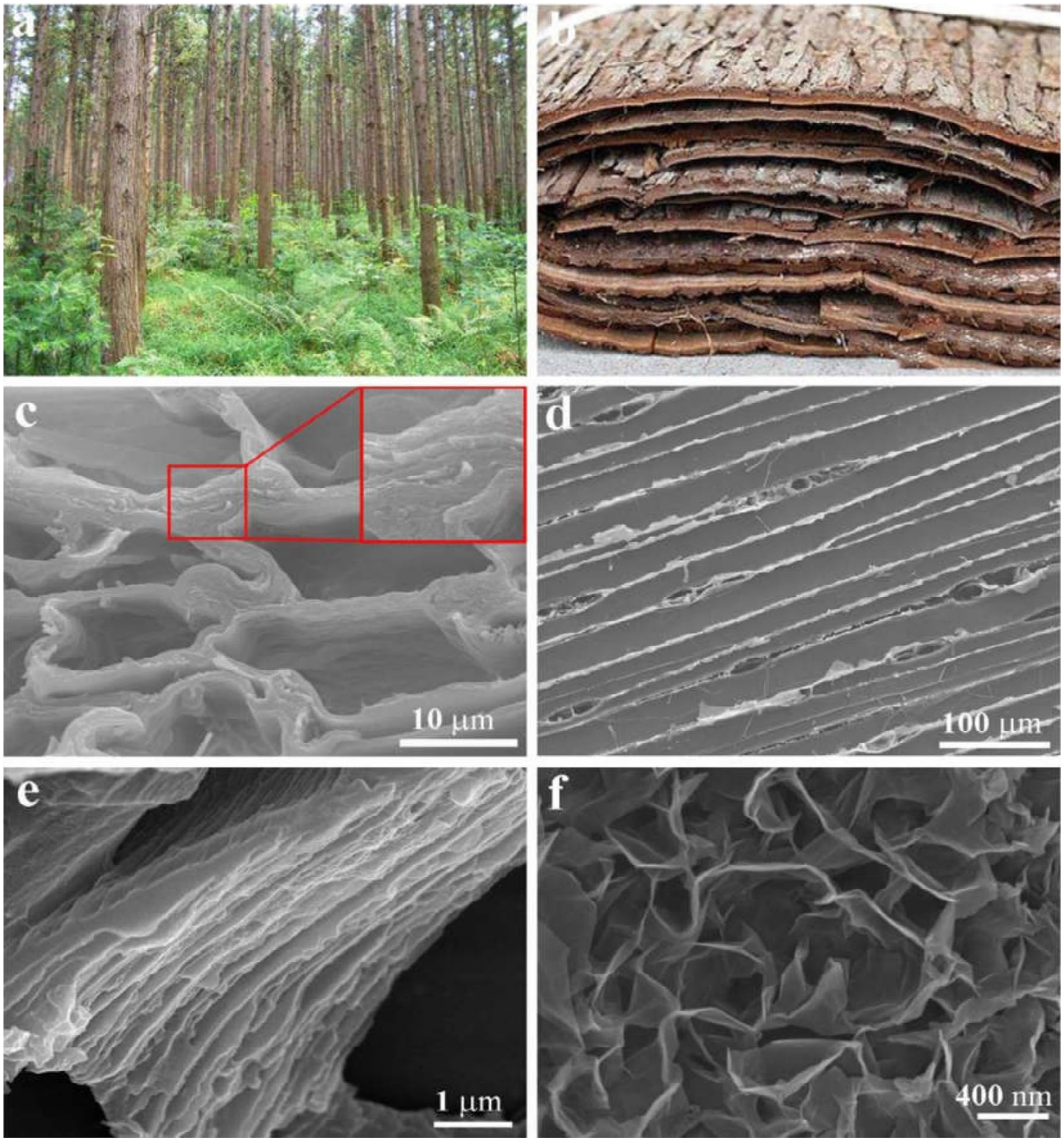

Fig. 23 **a** Digital photo of spruce trees and **b** its bark. **c** SEM image of the cross-section and **d** longitudinal section of the spruce bark. **e** SEM image of the hydrothermal carbonized precursor, a distinct multilayered stacking up structure was clearly observed. **f** The as-prepared 3D VAGNA-900 (Reprinted with the permission from Ref. [92])

the unreduced dispersion changes to black following reduction. This behavior suggests deoxygenation of the graphene nanosheets has effectively come about.

TGA and XPS measurements are done to understand the chemical transformations induced by reduction.

Thermogravimetric Analysis (TGA) The thermogravimetric (TG) and differential thermogravimetric (DTG) plots for the unreduced graphene oxide material (full and dotted orange curves, respectively) and the reduced material (solid and dotted black curves, respectively) are shown in Fig. 27. The reduced material also displays a significant mass loss (~10%) below 100 °C due to water desorption.

X-ray Photoelectron Spectroscopy (XPS) Figure 28 shows the presence of oxygen on both samples of unreduced graphene oxide material and the reduced material was directly evidenced by XPS.

Optical Imaging Optical microscope, atomic force microscopy (AFM), scanning electron microscopy (SEM), high-resolution transmission electron microscopy (TEM)

Table 3 Lists the various biomass resources for Graphene Quantum Dots (GQDs) synthesis via different techniques from Biomass-waste derived graphene quantum dots and their applications (Reprinted with the permission from Ref. [70])

Precursor	Preparation approach	Product	Yield (wt%)	Size (nm)	Height (nm)	References
Neem leaves	Pyrolysis and hydrothermal treatments	GODs Am-GQDs	–	5–6	0.4–1.7	[93]
Rice husks	Pyrolysis and hydrothermal treatment	GODs	15	3–6	0.8–1.6	[88, 94]
Wood charcoal	Electrochemical oxidation	GODs	–	3–6	~6	[88]
Coffee grounds	Hydrothermal treatment	GQDs PEI-GQDs	33	(GODs) 2.67(PEI-GQDS)	2.23 (GQDs) 3.18(PEI-GQDs)	[95]
Neem leaf extract	Pyrolysis and hydrothermal treatment	GQDs	25.2	2–8	–	[96]
Fenugreek leaf extract	Pyrolysis and hydrothermal treatment	GQDs	–	3–10	–	[96]
Honey	Emulsion templated carbonization	GODs	–	1.8–2.8	–	[97]
Rice grains	Pyrolysis	GODs	56	2–6.5	1–2	[97]

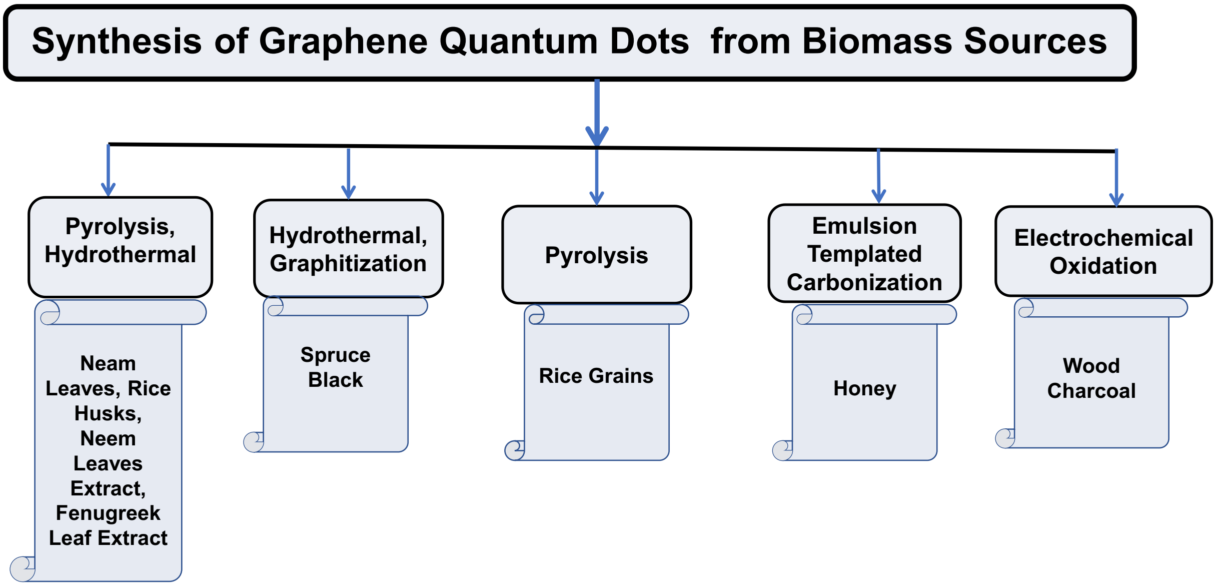

Fig. 24 Synthesis of graphene quantum dots from various biomass sources

techniques are used to image single layers, bi-layers and few layers of graphene.

Optical Microscopy Optical microscopy image of single-, double- and triple- layer graphene on Si with a 300 nm SiO_2 over-layer, labeled in the paper as 1L, 2L and 3L, respectively. The graphene regions were identified by both color contrast in the optical microscope image and atomic force microscopy (AFM) height measurements (as described next), as shown in Fig. 29.

Atomic Force Microscopy (AFM) AFM provides topographic information down to the Angstrom level. AFM technique of imaging of graphene can successfully determine the layer thickness at the nanometer scale as shown in Fig. 30. The images were recorded in the attractive regime of tip sample interaction. Superimposed onto each image is a line profile taken along the marked red line.

Raman Spectroscopy Raman scattering has been widely used in the fundamental spectroscopy study of excitations in solids, liquids, and gases and has also been extensively used in material characterization. Raman Spectroscopy is an effective tool for characterization of mono- or few-layer graphene's, and several theoretical and experimental studies have been reported recently [102].

Carbon allotropes show their fingerprints under Raman spectroscopy mostly by D, G, and 2D peaks around 1350 cm^{-1}, 1580 cm^{-1}, and 2700 cm^{-1} respectively due to the change in electron bands as shown in Fig. 31. Identification of these features allows characterization of graphene layers in terms of number of layers present, and their effect of strain, doping concentration, and effect of temperature and presence of defects. The single sharp 2D peak can be reported for mono layer that is four times more intense than the G peak. The properties of graphene

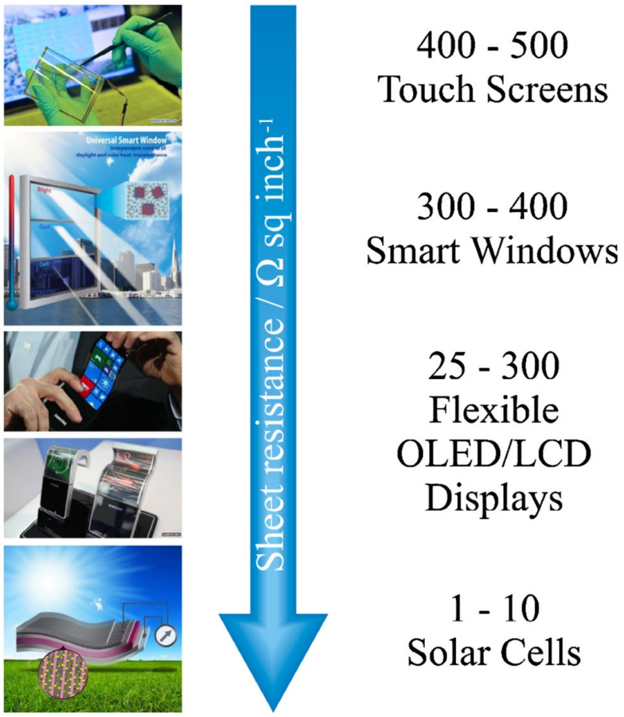

Fig. 25 Potential applications graphene has to offer, depending upon the resistivity of the type of graphene (Requested sought for printed with the permission from Ref. [99])

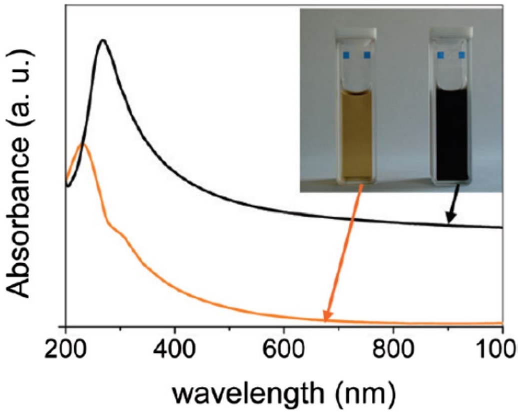

Fig. 26 UV–Vis spectra for unreduced (orange) and chemically reduced (black) graphene oxide dispersions in water. Inset: digital picture of the unreduced (left) and reduced (right) aqueous dispersions (Reproduced with permission from [100])

crucially depend on the number of layers and purity. Various researchers have used Raman spectra as a non-destructive tool to characterize and quality control of mono and few layers of graphene. Various effects on graphene have also been studied using Raman spectra including thickness determination, strain in graphene layers, defects, and doping.

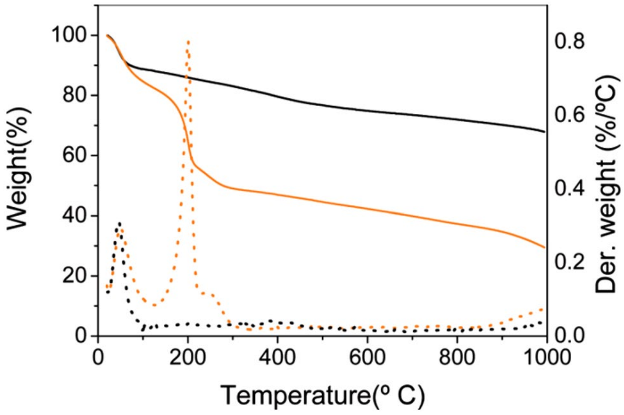

Fig. 27 TG (solid curves) and DTG (dotted curves) plots for unreduced (orange) and chemically reduced(black) graphene oxide material (Reprinted with permission from Ref. [100])

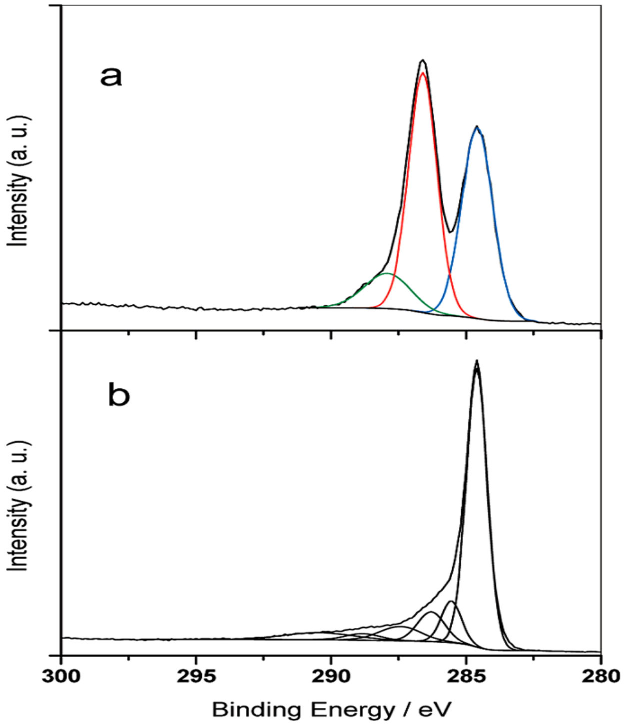

Fig. 28 High-resolution XPS spectra for unreduced (**a**) and chemically reduced (**b**) graphene oxide material (Reprinted with permission from Ref. [100])

Transmission Electron Microscopy (TEM) Transmission Electron Microscopy, TEM is a technique used to observe modulations in chemical identity, crystal orientation, and electronic structure. The TEM images of amine terminated graphene quantum dots (Am-GQDs), amine terminated graphene quantum dots (Am-GQD@Ag, and Am-GQD-Ag-Cys samples are shown in Fig. 32a, b and c respectively.

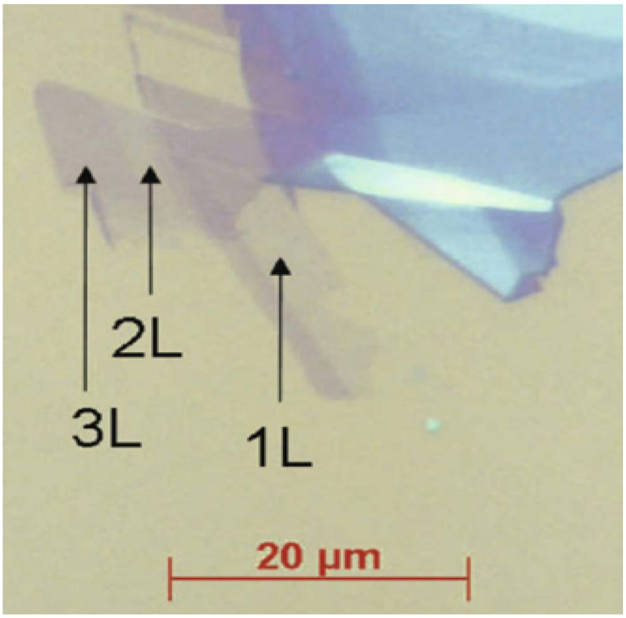

Fig. 29 Optical microscopy image of single-, double- and triple- layer graphene on Si with a 300 nm SiO_2 over-layer, labeled in the paper as 1L, 2L and 3L, respectively (Reprinted with permission from Ref. [101])

Scan Electron Microscopy (SEM) A scan electron microscope (SEM) is an imaging technique of a sample. Field emission SEM (FE-SEM) produces clearer, less electrostatically distorted images with spatial resolution down to 1.5 nm and it is 3–6 times better than conventional SEM. The morphologies of samples can be revealed by SEM based on the different brightness for different angles of the sample surface as shown in Fig. 33. At a vertical surface, the higher proportion of secondary electrons can be collected than at a horizontal surface. Therefore, the thin carbon sheets or wrinkles can be detected by the SEM [71].

X-ray Diffraction (XRD) XRD is a nondestructive technique and qualitative and quantitative analysis of crystalline materials, form of powder or solid. Figure 34 shows the XRD spectra of pristine graphite, graphite oxide, and graphene. The strong and sharp diffraction peak of pristine graphite at 26.6 completely disappeared after oxidization and instead a new peak at 13.9 appeared, indicating a complete oxidization of graphite, which is a prerequisite to obtain exfoliated graphene nanosheets by ultrasonication or thermal expansion. After thermal exfoliation of the completely oxidized graphite (GO), there was no apparent diffraction peak detected, which means the periodic structure of GO was eliminated and graphene nanosheets were formed.

Fourier Transform Infrared Spectroscopy (FTIR) In the FT-IR spectrum of the graphene oxide sample, the peaks at 3432 and 1711 cm^{-1} are attributed to –OH and C=O bands, respectively as shown in Fig. 35. Upon reduction of graphene oxide to graphene, the C=O band disappears and new bands at 2928 and 2865 cm^{-1} arise representing the C–H stretch vibrations of the methylene group. Functionalised graphene displays a peak at 1731 cm^{-1} characteristic band for C=O stretch of the COOH group. The presence of carboxylic functional group is further confirmed by the strong and broad band at 3412 cm^{-1}.

Spectroscopic Ellipsometry Spectroscopy ellipsometry (SE) technique is a nondestructive diagnostic test of thin films. SE is essential for determination of layer thickness, surface roughness, and the optical as well as electrical properties of thin films. For thin films, the optical properties vary considerably depending on the microstructure and growth conditions. The SE data analysis process for most samples begins by building a layered optical model, which corresponds to the nominal sample structure.

As shown in Fig. 36 below, where spectroscopic ellipsometry is used to characterize the complex refractive index of chemical vapor deposition CVD graphene grown on copper foils and transferred to glass substrates. The spectroscopic ellipsometry, with respective wavelength ranges extending into the ultraviolet and infrared IR, have been used to characterize the CVD graphene optical functions.

Electrical and Electronic Characterization

Microwave Characterization Microwave measurements of the dielectric properties of materials are finding increasing applications in new electrotechnology. Measurement of the bulk dielectric properties (dielectric constant, dielectric loss factor) is not only testing, but these properties are in intermediary vehicle for understanding, explaining, and empirically relating certain physicochemical properties of the test material. The EM (Electromagnetic) absorption characteristics of materials depend on its dielectric properties (complex permittivity), magnetic properties (complex permeability), thickness, and the frequency of operation.

Near-field measurements were performed at X-band frequencies (8–12 GHz) for graphene on copper microstrip transmission lines. An improvement in radiation of 0.88 dB at 10.2 GHz is exhibited from the monolayer graphene antenna which has dc sheet resistivity of 985 X/sq. Emission characteristics were validated via ab initio simulations and compared to empirical findings of geometrically comparable copper patches. The S-parameters of were measured, as depicted in Fig. 37. The graphene enhances the dielectric losses. The impedance mismatch caused by the copper patch, as illustrated in Fig. 37b, is similarly severe and increases reflections by at least 10 dB whilst reducing transmission by 1 dB.

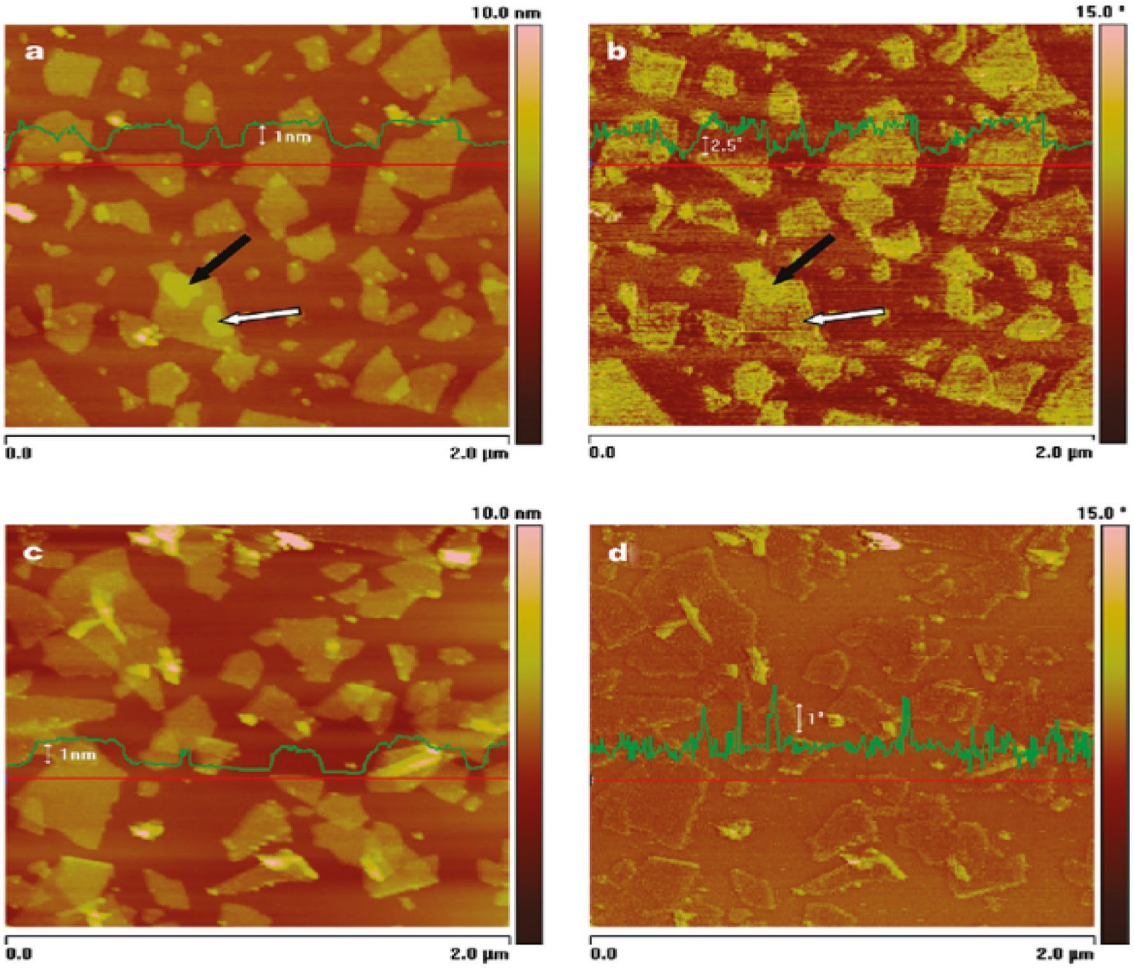

Fig. 30 Height **a** and **c** and corresponding phase **b** and **d** tapping-mode AFM images of unreduced (**a** and **b**) and chemically reduced **c** and **d** graphene oxide nanosheets deposited from aqueous dispersions onto freshly cleaved HOPG (Printed with the permission [100])

This section has presented various novel analysis and characterization techniques for graphene required for various application. These include structural, thermal, surface, optical, electrical, and microwave characterization for graphene as shown in Fig. 38. Moreover, electrical, thermal, parameters (conductivity, stability, etc.), microwave properties (scattering parameters i.e. complex permittivity, attenuation, dielectric loss, and reflection loss in the gigahertz range) are also discussed. The next section various applications of graphene are discussed.

Application

Graphene can be used in a multitude of applications for improved energy storage (capacitors, batteries, and fuel cells), energy generation (solar cells), sensors or even as an advanced membrane material for separations. For example, graphene-based wireless sensor is used for bacteria detection on tooth enamel [112, 113].

Graphene in Energy Storage and Eenergy Generation Devices The Graphene Quantum Dots (GQDs) are strongly luminescent, biocompatible, dispersible in a number of solvents, and usually nontoxic, demonstrating a great potential for integration onto devices of bio-imaging, batteries, supercapacitors, photovoltaics and light emitting diodes (Fig. 39).

Graphene-Based Ultracapacitors Figure 40A shows a schematic of the two-electrode ultracapacitor test cell and fixture assembly along with SEM and TEM images of the surface of the chemically modified graphene (CMG) agglomerate particles and individual graphene sheets. Figure 40B shows lithium batteries with cross-sectional TEM images of graphene nanoplatelets and CNT (carbon nanotubes).

Graphene in Biomedical applications The properties of graphene and its derivatives are strong UV absorption, fluorescence, fluorescence quenching ability, SERS, functionalizable surfaces. This unique property of graphene and its derivatives make them the desirable material for biosensors,

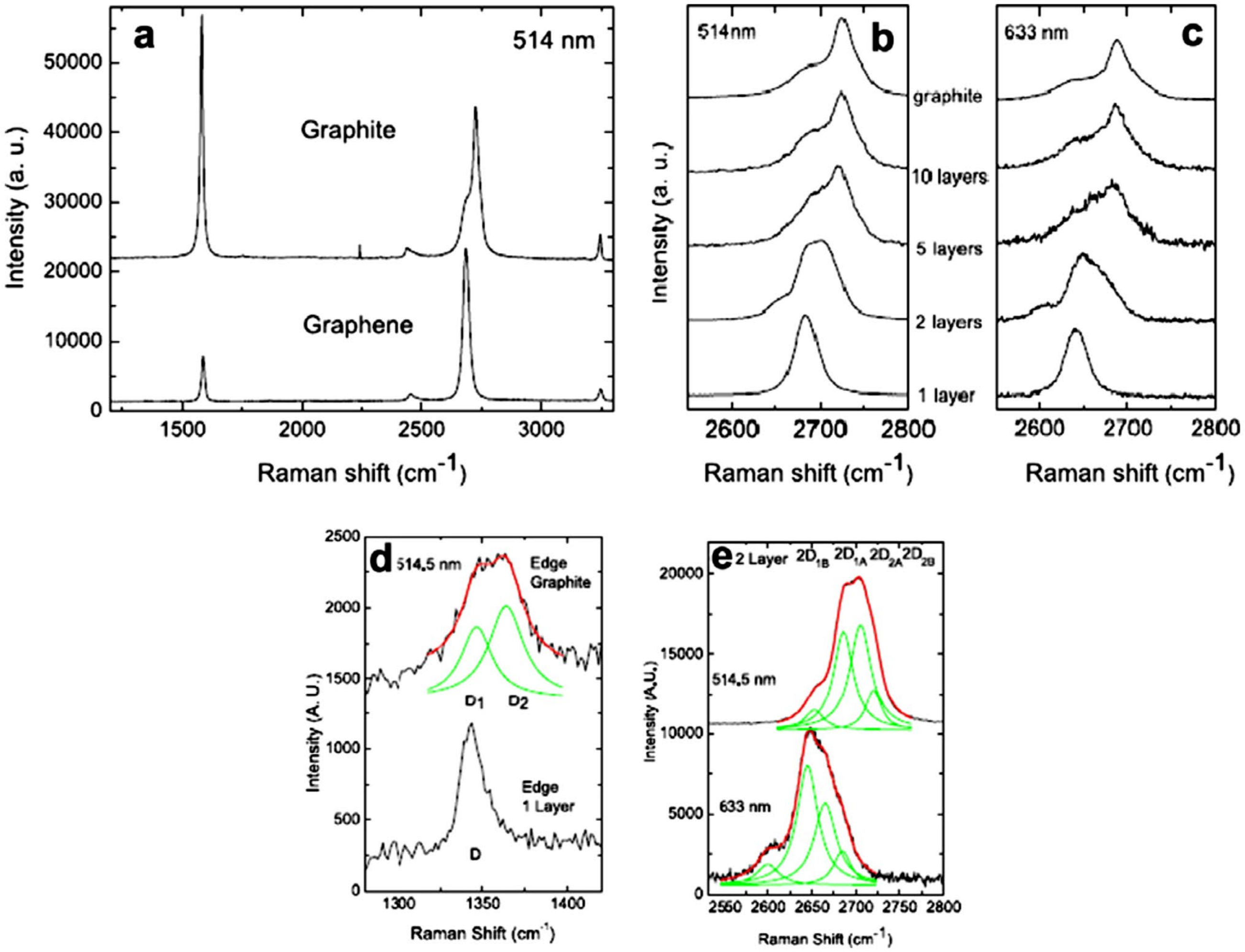

Fig. 31 **a** Comparison of Raman spectra at 514 nm for the graphite and single layer graphene. **b** and **c** Evolution in 2D band as a function of layers at 514 and 633 nm excitations. **d** and **e** Comparison of the D band at 514 nm at the edge of bulk graphite and single layer graphene. The fit of the D1 and D2 components of the D band of bulk graphite is shown. **e** The four components of the 2D band in 2-layer graphene at 514 and 633 nm (Reprinted with the permission from Ref. [102, 103])

tissue engineering, electronics, and therapeutics. Graphene also possesses excellent surface functionalizability, aqueous processability, hydrophobicity (important for cell growth and differentiation) and amphiphilicity which is desirable for biological applications [116]. Figure 41 shows the potential biomedical applications of graphene and graphene oxide in mass spectrometry, sensors, gene & drug delivery, cancer treatment, cell growth.

Yin Zhang et al. states that graphene has a vast scope in biomedical application because of its exceptional properties and structure. The main concern that lies in the full implementation is the toxicity of graphene and its effect on the body. If graphene and its derivatives can be functioned and modified in such a way that it does not display any toxic behavior or it can be eliminated from the body over a period, then it can be best used. Graphene and graphene oxide have many development of graphene and graphene derivatives for energy, sensing, and biomedical applications in biomedical field such as in cell replacement, bone tissue repair, restoring neuronal circuits and in cardiovascular diseases. The schematic overview of various biomedical applications of graphene is shown in Fig. 42. The main aim is to develop a material than can efficiently deliver the therapeutic agents without toxicity [120].

Martin Pumera et al. reviews about the electrochemistry property of graphene for sensing and energy applications. Graphene sheets and nanoplatelets have exceptional conductivity, large surface area, lower cost and are free from impurity. There electrochemical properties are noteworthy as compared to other electrodes [121].

The fast heterogeneous electron transfer kinetics and sensitive sensing properties towards the detection of dopamine

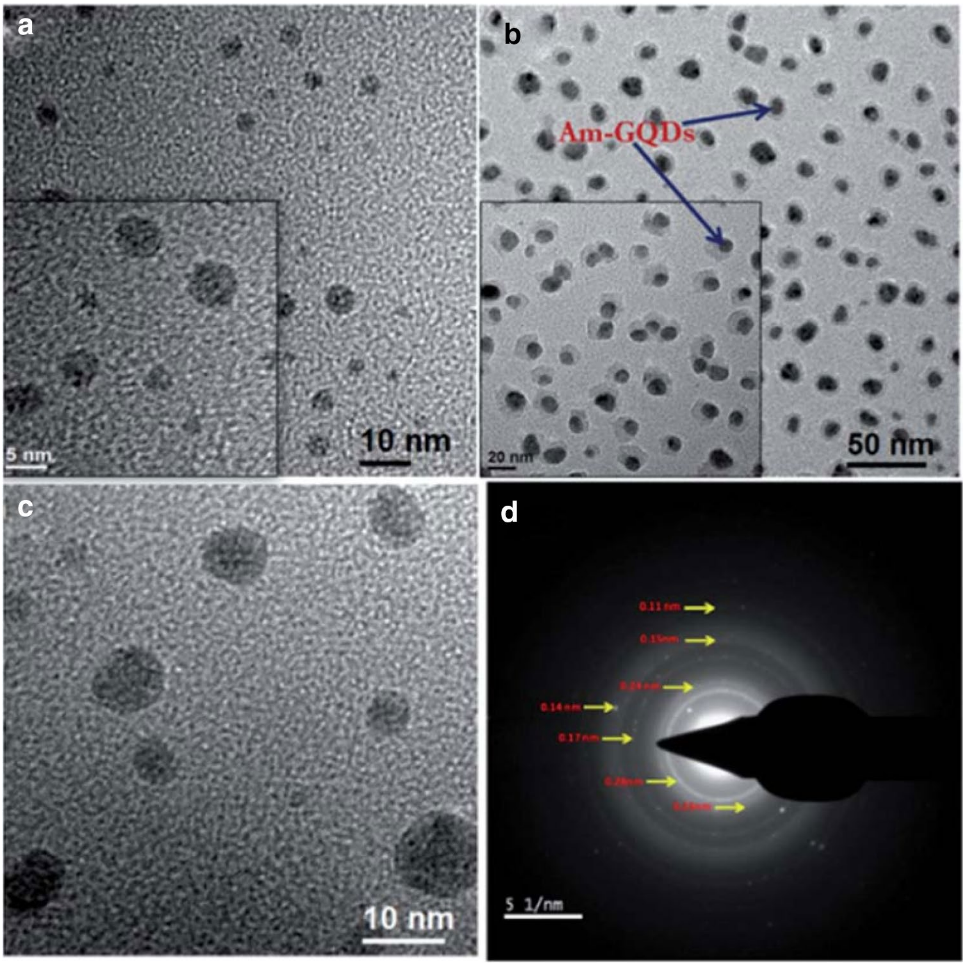

Fig. 32 HRTEM images of **a** Am-GQDs, **b** Am-GQD@Ag (with the addition of Ag + ions to the 5–6 nm size amine terminated GQDs results in the formation of a complex which arranges on the Am-GQD surface to get Am-GQD@ Ag particles. Interestingly a distinct shell appears around the GQDs), **c** AmGQD-Ag-Cys (addition of L-cysteine solution this shell in **b** disappears), and **d** SAED pattern of Am-GQD@ Ag (shell surrounding the quantum dots possibly arises due to nucleation of Na_2SO_4 and Ag_2SO_4 around the AmGQD-Ag particle system during the process of drying the sample on the TEM grid) (Reprinted with the permission fromRef. [104])

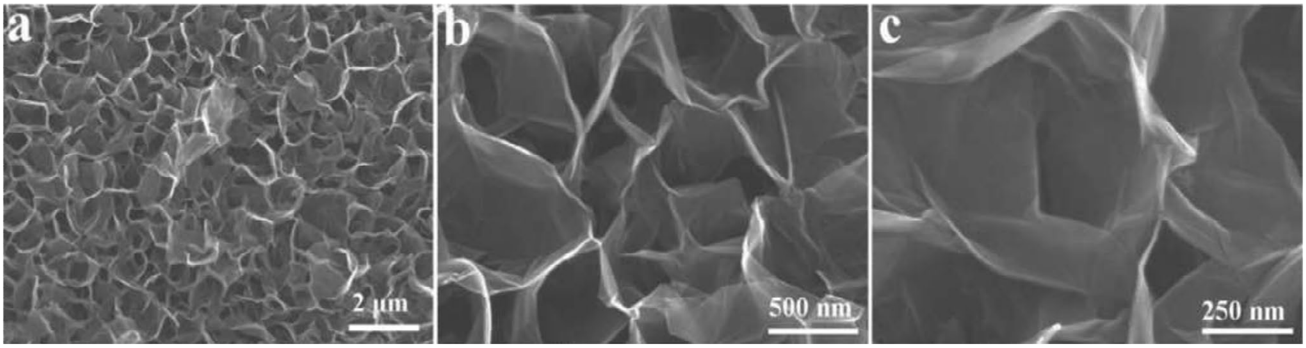

Fig. 33 SEM images of vertically aligned graphene nanosheet arrays (VAGNA) obtained by pyrolysis at 900 °C from spruce bark via coupling with hydrothermal carbonization method. **a** SEM image; **b**, **c** High-magnification of SEM; **d**) (Reproduced with permission from Ref. [105])

in the presence of typical interferences, such as ascorbic and uric acid, arises from the high density of edge plane sites at the ends of the graphene nanoplatelets and their ability to act as nano connectors for electrical connection with electrode substrates as shown in Fig. 43.

Fluorescence microscopy of MCF-7 cells incubated for 24 h, QDUS-rGO could be observed in the cytoplasm (Fig. 44a) and Henrietta Lacks (HeLa) cells, shown in Fig. 44b (QD-US-rGO). In vivo fluorescence imaging of mice bearing different tumors (indicated by arrows) after intravenous injection of Cy7-labeled GO are shown in Fig. 44b.

Yuqi Yang et al. talks about the use of graphene in drug delivery, phototherapy and in vivo imaging [124]. Due to

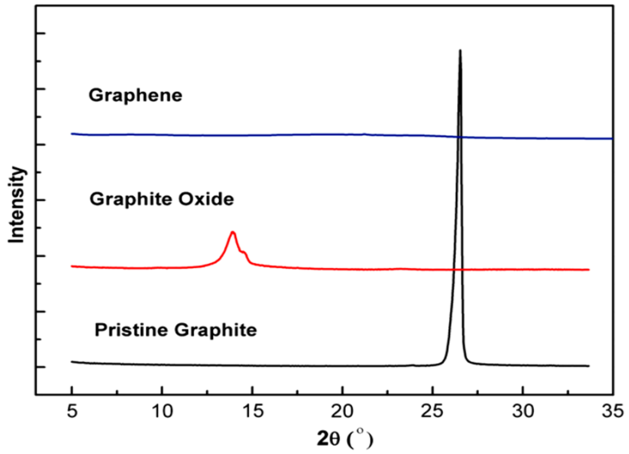

Fig. 34 X-ray diffraction patterns of pristine graphite, graphite oxide and graphene (Reproduced with permission from Ref. [106])

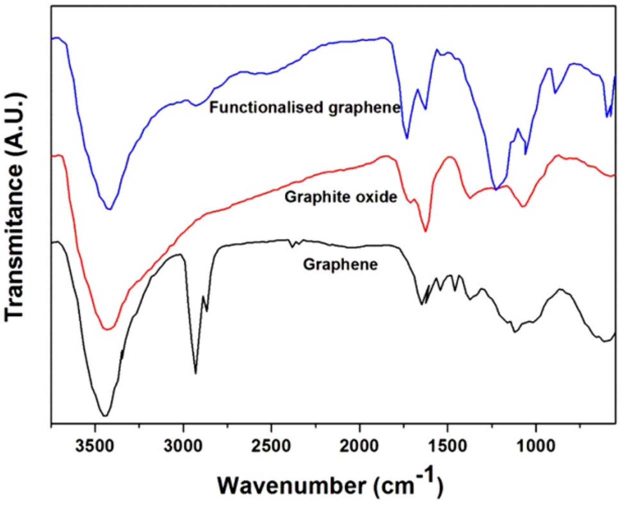

Fig. 35 FTIR spectra of graphene, thermally reduced graphite oxide and functionalized graphene (Reproduced with permission from Ref. [107])

its excellent properties, graphene-based materials have an excellent future in biomedical fields but there are some hurdles which need to be overcome to get a desired efficacy. There needs to be more study on its toxicity, intracellular pathway and cellular-uptake mechanism. Another concern is increasing the productivity of graphene quantum dots and developing effective methods to produce inerratic graphene sheets [125].

Owing to the excellent biocompatibility, ready cellular uptake, flexible chemical modifications and unique optical properties, GO has been explored for biological imaging. The protection of DNA from enzymatic digestion by the self-assembly of ssDNA on GO sheets was reported by Tang et al. [126] as shown in Fig. 45.

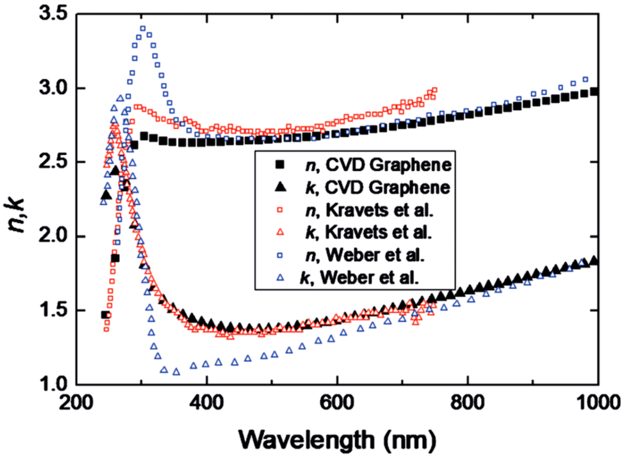

Fig. 36 Color Comparison of *n* and *k* values between CVD graphene [108] and exfoliated graphene by Kravets et al. Ref. [109] and Weber et al. Ref. [110]; (Reproduced with permission from Ref. [108–110])

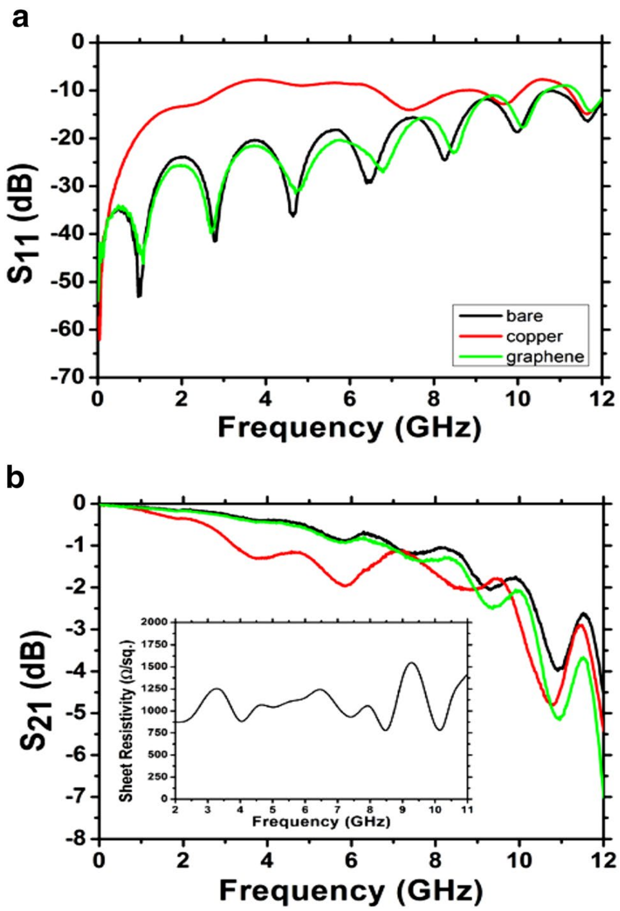

Fig. 37 **a** Reflection (S_{11}) and **b** transmission (S_{21}) coefficients of the bare transmission line (black), the graphene patch (green), and the copper patch (red). Inset: Optimized surface conductivity of graphene (Reproduced with permission from Ref. from [111])

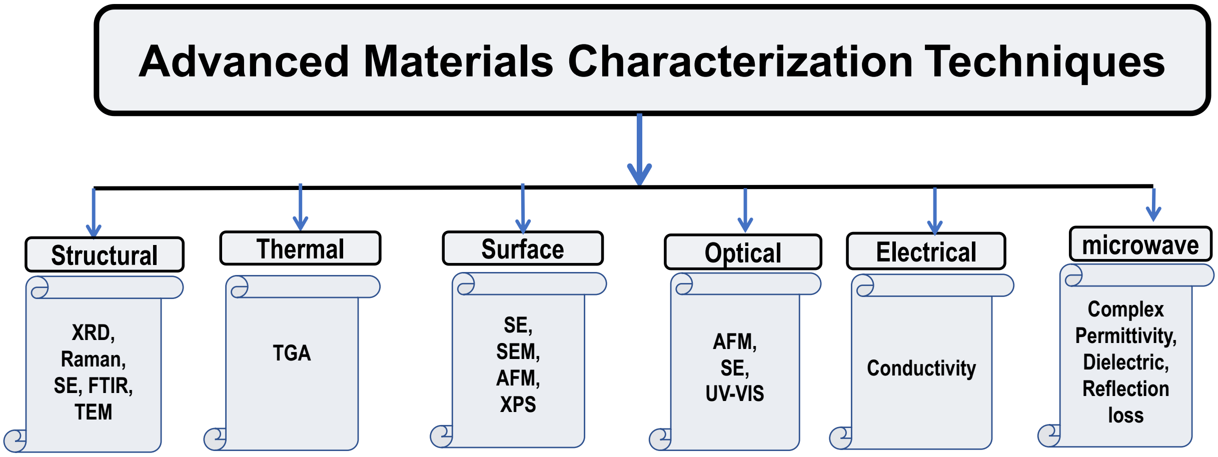

Fig. 38 Advanced materials characterization techniques for graphene

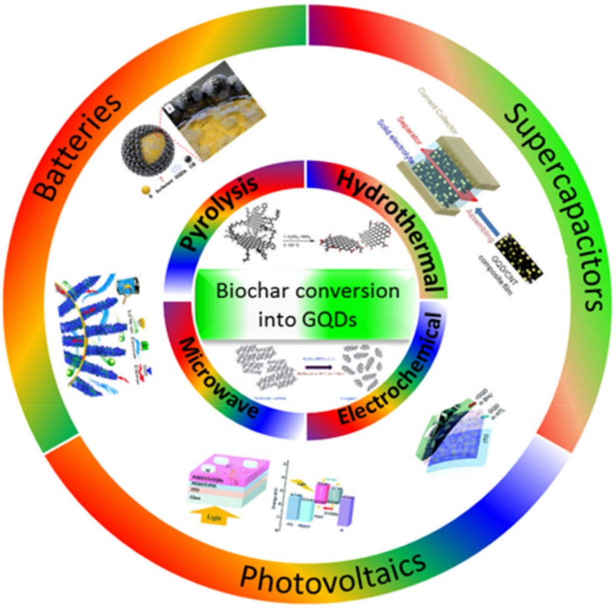

Fig. 39 Schematic illustration of the conversion of biowaste into GQDs through various approaches and their energy applications (Reprinted with permission from [70])

Shumao Cui et al. describes the use of graphene coupled with nanocrystals for sensing and energy applications. The biosensor developed using thermally reduced graphene oxide (TRGO) coupled with Au nanocrystals was highly sensitive and reliable with stable structure. The addition of nanocrystal proves to be appropriate in increasing the sensitivity of graphene. The main challenge lies in the understanding of interaction between graphene and nanocrystals on which the properties of the hybrid structure depends. The application and development of graphene-nanocrystals structure highly depends on the orientation and morphology of the structure [126]. A sensitive and selective field-effect transistor (FET) biosensor is demonstrated using vertically oriented graphene (VG) sheets labeled with gold nanoparticle (NP)-antibody conjugate in Fig. 46.

Ernie W. Hill et al. reviews the use of graphene as a material for different types of sensors. Graphene has properties which can be utilized to produce different types of sensors such as electrochemical sensors, magnetic sensors, bio sensors, photoelectric sensors, strain sensors, optical sensors, chemical sensors, and mass sensors. Graphene has superior mechanical stability comparatively which can be utilized for flexible touch screens. The future of graphene-based sensors looks bright but there must be an abundant source of high-quality of graphene available on wafer scale [128].

Application in COVID-19 Graphene joins the fight against COVID-19. The world is currently experiencing one of the most significant cases of lockdown since the second world war and has had a profound medical, economic and social impact on the lives of people in all corners of the world. The current situation is one that is likely to proceed for a significant period. Still, a concerted effort is being made by governments, scientists and healthcare professionals to test people with symptoms, to confirm if they have the novel SARS-CoV-2 coronavirus, so that they can either self-isolate or seek appropriate medical treatment if needed.

However, one of the issues around the globe is a lack of testing in some areas, whereas the quality of testing in other areas is coming under fire for producing false results. There are already several tests on the market which are being sold and used by many companies. Still, ways of creating more effective tests to diagnose if people have or had the coronavirus are coming to the fore. These tests will hopefully help to alleviate any issues about the quality of tests on the market soon—this will be especially important in the coming months before (and if) researchers find a vaccine that

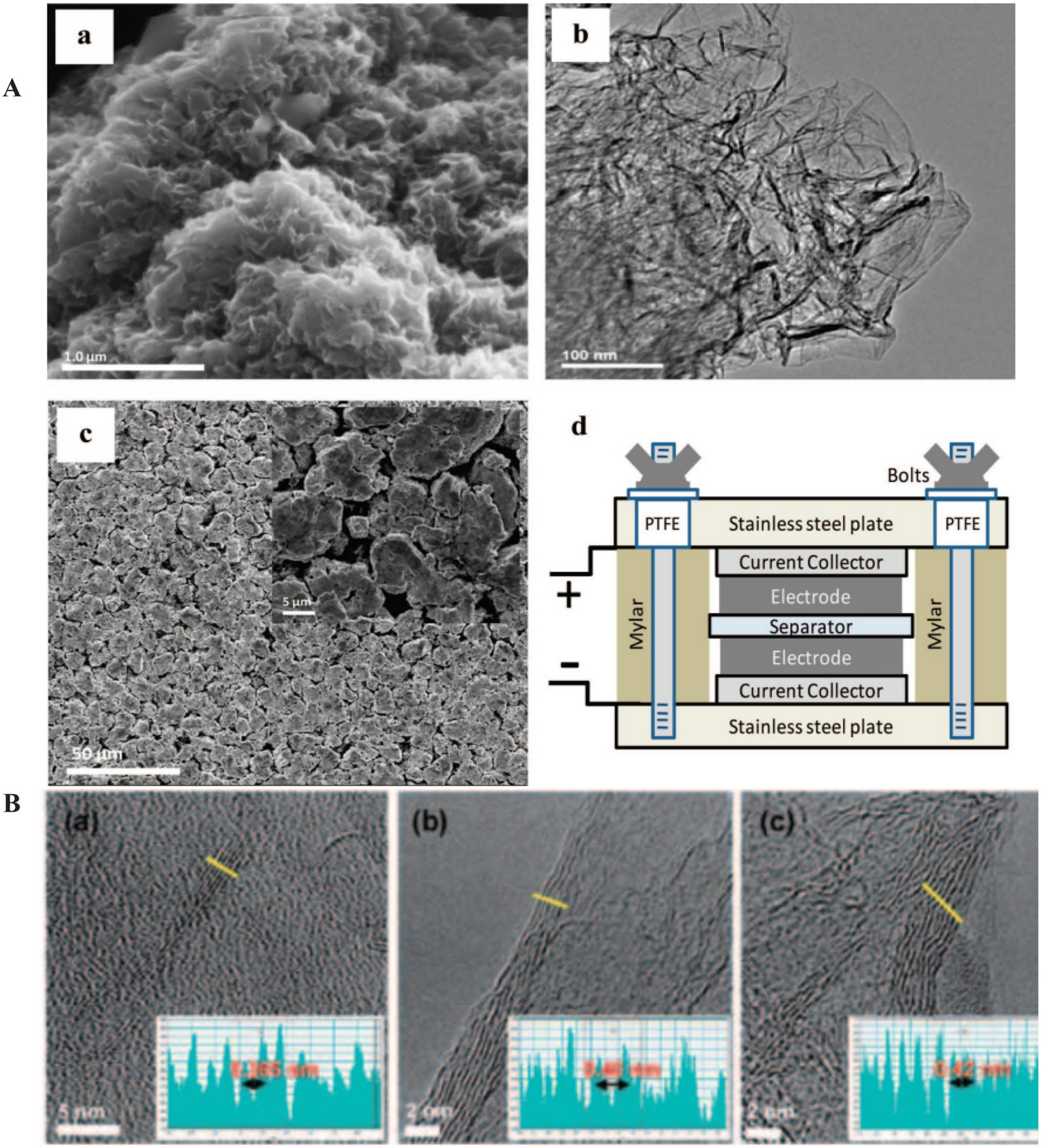

Fig. 40 Graphene for energy storage. **A** Ultracapacitors: (a) SEM image of CMG particle surface, (b) TEM image showing individual graphene sheets extending from chemically modified graphene surface, (c) low and high (inset) magnification SEM images of chemically modified graphene electrode surface, and (d) schematic of test cell assembly. **B** Lithium batteries: Cross-sectional TEM images of graphene nanoplatelets with almost the same numbers (5–6) of graphene stacking layers for (a) graphene nanosheets, (b) graphene nanosheets separated by CNT, and (c) grapheme nano-sheets separated by C60 (Reprinted with permission from Ref. [114–116])

can contain the spread of the virus [129]. Graphene sensors arrays can be implemented on standard utility textiles and drug efficacy screening. Thanks to its high versatility, we foresee that graphene may have a leading role in the fight against COVID-19 [130].

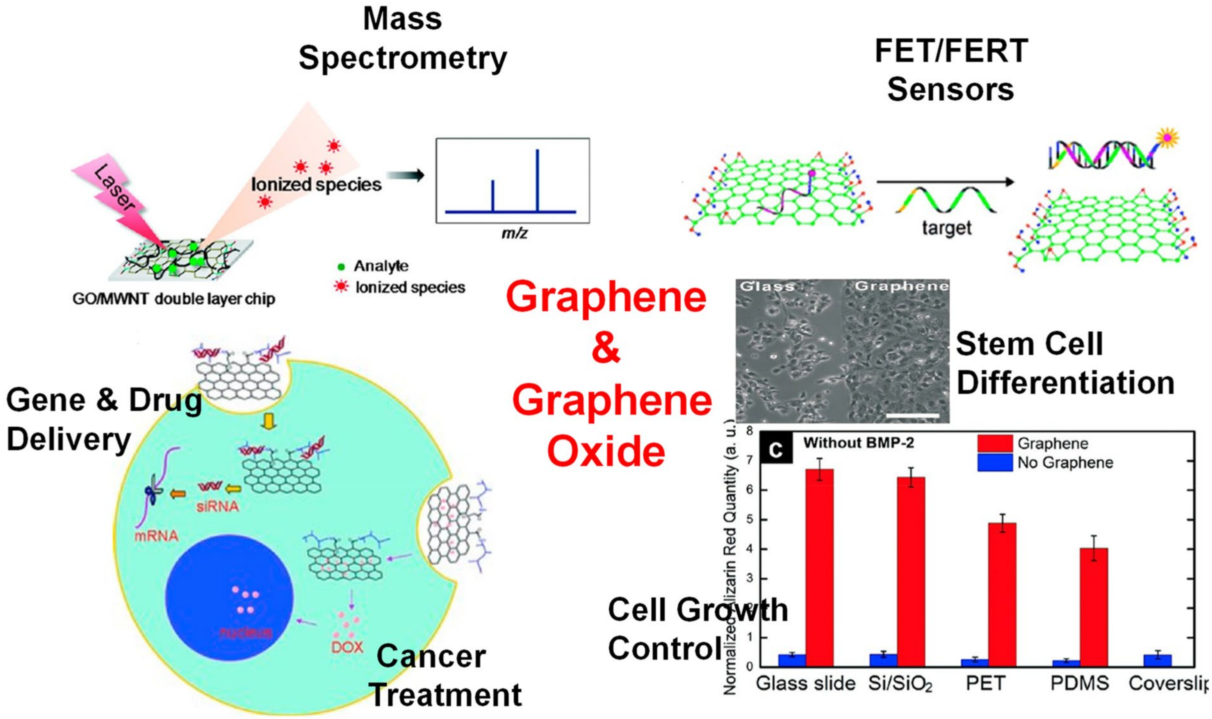

Fig. 41 Biomedical applications of graphene and graphene oxide (Reproduced with permission from Ref. [117–119])

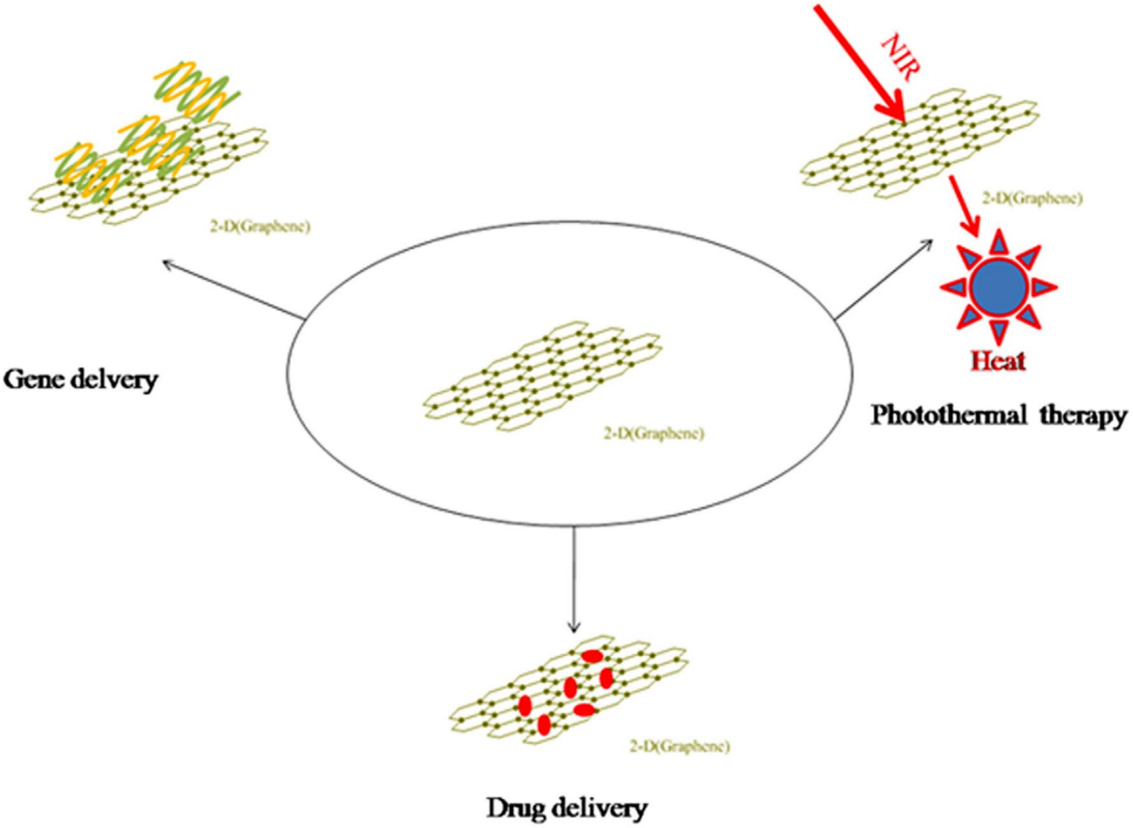

Fig. 42 Schematic overview of various biomedical applications of graphene (Reproduced with permission from Ref. [119])

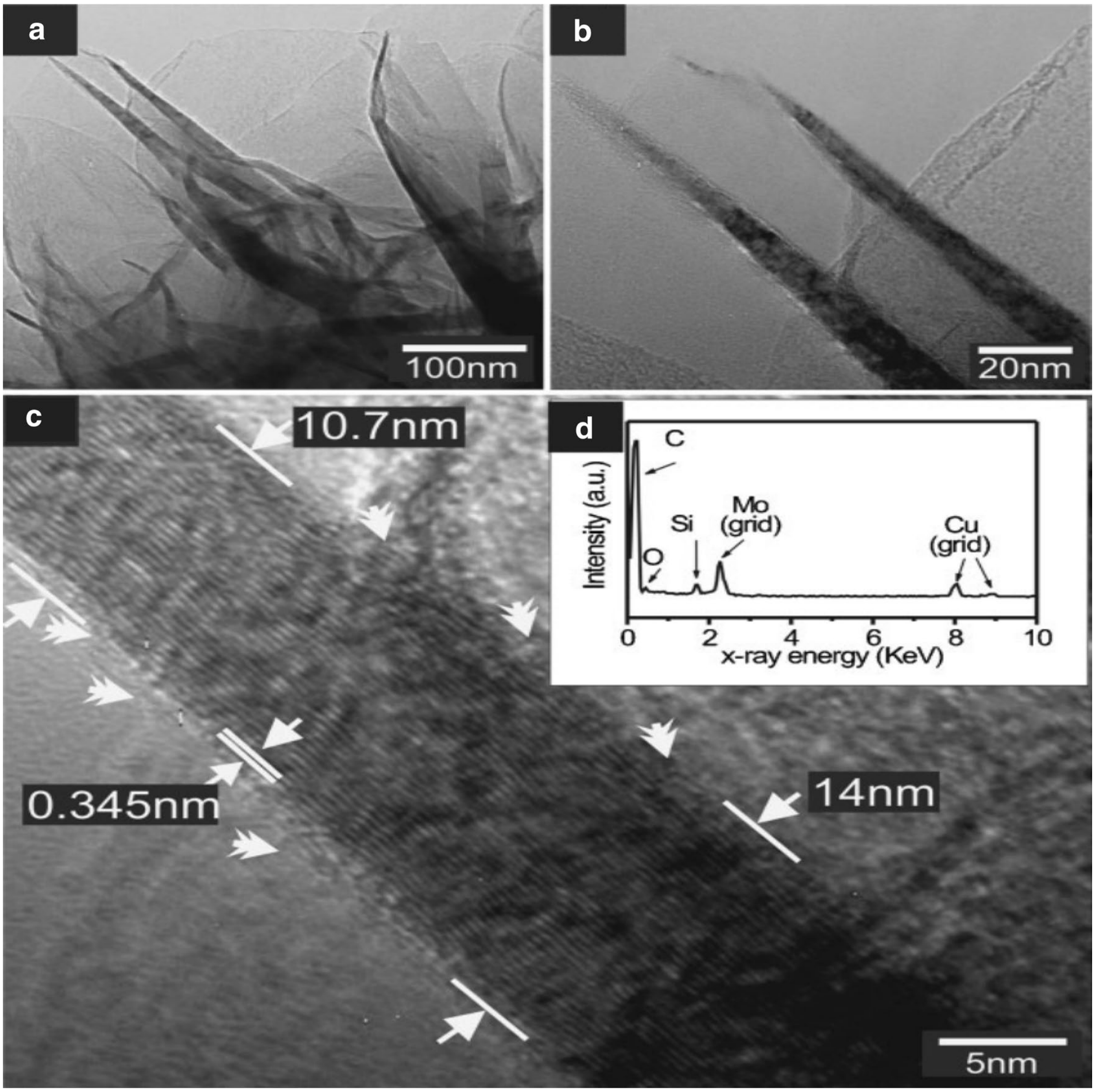

Fig. 43 Graphene nanoplatelets for electrochemical biosensing. **a** and **b** Different magnification TEM images of nanoplatelets; **c** High-resolution TEM image of graphene nanoplatelets showing the nanoflake with a knife edge or conical structure with open graphitic planes; **d** EDX spectrum, showing the chemical composition of graphene nanoplatelet films [Reproduced with permission from Ref. [121])

Biomass Derived GQDs Graphene Quantum Dots, GQDs stand out as a new material combining the exceptional properties of both graphene and quantum dots [131]. As a result of the intriguing properties, such as good electrical conductivity, enlarged surface area, high solubility in many solvents, strong luminescence, high mobility, decreased chemical impedance, and tunable bandgap, GQDs exhibit an edge over other graphene based materials and have indicated a bright promise in fluorescence sensors, photovoltaic devices, light-emitting diodes, solar cells, fuel cells, batteries, and supercapacitors.

PL Sensors The numerous applications of biomass derived GQDs include PL Sensors for detection of chlorine in water, detection of range of metal ions in water based on their strong fluorescence properties,

Light Emitting Diodes The biomass derived GQDs are also used for the development of range of white, green, red, blue, orange light emitting diodes and other devices.

Biomedical Biomass derived GQDs from natural food precursor such as rice grains [98], rice husks [88, 94], coffee beans [95] and have been widely investigated for biomedical applications, especially bioimaging. Very recently, Ding et al. reported on the bioimaging of fibroblast cells with sulphur doped GQDs synthesized by the hydrothermal treatment of durian [132]. Different GQDs with varying amount of S doping indicate different color in bioimaging of the

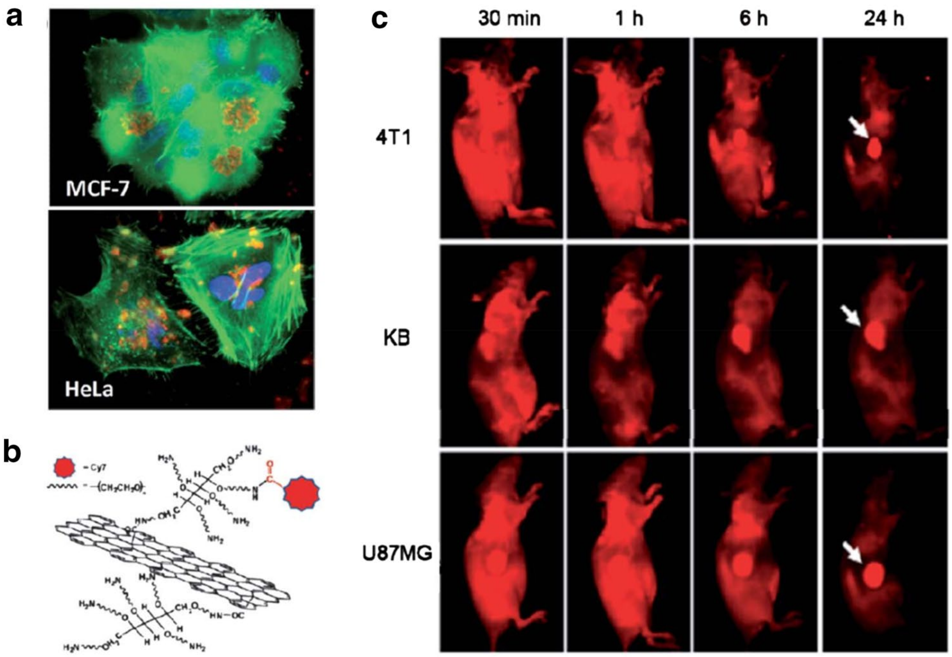

Fig. 44 Optical imaging of graphene-based nanomaterials. **a** Cellular uptake of folic acid-conjugated QD–rGO in human breast cancer MCF-7 and HeLa cells, where QD fluorescence is shown in red orange. **b** A schematic representation of Cy7-labeled GO through six-arm branched PEG chains. **c** In vivo fluorescence imaging of mice bearing different tumors (indicated by arrows) after intravenous injection of Cy7-labeled GO. Adapted from Ref. [122] and [123] with permission Fabrication and properties of a high-performance chlorine doped graphene quantum dot based photovoltaic detector

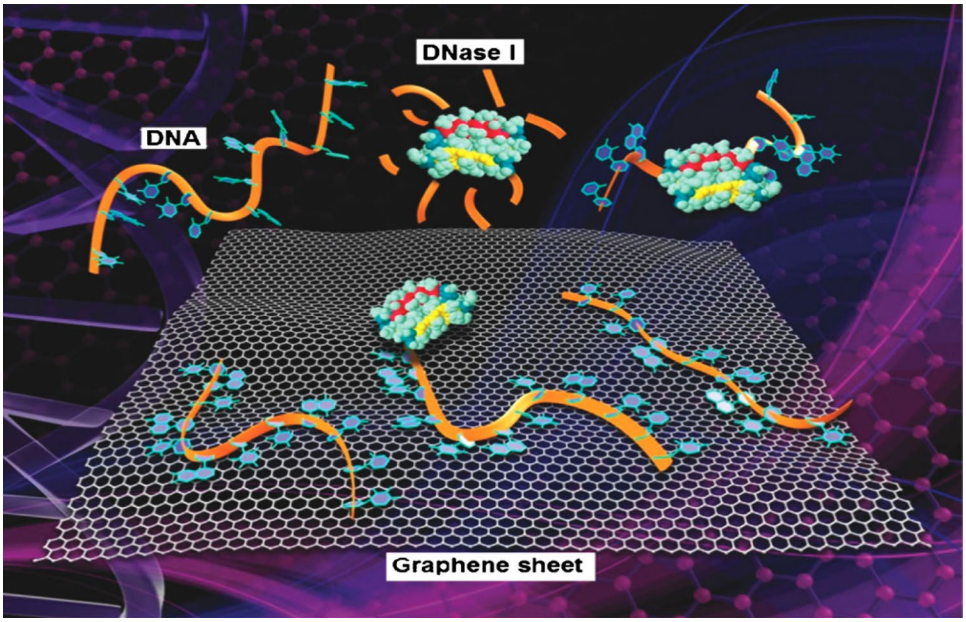

Fig. 45 Schematic illustration of the constraint of DNA molecules on functionalized graphene and its effects. Single stranded DNA can be effectively constrained on the surface of graphene through adsorption. The enzyme DNase I can digest free DNA but not graphene-bound DNA (Printed with the permission Ref. [124, 125])

fibroblast cells, showing their high bioimaging capability (Fig. 47).

Energy Owning to the extraordinary properties of graphene, such as large surface area, good electrical conductivity, tunable luminescence, decreased chemical impedance, and tunable bandgap, GQDs have shown great promise in energy applications, such as photovoltaics devices, batteries, and supercapacitors.

Liu et al. [133] synthesized a GQD-based symmetric micro-supercapacitor by electrophoretic deposition of GQDs on the interdigital Au finger microelectrode and acquired fast power response, high rate performance, and long cycling life (97.8% stability after 5000 cycles) as shown in Fig. 48.

Owning to the extraordinary electronic/optical properties, GQDs may be implemented in various components of photovoltaics, such as sensitizers, activators, active layers, catalysts for the counter electrode. GQDs are used as active layer to fabricate Si/GQD heterojunction solar cell [134] as shown in Fig. 49a. PbS QD/GQD core/shell hybrids were synthesized [135]. An improved current

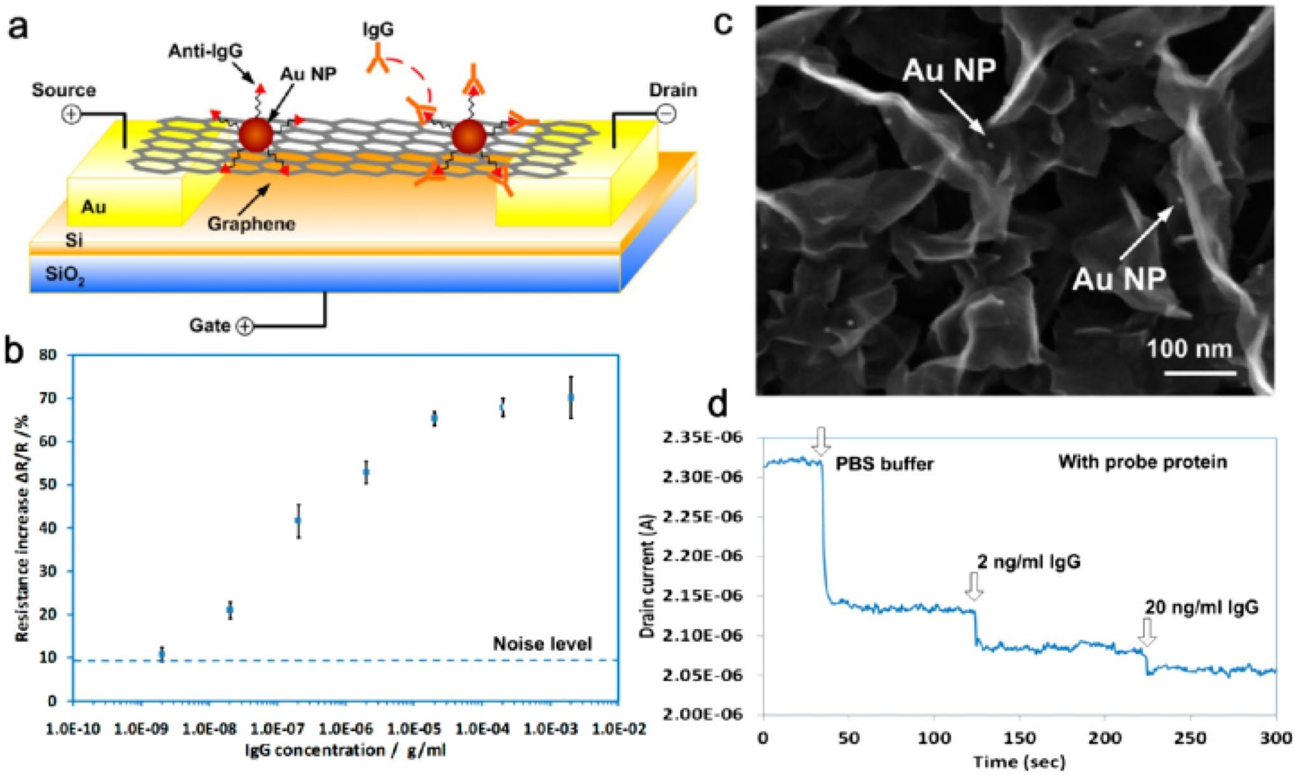

Fig. 46 **a** Schematic of a TRGO FET device by direct growth of VG between the drain and the source electrodes. Probe antibody is labeled to the VG surface through Au NPs. **b** Sensor sensitivity versus IgG concentration (g/mL). The dashed line represents the noise level (9.8%) from the buffer solution. **c** SEM image of the VG network deposited with Au NP-antibody conjugates (top view). **d** Dynamic response of the VG sensor exposed to different concentrations of IgG with probe proteins (Reprinted with permission from Ref. [127])

density (13.4 mA cm^2), PCE (3.6%) and open voltage (0.58 V) was obtained for solar cell with PbS QD/GQDs active layers than that of organic molecules capped PbS QDsbased devices [135].

Figure 50 shows the summary of application areas of Graphene including energy generation, energy storage, sensors, composites, coating membranes, biomedical fields.

Discussion

Since 2004, the number of graphene-related academic publications has substantially increased. Figure 45 illustrates the surge in graphene as well as reporting some historical points of interest; there were over 14,000 papers published with the keyword ‘graphene’ (Web of Knowledge 2020). As of 2020, the time of writing this review, there are a range of graphene production methods (as briefly discussed above), each of which carry their respective benefits, whilst at the same time producing different types of graphene (monolayer, multi-layer, etc.) which have different applications depending on the properties exhibited by each type of graphene.

So far various synthesis techniques of graphene have been discussed and their properties are identified, analyzed, and classified. The synthesis of graphene can be divided into two main categories as listed in Table 4: the top-down approach and the bottom up approach. A general survey and comparison on the state of art synthesis of graphene are summarized with their merits and challenges.

Very few commercial technologies involving graphene-based materials have emerged, in large part due to the difficulty in processing these 2D sheets into useful, 3D materials with predicable structure and thus function. To address this challenge, for developing processes capable of depositing large-area monolayer graphene films onto a variety of substrates from biomass sources are summarized in Table 5.

Table 6 shows the summary of critical material properties for each characterization techniques that have been discussed so far. This will lead to an interdisciplinary research field of graphene development from biomass sources.

The various microscopic materials characterization techniques such as TEM, SEM, AFM are very different each

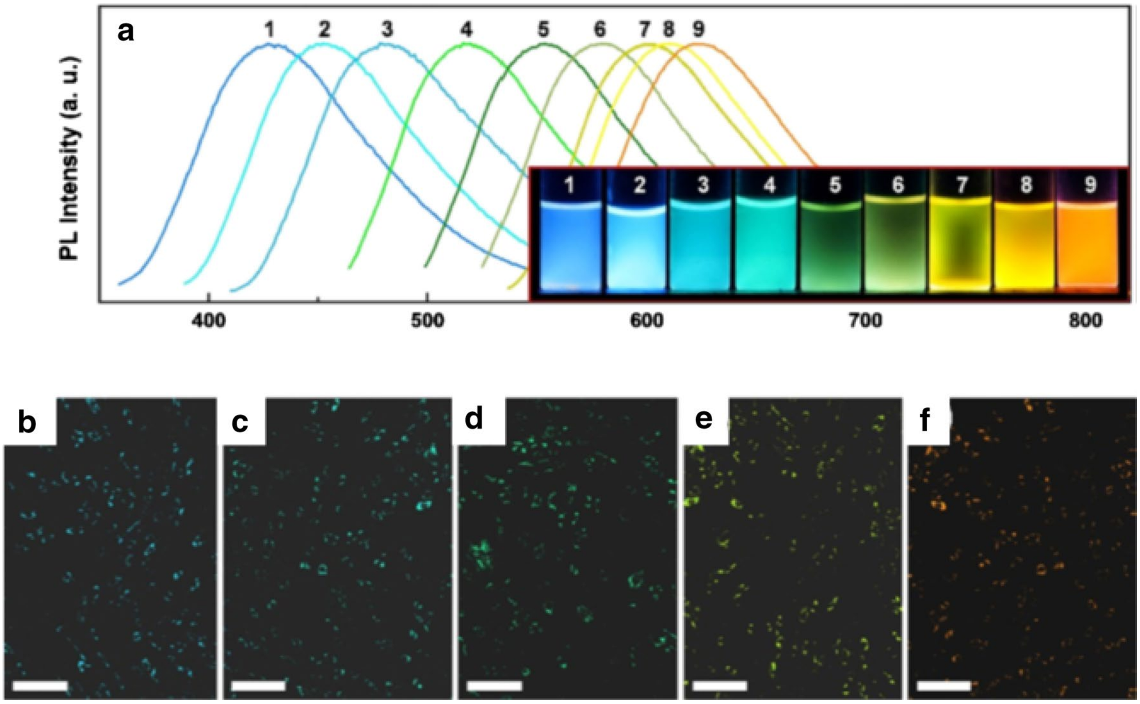

Fig. 47 **a** PL spectra of S-GQDs with varying concentration of heteroatom doping, and **b** respective imaging of fibroblast cells incubated with S-GQD series 1, 3, 5, 7, and 9 (scalebar: 20 mm). Reprinted with permission from Ref. [132]

other. SEM/TEM is conducted in vacuum environment, and AFM is conducted in an ambient or fluid environment. The above techniques are used for topography (the surface features of an object or how it looks, its texture), morphology (the shape and size of the particles making up the object), composition (the elements and compounds that the object is composed of and the relative amount of them), crystallographic information (how the atoms are arranged in the object) of materials.

If the expected value is in the > 100 nm range, standard SEM on sample cross section may be used. In the 30–100 nm range a FESEM (Field Emission SEM) is better. For thinner samples, a TEM cross sectional analysis is needed, that however require a proper sample preparation. Of course, some special care must be taken in all the above measurements. First, the sample must be properly prepared even in the case of SEM analysis. For example. if the interested film is the top most one, need to deposit a dummy thin coating (e.g. a thin Au layer) before cutting the cross-sectional sample. High-resolution transmission electron microscopy (HR-TEM) has been used as the ultimate method of thickness measurement for thin films. SEM/AFM images are three dimensional and are accurate representations while TEM pictures are two-dimensional and might require little bit of interpretation. In terms of resolution and magnification, TEM gains more advantages compared to SEM. SEM/TEM gives information regarding surface morphology, while AFM gives true surface topography and various types of surface measurements. Compared with SEM, AFM provides extraordinary topographic contrast direct height measurements and un-obscured views of surface features (no coating is necessary).

Table 7 shows the various applications of graphene and its derivatives eg. graphene oxide, graphene quantum dots (GQDs).

Conclusion

Biomass is a sustainable and rich source of carbon production. For the proficient utilization of carbon resources, it is necessary to understand the carbon chemistry and factors influencing its properties. This review highlighted the novel research on different sources specially from biomass derived several synthetic schemes for the preparation of graphene including 3D graphene-based materials, advanced characterization techniques and their application for energy generation, storage, sensing, biomedical fields.

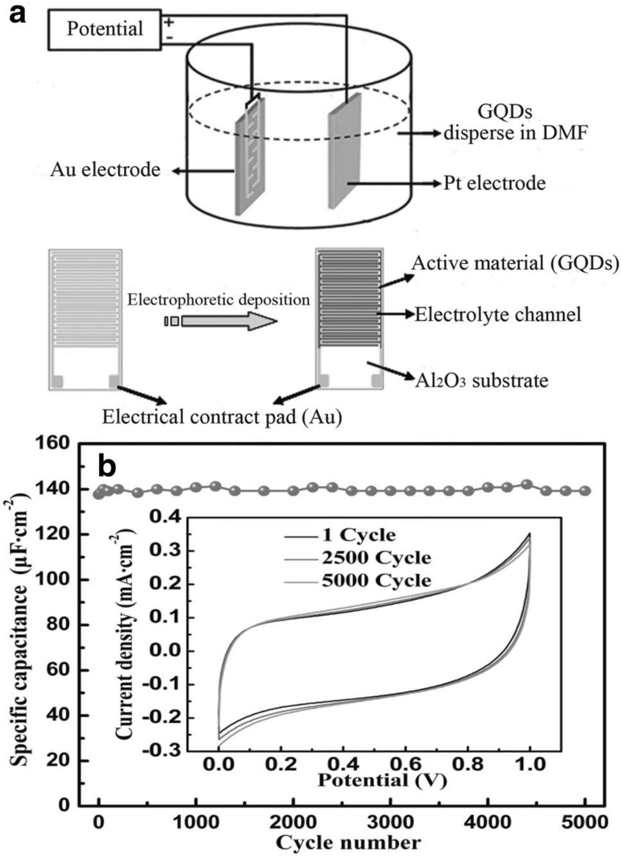

Fig. 48 **a** The preparation of a symmetric micro-supercapacitor by depositing GQDs on an interdigital Au finger microelectrode, **b** specific capacitance retention after 5000 cycles (Reprinted with permission from Ref. [133]

This article presents a comprehensive review of graphene synthesis, advanced characterization techniques, and their applications. The contributions of the article can be summarized as follows:

(i) identification of synthesis techniques for the development of graphene from various sources including graphite, non-graphite sources specially from graphene synthesis from bio-mass sources.
(ii) Synthesis techniques of graphene quantum dots (GQDs) from various biomass sources and biomass-wastes.
(iii) Advanced material analysis and characterization techniques to understand the structural, surface and optical. behaviors of graphene as well as electrical, thermal parameters, microwave properties.
(iv) Finally, multidimensional real-world applications for graphene.

(i) Identification of synthesis techniques for the development of graphene from various sources including graphite, non-graphite sources specially from graphene synthesis from bio-mass sources.

The synthesis techniques section has presented a comprehensive review of various synthesis techniques for the development of graphene from various sources including graphite, non-graphite sources specially from graphene synthesis from bio-mass sources. The graphene synthesis from graphite sources such as micromechanical cleavage-the scotch tape method, chemical cleavage and exfoliation were discussed. Next graphene synthesis from non-graphitic sources such as epitaxial growth from silicon carbide, physical vapor deposition (PVD), chemical vapor deposition (CVD) from $CH_{4,}$ conversion of carbon dioxide to graphene, growth of graphene from solid carbon sources, graphene synthesis from polymers, facile synthesis of graphene from plastic by pyrolysis of poly(methyl ethacrylate) were discussed. Among these methods, mechanical exfoliation and CVD can produce good-quality graphene. However, the practical application of graphene is blocked by the high price and insufficient supply.

Recently, many researchers have suggested to develop green production methods for synthesizing graphene using environmentally friendly biomass resources. The synthesis of monolayer-patched graphene from glucose via pyrolysis, graphene from fungus via pyrolysis coupling with hydrothermal carbonization pretreatment, graphene synthesis using one-step pyrolysis from dead camphor leaves porous 3D graphene-based bulk materials, growth of graphene from food, insects, waste (cookies, chocolate, grass, plastics, roaches, and dog feces without purification), graphene from rice husk (RH) by microwave plasma irradiation (MPI), high-quality graphene sheets from wheat straw via a combined hydrothermal and graphitization approach, catalyst-free plasma enhanced growth of graphene from sustainable sources from tea tree plant, chemical converted graphene sheets derived from pulping black liquor were discussed. Moreover, large area few-layer graphene with scalable preparation from waste biomass such as peanut shell, coconut shell, wheat straw, tee tree plant, Auricularia, wastepaper was discussed.

(ii) Synthesis techniques of graphene quantum dots (GQDs) from various biomass sources and biomass-wastes

Graphene Quantum Dots (GQDs) synthesis from various biomass resources via different techniques such as pyrolysis from rice grains, hydrothermal from coffee grounds, combining pyrolysis and hydrothermal treatments from neem leaves and fenugreek leaf extract, electrochemical oxidation emulsion templated carbonization from honey was discussed.

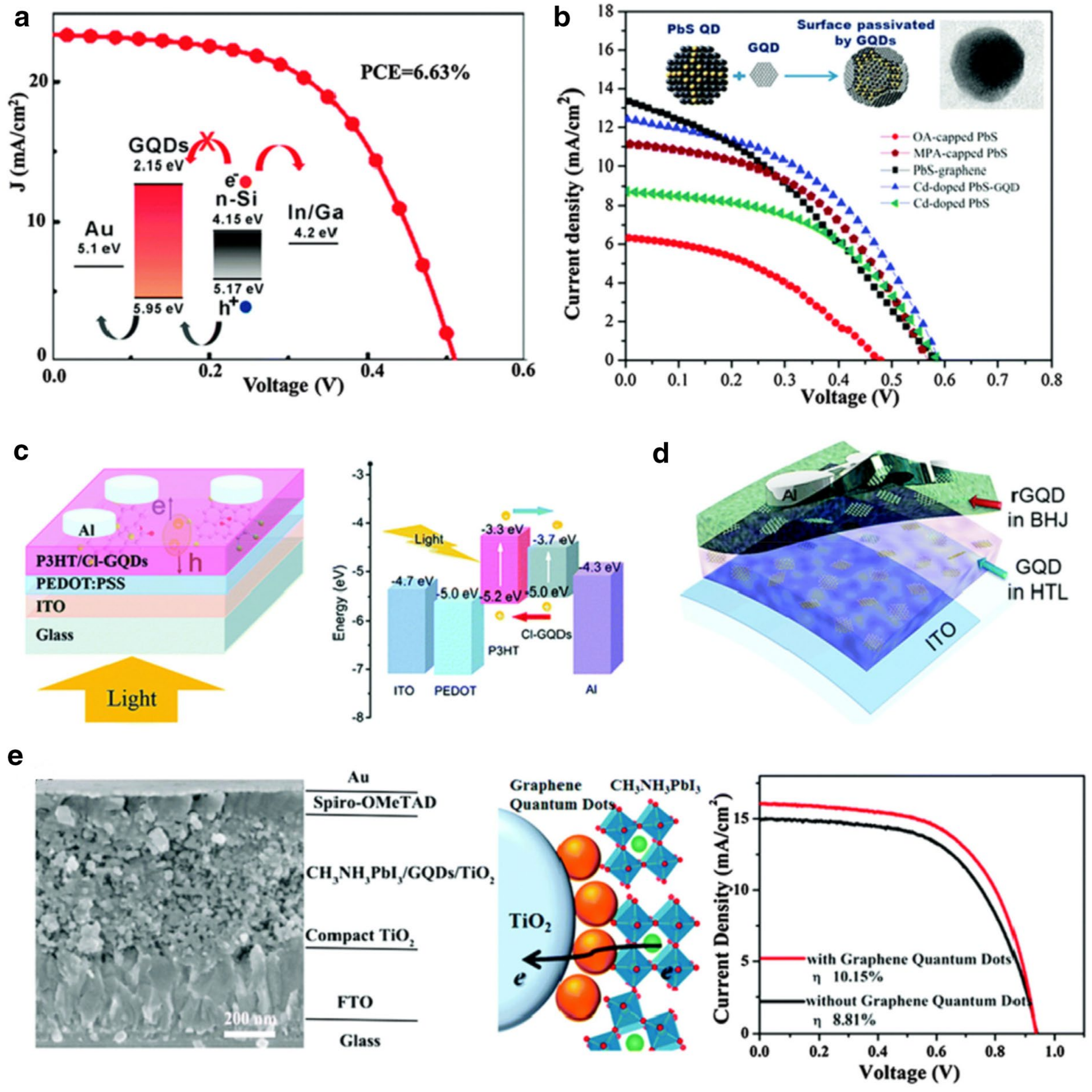

Fig. 49 **a** CH_3-Si/GQD heterojunction solar cell showing J-V curve at Am1.5G (the inset shows its energy band diagram), [Reproduced with permission from Ref. [134]), **b** A schematic diagram of PbS QDs surface passivated by GQDs and PbS based solar cells' J-V curves under Am1.5G. Reprinted with permission from Ref. [135], **c** Schematic of a photovoltaic device based on GQD-Cl hybrid and its working mechanism (Reprinted with permission from Ref. [136]). **d** Illustration of a photovoltaic device based on GQDs in hole-transport layer (HTL) and hydrothermally reduced GQDs in the BHJ layer (Reprinted with permission from Ref. [137]). **e** SEM image (cross sectional view) of perovskite solar cell on left side, illustration of its working mechanism in middle, and J-V curves of the cell without or with GQD on right (Adopted with permission from Ref. [138])

(iii) Advanced material analysis and characterization techniques to understand the structural, surface and optical, thermal behaviors of graphene as well as electrical parameters, microwave properties

From the advanced material analysis and characterization techniques such as structural, thermal, surface, optical, electrical, and microwave characterization for graphene the following interferences are drawn:

(a) Structural characterization of graphene: The XRD, Raman spectroscopy, SE, TEM, and FTIR techniques are used for structural characterization of graphene. The structural characterization of graphene is required for material identification, verification, and to under-

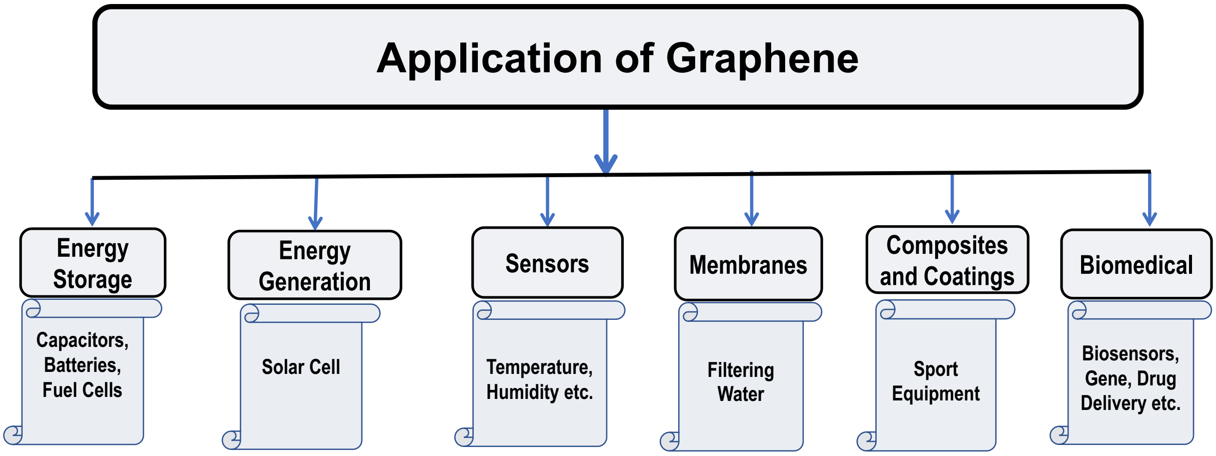

Fig. 50 Application areas of graphene

stand the definitive information to develop graphene for various application.

(b) Thermal characterization of graphene: The TGA is used for thermal characterization of graphene to understand the weight loss with temperatures.

(c) Surface characterization of graphene: The SE, SEM, and AFM techniques are used for surface characterization of graphene. The surface characterizations are used to understand the topographic information to develop graphene for various application.

(d) Optical characterization of graphene: The SE, UV–Vis techniques are used for optical characterisation of graphene. The SE with an optical model is used to extract the complex refractive index, dielectric constant, layer thickness, surface roughness, and so on. The UV–Vis provides information about the transmittance, reflection, absorption coefficient, and so on to develop graphene for various application.

(e) Electrical and microwave characterization of graphene: The electrical conductivity measurement is used for graphene for energy and sensing applications. The microwave characterization is used for measurement of scattering parameters, that is, complex permittivity, dielectric, reflection loss of graphene at microwave and mm-wave frequencies. The graphene characterisation in the microwave domain is a novel approach in chipless RFID sensor development. This approach enables the use of smart sensing in low-energy levels for short-range communications in a wider bandwidth to understand the behaviour of graphene oxide and its dielectric properties in various environmental parameters.

(iv) Multidimensional real-world applications for graphene.

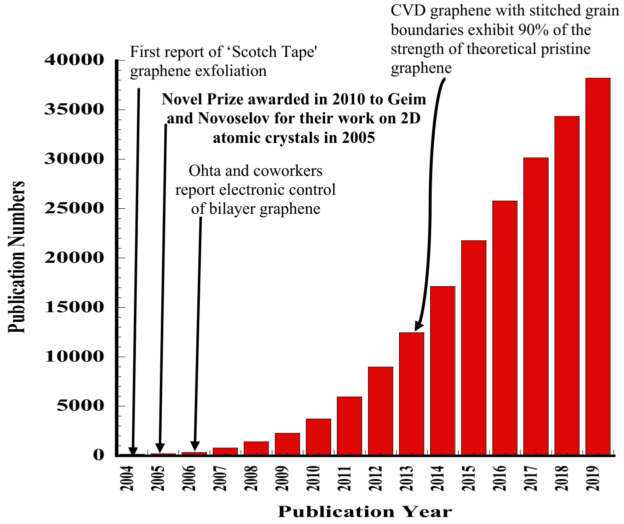

Fig. 51 A short post-2004 graphene timeline representing the number of graphene-related academic publications (Source: Web of Knowledge, 08/09/20) and some pertinent graphene breakthroughs Information acquired from (Reproduced with permission from Ref. [139–141])

The graphene can be used for energy generation such as solar cell, energy storages (capacitors, batteries, fuel cells), sensors, composites (sport equipment's such as head ski and ski boots), coating membranes (filtering water), biomedical fields (Fig. 51).

Owning to the extraordinary properties of graphene, such as large surface area, good electrical conductivity, tunable luminescence, decreased chemical impedance, and tunable bandgap, GQDs have shown great promise in energy applications, such as solar cells or photovoltaics devices, batteries, fuel cells electrodes, and supercapacitors.

Graphene and graphene-based materials can be used for energy storage systems, i.e., lithium-ion batteries,

Table 4 State of art synthesis of graphene [141]

Type	Method	Figure/Illustration	Merits	Challenges
Top-down (from Graphite)	Mechanical exfoliation	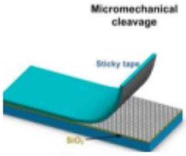	Less defects	Neither scalable nor capable for mass production
	Chemical method	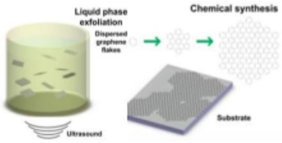	Cost-effective and suitable for mass production	Utilize many toxic chemical throughout the synthesis process
Bottom-up Approach (From Carbon)	Chemical Vapor Deposition (CVD)	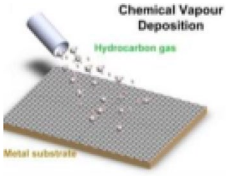	Compatible with the current complementary metal–oxide–semiconductor (CMOS) technology due to large area and high-quality graphene produced	Expensive and involves complex transfer process
	Epitaxial growth	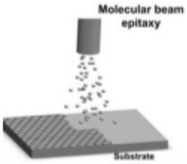	No defects for every single graphene island	Discontinuous

supercapacitors, lithium-sulfur batteries and lithium-air batteries [142]. Figure 52 shows the illustration of the formation process of the graphene-Sulfur hybrid as a self-supporting electrode.

To demonstrate how the transparent graphene films are potential window electrodes for optoelectronics, a dyesensitized solid solar cell was fabricated using the graphene film as anode and Au as cathode as shown in Fig. 53 [144].

Potential biomedical applications of graphene and graphene oxide include in mass spectrometry, sensors, gene & drug delivery, cancer treatment, cell growth.

Graphene offers the ability to efficiently transfer graphene films to other substrates over large areas for biocompatible sensing and flexible electronics. These properties render graphene an ideal active material for direct interfacing onto rugged surfaces. For example, electronic sensors based on graphene can be used for various applications including detection of pathogenic bacteria on tooth as well as microbial growth in the food. Measuring relative humidity using wireless sensing is also quite novel in the art, and it is imperative in the food industry as the humidity control of the packaging ensures food safety. Increase humidity conditions lead to an increase in the chance of microbial growth, which is a common problem, especially in perishable food items. Chipless RFID sensors using graphene are comparatively low-cost, but they provide enormous design flexibility in diversified applications especially in smart packaging applications in a remote setting. A fully printable multiparameter chipless RFID sensor for sensing temperature, pH, and humidity in a single platform is shown in Fig. 54 [127].

Graphene is a disruptive technology; one that could open up new markets and even replace existing technologies or materials. It is when graphene is used both as an improvement to an existing material and in a transformational capacity that its true potential could be realized. The vast number of products, processes, and industries which graphene could create a significant impact all stems from its amazing properties. No other material has the breadth of superlatives that graphene boasts making it ideal for countless applications. Graphene, which is currently called the material of the next century, is around 200 times stronger than steel, lightweight, flexible, and more conductive than copper, it’s possible uses are not limited to electronics but also include many areas of transport. It is electrically and thermally conductive but also transparent. It is the world's first 2D material and is one million times smaller than the diameter of a single human hair. At present the global market for graphene-based products is 675 million USD.

Graphene sensors arrays can also be implemented on standard utility textiles and drug efficacy screening, that may have a leading role in the fight against COVID-19 [130].

Table 5 Synthesis of graphene and its derivatives from biomass sources

Method	Sources	Figure/Illustration	Features	References
HTC, Pyrolysis	Fungus, Glucose	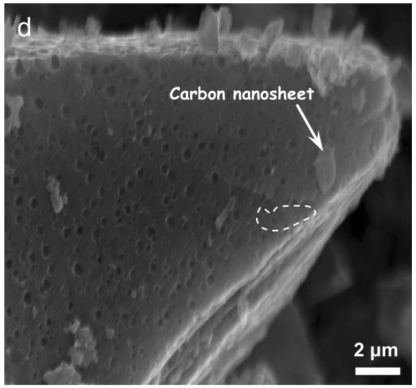 SEM image of the obtained densely porous layer-stacking carbon (PGC) material [Reproduced with permission from Ref. [73])	Low-cost and environmentally friendly design of electrode materials for high volumetric-performance supercapacitors	[73]
CVD	Cookies, Chocolate, Grass, Plastics, Roaches, Dog Feces	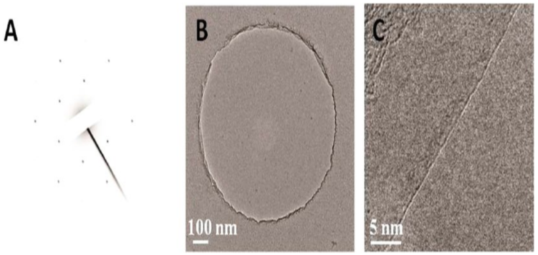 Diffraction pattern and TEM images of the cookie-derived graphene. (A) SAED pattern, (B) suspended graphene film on a 1 μm diameter hole, and (C) the edge of monolayer graphene [Reproduced with permission from Ref. [77])	Monolayer graphene derived from carbon sources is of high quality	[77]
Microwave Plasma Irradiation	Rice Husk	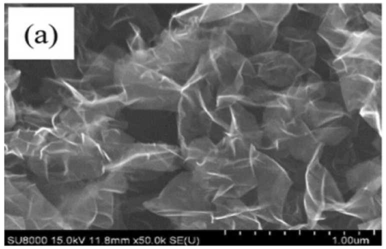 SEM images of the Rice Husk -derived (a) graphene [Reproduced with permission from Ref. [80])	Fabricate high-added-value nanocarbons including graphene, CNTs, and g-CNTs, which were dependent of experimental pressure	[80]

Table 5 (continued)

Method	Sources	Figure/Illustration	Features	References
Hydrothermal Calcination, Graphitization	Wheat Straw	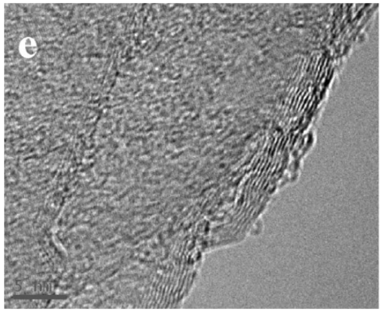 TEM image (e) of graphene [Reproduced with permission from Ref. [81])	less expensive method to synthesize high-quality graphene sheets from wheat straw via a combined hydrothermal and graphitization approach	[81]
Plasma Enhanced Growth	Tea Tree Plant	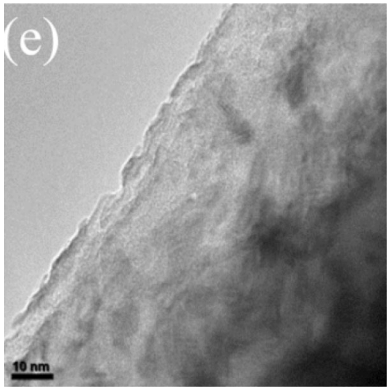 TEM image of a graphene sample [Reproduced with permission from Ref. [82])	The as-fabricated graphene films yielded a stable contact angle of 135°, indicating their potential application in very high hydrophobic coatings	[82]

Table 5 (continued)

Method	Sources	Figure/Illustration	Features	References
Chemical	Pulping black Liquor	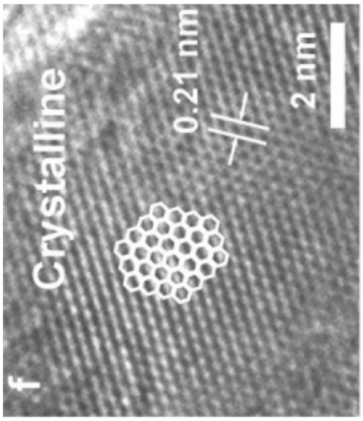 The HR-TEM image of gradual ordered graphene lattice, from amorphous to crystalline, indicating the forming mechanism of graphene formation process [Reproduced with permission from Ref. [83])	The pulping black liquor mainly consisting of lignin component was successively converted from amorphous heterogeneous chemical states to micron-sized graphene crystalline structure	[83]

Graphene could be the major reinforcing component of many polymer composites. The road transport generates 76% of global CO_2 emissions for all vehicles. Starting from 2016 in North America the transport sector emitted more CO_2 than energy sector. This change is due to the increasing use of low-emission and renewable energy technologies. The use of bio-graphene in production of lightweight car components will lead to the revolution in transport.

The Graphene is expected to have significant impact on various levels through the development of new synthesis techniques, new processes, and an improved understanding of how structure affects materials performance in a range of applications for energy including solar cell, super capacitor as well as sensors for food safety, health, agriculture, biomedical sectors etc. Continued development and successful implementation of the technologies that could lead to new jobs and a potentially huge source of revenue to fuel the future economy.

Table 6 Advanced material characterization techniques for graphene and its derivatives

Name of techniques	Type of techniques	Materials properties	References
X-ray Diffraction, XRD	Structural	Crystalline Quality	[106]
Raman Spectroscopy	Structural	Order or disorder structural information, Crystalline Quality	[65, 102, 103]
Spectroscopic Ellipsometry, SE	Structural, Surface, Optical, Electronic	Layer thickness, surface roughness, and dielectric constant, refractive index	[108–110]
Ultraviolet–Visible (UV–VIS) Absorption Spectroscopy	Optical, Electronic	Transmittance, reflection, and absorption coefficient	[100]
Atomic Force Microscopy, AFM	Surface	Surface roughness, morphology, topographical images	[100]
Scan Electron Microscopy, SEM	Surface	Morphology	[105]
Transmission Electron Microscopy, TEM	Structural, thickness, surface, morphology	Examine fine detail—even as small as a single column of atom	[104]
Fourier Transformation Infrared Spectroscopy, FTIR	Surface	Surface bonding	[107]
X-ray Photoelectron Spectroscopy**,** XPS	Surface	Chemical nature, surface composition	[100]
Thermogravimetric Analysis (TGA)	Nature of the materials	Deviation of the weight with temperature	[100]
Electrical and Electronic Characterization	Electrical, Electronic	Electrical, Dielectric properties	[111]

Table 7 Applications for graphene and its derivatives

Application	Capabilities	Examples	References
Energy storage and generation devices, membranes, coatings, composites	Graphene could dramatically increase the lifespan of a traditional lithium ion battery, meaning devices can be charged more quickly—and hold more power for longer Graphene supercapacitors could provide massive amounts of power while using much less energy than conventional devices. Because they are light, they could also reduce the weight of cars or planes Graphene has the potential to create the next generation of electronics currently limited to sci-fi. Faster transistors; semiconductors; bendable phones and other electronics Storing wind and solar power	Integration onto devices of bio-imaging, batteries, supercapacitors, photovoltaics, and light emitting diodes	[133–138]
Biomedical	Graphene's unique properties allow for ground-breaking biomedical applications. Targeted drug delivery; improved brain penetration; health-testing kits and 'smart' implants Graphene applications in biomedicine are numerous and can be classified into several main areas: transport (delivery) systems, sensors, tissue engineering and biological agents (for example antimicrobials) Graphene detects. Ultra-sensitive sensors made from graphene could detect minute dangerous particles helping to protect potentially dangerous environments	Mass spectrometry, gene & drug delivery, photothermal & cancer treatment, cell growth control, stem cell differentiation, COVID-19, sensors for food waste, crop protection, defence etc	[98, 117–132]

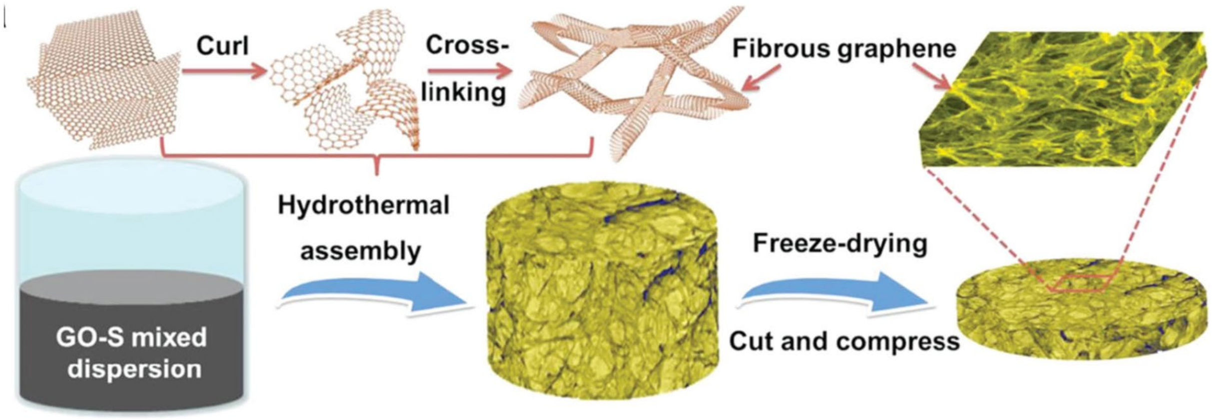

Fig. 52 Illustration of the formation process of the graphene-Sulfur hybrid and schematic of fabrication of a self-supporting electrode (Reprinted with permission from Ref. [143])

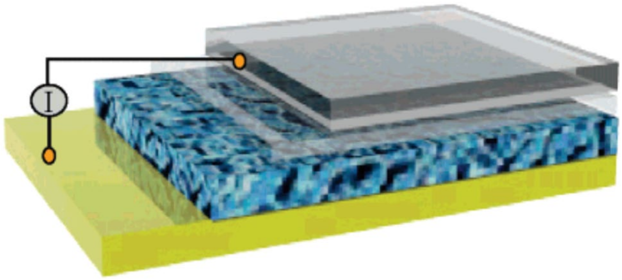

Fig. 53 Illustration of dye-sensitized solar cell using graphene film as electrode, the four layers from bottom to top are Au, dye-sensitized heterojunction, compact TiO_2, and graphene film (Reprinted with permission from Ref. [144])

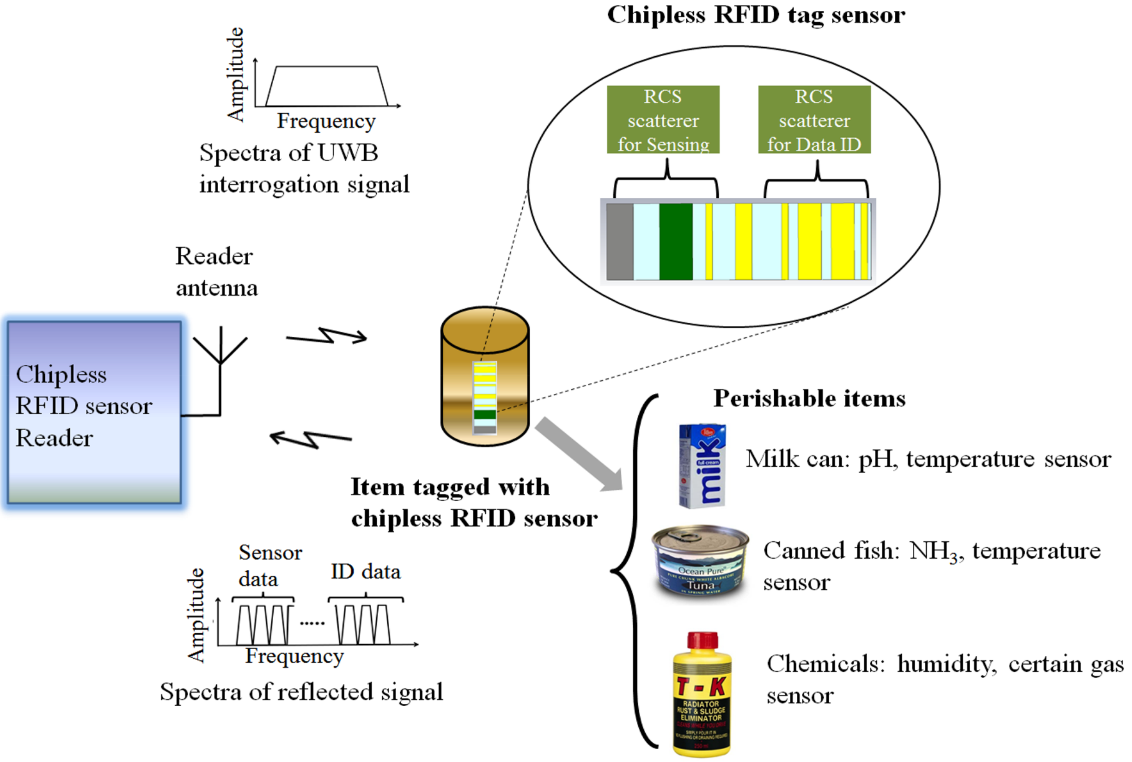

Fig. 54 Generic block diagram of proposed chipless RFID sensor system (Reprinted with permission from Ref. [113])

Acknowledgements The research funding supports from Natural Sciences and Engineering Research Council (NSERC) and The Ontario Ministry of Agriculture, Food and Rural Affairs (OMAFRA) Project Grants are highly acknowledged.

References

1. Geim, A.K., Novoselov, K.S.: The rise of graphene. Nature **6**, 183–191 (2007)
2. Novoselov, K.S., Geim, A.K., Morozov, S.V., Jiang, D., Zhang, Y., Dubonos, S.V., Grigorieva, I.V., Firsov, A.A.: Electric field effect in atomically thin carbon film. Science **306**(5696), 666–669 (2004)
3. Berger, C., Song, Z.M., Li, T.B., Li, X.B., Ogbasghi, A.Y., Feng, R., Dai, Z.T., Marchenkov, A.N., Conrad, E.H., First, P.N., de Heer, W.A.: Ultrathin epitaxial graphite: 2D electron gas properties and a route toward graphene-based nanoelectronics. J. Phys. Chem. B **108**, 19912–19916 (2004)
4. Berger, C., Song, Z.M., Li, X.B., Wu, X.S., Brown, N., Naud, C., Mayou, D., Li, T.B., Hass, J., Marchenkov, A.N., Conrad, F.H., First, P.N., de Heer, W.A.: Electronic confinement and coherence in patterned epitaxial graphene. Science **312**, 1191–1196 (2006)
5. Kunc, J., Hu, Y., Palmer, J., Berger, C., de Heer, W.A.: A method to extract pure Raman spectrum of epitaxial graphene on SiC. Appl. Phys. Lett. **103**, 201911 (2013)
6. Fukidome, H., Kawai, Y., Fromm, F., Kotsugi, M., Handa, H., Ide, T., Ohkouchi, T., Miyashita, H., Enta, Y., Kinoshita, T., Seyller, Th., Suemitsu, M.: Precise control of epitaxy of graphene by microfabricating SiC substrate. Appl. Phys. Lett. **101**, 41605 (2012)
7. Emtsev, K.V., Bostwick, A., Horn, K., Jobst, J., Kellogg, G.L., Ley, L., McChesney, J.L., Ohta, T., Reshanov, S.A., Röhrl, J., Rotenberg, E., Andreas, K.S., Waldmann, D., Heioko, B.W., Seyller, T.: Towards wafer-size graphene layers by atmospheric pressure graphitization of silicon carbide. Nat. Mater. **8**, 203–207 (2009)
8. Virojanadara, C., Syvajarvi, M., Yakimova, R., Johansson, L.I., Zakharov, A.A., Balasubramanian, T.: Homogeneous large-area graphene layer growth on 6H-SiC 0001. Phys. Rev. B **78**, 245403 (2008)
9. Sutter, P.W., Flege, J.I., Sutter, E.A.: Epitaxial graphene on ruthenium. Nat. Mater. **7**, 406–411 (2008)
10. Zeller, P., Speck, F., Weinl, M., Ostler, M., Schreck, M., Seyller, T., Wintterlin, J.: Healing of graphene on single crystalline Ni(111) films. Appl. Phys. Lett. **105**, 191612 (2014)
11. Usachov, D., Dobrotvorskii, A.M., Varykhalov, A., Rader, O., Gudat, W., Shikin, A.M., Adamchuk, V.K.: Experimental and theoretical study of the morphology of commensurate and incommensurate graphene layers on Ni single-crystal surfaces. Phys. Rev. B **78**, 085403 (2008)
12. N'Diaye, A.T., Bleikamp, S., Feibelman, P.J., Michely, T.: Two-dimensional Ir cluster lattice on a graphene Moire' on Ir(111). Phys. Rev. Lett. **97**, 215501 (2006)
13. Coraux, J., N'Diaye, A.T., Busse, C., Michely, T.: Structural coherency of graphene on Ir(111). Nano Lett. **8**, 565–570 (2008)
14. Pan, Y., Zhang, H., Shi, D., Sun, J., Du, S., Liu, F., Gao, H.J.: Highly ordered millimeter-scale continuous single-crystalline graphene monolayer formed on Ru (001). Adv. Mater. **21**, 2777–2780 (2009)

15. Li, X.S., Cai, W.W., An, J.H., Kim, S., Nah, J., Yang, D.X., Piner, R.D., Velamakanni, A., Jung, I., Tutuc, E., Banerjee, S.K., Colombo, L., Ruoff, R.S., R.S. : Large-area synthesis of high-quality and uniform graphene films on copper foils. Science **324**, 1312–1314 (2009)
16. Reina, A., Jia, X.T., Ho, J., Nezich, D., Son, H., Bulovic, V., Dresselhaus, M.S., Kong, J.: Large area, few-layer graphene films on arbitrary substrates by chemical vapor deposition. Nano Lett. **9**, 30–35 (2009)
17. Li, X.S., Magnuson, C.W., Venugopal, A., An, J., Suk, J.W., Han, B., Borysiak, M., Cai, W.W., Velamakanni, A., Zhu, Y., Fu, L.F., Vogel, E.M., Voelkl, E., Colombo, L., Ruoff, R.S.: Graphene films with large domain size by a two-step chemical vapor deposition process. Nano Lett. **10**, 4328–4334 (2010)
18. Hao, Y., Bharathi, M.S., Wang, L., Liu, Y., Chen, H., Nie, S., Wang, X., Chou, H., Tan, C., Fallahazad, B., Ramanarayan, H., Magnuson, C.W., Tutuc, E., Yakobson, B.I., McCarty, K.F., Zhang, Y.W., Kim, P., Hone, J., Colombo, L., Ruoff, R.S.: The role of surface oxygen in the growth of large single-crystal graphene on copper. Science **342**, 720–723 (2013)
19. Li, X.S., Magnuson, C.W., Venugopal, A., Tromp, R.M., Hannon, J.B., Vogel, E.M., Colombo, L., Ruoff, D.R.S.: Large-area graphene single crystals grown by low-pressure chemical vapor deposition of methane on copper. J. Am. Chem. Soc. **133**, 2816–2819 (2011)
20. Zurutuza, A., Marinelli, C.: Challenges and opportunities in graphene commercialization. Nat. Nanotechnol. **9**, 730–734 (2014)
21. Sukang, B., Hyeongkeun, K., Youngbin, L., Xiangfan, X., Jae-Sung, P., Yi, Z., Jayakumar, B., Tian, L., Hye, R.K., Young, S., Young-Jin, K., Kwang, S.K., Barbaros, O., et al.: Roll-to-roll production of 30-inch graphene films for transparent electrodes. Nat. Nanotechnol. **5**, 574–578 (2010)
22. Li, X.S., Zhu, Y.W., Cai, W.W., Borysiak, M., Han, B.Y., Chen, D., Piner, R.D., Colombo, L., Ruoff, R.S.: Transfer of large-area graphene films for high-performance transparent conductive electrodes. Nano Lett. **9**, 4359–4363 (2009)
23. Gao, L., Ren, W., Zhao, J., Ma, L.P., Chen, Z., Cheng, H.M.: Efficient growth of high-quality graphene films on Cu foils by ambient pressure chemical vapour deposition. Appl. Phys. Lett. **97**, 183109 (2010)
24. Kobayashi, T., Bando, M., Kimura, N., Shimizu, K., Kadono, K., Umezu, N., Miyahara, K., Hayazaki, S.N., Mizuguchi, Y., Murakami, Y., Hobara, D.: Production of a 100-m-long high-quality graphene transparent conductive film by roll-to-roll chemical vapor deposition and transfer process. Appl. Phys. Lett. **102**, 023112 (2013)
25. Kim, K.S., Zhao, Y., Jang, H., Lee, S.Y., Kim, J.M., Kim, S.S., Ahn, J.H., Kim, P., Choi, J.Y., Hong, B.H.: Large-scale pattern growth of graphene films for strechable transparent electrodes. Nature **457**, 706–710 (2009)
26. Lee, S., Lee, K., Zhong, Z.: Wafer scale homogeneous bilayer graphene films by chemical vapor deposition. Nano Lett. **10**, 4702–4707 (2010)
27. Ago, H., Ogawa, Y., Tsuji, M., Mizuno, S., Hibino, H.: Catalytic growth of graphene-toward large-area single-crystalline graphene. J. Phys. Chem. Lett. **3**, 2228–2236 (2012)
28. Yu, Q., Jauregui, L.A., Wu, W., Colby, R., Tian, J., Su, Z., Cao, H., Liu, Z., Pandey, D., Wei, D., Chung, T.F., Peng, P., Guisinger, N.P., Stach, E.A., Bao, J., Pei, S.S., Chen, Y.P.: Control and characterization of individual grains and grain boundaries in graphene grown by chemical vapour deposition. Nat. Mater. **10**, 443–449 (2011)
29. Su, C.Y., Lu, A.Y., Wu, C.Y., Li, Y.T., Liu, K.K., Zhang, W., Lin, S.Y., Juang, Z.Y., Zhong, Y.L., Chen, F.R., Li, L.J.: Direct formation of wafer scale graphene thin layers on insulating substrates by chemical vapor deposition. Nano Lett. **11**, 3612–3616 (2011)
30. Emstev, K.V., Bostwick, A., Horn, K., Jobst, J., Kellogg, G.L., Ley, L., Jessica, L.M., Ohta, T., Reshanov, S.A., Röhrl, J., Rotenbery, E., Andreas, K.S., Waldmann, D., Heiko, B.W., Seyller, T.: Towards wafer-size graphene layers by atmospheric pressure graphitization of silicon carbide. Nat. Mater. **8**, 203–207 (2009)
31. Robertson, A.W., Warner, J.H.: Hexagonal single crystal domains of few-layer graphene on copper foils. Nano Lett. **11**, 1182–1189 (2011)
32. Yao, Y., Wong, C.P.: Monolayer graphene growth using additional etching process in atmospheric pressure chemical vapor deposition. Carbon **50**, 5203–5209 (2012)
33. Vlassiouk, I., Fulvio, P., Mayer, H., Lavrik, N., Dai, S., Datskos, P., Smirnov, S.: Large scale atmospheric pressure chemical vapor deposition of graphene. Carbon **54**, 58–67 (2013)
34. Liu, L., Zhou, H., Cheng, R., Chen, Y., Lin, Y.C., Qu, Y., Bai, J., Ivanov, I.A., Liu, G., Huang, Y., Duan, X.: A systematic study of atmospheric pressure chemical vapor deposition growth. J. Mater. Chem. **22**, 1498–1593 (2012)
35. Somekh, M., Shawat, E., Nessim, G.D.: Fully reproducible, low-temperature synthesis of high-quality, few-layer graphene on nickel via preheating of gas precursors using atmospheric pressure chemical vapor deposition. J. Mater. Chem. A **2**(46), 19750–19758 (2014)
36. Sun, Z., Yan, Z., Yao, J., Beitler, E., Zhu, Y., Tour, J.M.: Growth of graphene from solid carbon sources. Nature **468**, 549–552 (2010)
37. Peng, Z., Yan, Z., Sun, Z., Tour, J.M.: Direct growth of bilayer graphene on SiO_2 substrates by carbon diffusion through nickel. ACS Nano **5**(10), 8241–8247 (2011)
38. Byun, S.J., Lim, H., Shin, G.Y., Han, T.H., Oh, S.H., Ahn, J.H., Choi, H.C., Lee, T.W.: Graphenes converted from polymers. J. Phys. Chem. Lett. **2**(5), 493–497 (2011)
39. Papon, R., Kalita, G., Sharma, S., Shinde, S.M., Vishwakarma, R., Tanemura, M.: Controlling single and few-layer graphene crystals growth in a solid carbon source based chemical vapor deposition. Appl. Phys. Lett. **105**(13), 133103 (2014)
40. Garcia, J.M., He, R., Jiang, M.P., Kim, P., Pfeiffer, L.N., Pinczuk, A.: Multilayer graphene grown by precipitation upon cooling of nickel on diamond. Carbon **49**, 1006 (2011)
41. Weatherup, R.S., Baehtz, C., Bruno, B.C., Kidambi, P.R., Blume, R., Schloegl, R., Hofmann, S.: Introducing carbon diffusion barriers for uniform, high-quality graphene growth from solid sources. Nano Lett. **13**(10), 4624–4631 (2013)
42. Hofrichter, J., Szafranek, B., Otto, M., Echtermeyer, T.J., Baus, M., Majerus, A., Geringer, V., Ramsteiner, M., Kurz, H.: Synthesis of graphene on silicon dioxide by a solid carbon source. Nano Lett. **10**(1), 36–42 (2010)
43. Li, X., Cai, W., Colombo, L., Ruoff, R.S.: Evolution of graphene growth on Ni and Cu by carbon isotope labeling. Nano Lett. **9**(12), 4268–4272 (2009)
44. Yu, Q., Lian, J., Siriponglert, S., Li, H., Chen, Y.P., Pei, S.S.: Graphene segregated on Ni surfaces and transferred to insulators. Apl. Phys. Lett. **93**(11), 113103 (2008)
45. Koh, A.T.T., Foong, Y.M., Y.M., and D. H. C. Chua, : Cooling rate and energy dependence of pulsed laser fabricated graphene on nickel at reduced temperature. Appl. Phys. Lett. **97**(11), 114102 (2010)
46. Hofrichter, J., Szafranek, B., Otto, M., Echtermeyer, T.J., Baus, M., Majerus, A., Geiringer, V., Ramsteiner, M., Kurz, H.: Synthesis of graphene on silicon dioxide by a solid carbon source. Nano Lett. **10**(1), 36 (2010)
47. Serry, M., Sakr, M.A.: Graphene-metal-semiconductor composite structure for multimodal energy conversion. Sens. Actuators A (2016). https://doi.org/10.1016/j.sna.2016.04.061

48. Dong, Y., Cheng, C., Xu, C., Mao, X., Xie, Y., Chen, H., Huang, B., Zhao, Y., Deng, J., Guo, W., Pan, G., Sun, J.: Metal-catalyst-free growth of patterned graphene on SiO_2 substrates by annealing plasma-induced cross-linked parylene for optoelectronic device applications. ACS Appl. Mater. Interfaces (2019). https://doi.org/10.1021/acsami.9b00124
49. Bae, S., Kim, S.J., Shin, D., Ahn, J.H., Hong, B.H.: Towards industrial applications of graphene electrodes. Phys. Scr. (2012). https://doi.org/10.1088/0031-8949/2012/T146/014024
50. Mittal, G., Dhand, V., Rhee, K.Y., Park, S.-J., Lee, W.R.: A review on carbon nanotubes and graphene as fillers in reinforced polymer nanocomposites. J. Ind. Eng. Chem. **21**, 11–15 (2015)
51. Biswal, M., Banerjee, A., Deo, M., Ogale, S.: From dead leaves to high energy density supercapacitors. Energy Environ. Sci. **6**, 1249–1259 (2013)
52. Dong, Y., Cheng, C., Xu, C., Mao, X., Xie, Y., Cheng, H., Huang, B., Zhao, Y., Deng, J., Guo, W., Pan, G., Sun, J.: Metal-catalyst-free growth of patterned graphene on SiO_2 substrates by annealing plasma-induced cross-linked parylene for optoelectronic device applications. ACS Appl. Mater. Interfaces **11**, 14427–14436 (2019)
53. Niu, J.: Growth mechanisms, and mechanical and thermal properties of junctions in 3d carbon nanotube-graphene nano-architectures, University of North Texas, Ph.D Thesis (2014)
54. Subramanian, V., Luo, C., Stephan, A.M., Nahm, K.S., Thomas, S., Wei, B.: Supercapacitors from activated carbon derived from banana fibers. J. Phys. Chem. C **111**, 7527–7531 (2007)
55. Wu, F.C., Tseng, R.L.: Preparation of highly porous carbon from fir wood by KOH etching and CO_2 gasification for adsorption of dyes and phenols from water. J. Colloid Interface Sci. **294**, 21–30 (2006)
56. Ismanto, A.E., Wang, S., Soetaredjo, F.E.: Preparation of capacitor's electrode from cassava peel waste. Bioresour. Technol. **101**, 3534–3540 (2010)
57. Li, X., Xing, W., Zhuo, S., Zhou, J., Li, F., Qiao, S.Z., Lu, G.Q.: Preparation of capacitor's electrode from sunflower seed shell. Bioresour. Technol. **102**, 1118–1123 (2011)
58. Singh, V., Joung, D., Zhai, L., Das, S., Khondaker, S.L.: Seal, S: Graphene based materials: past, present, and future. Prog. Mater. Sci. **56**, 1178 (2011)
59. Robinson, J.T., Zalalutdinov, M., Baldwin, J.W., Snow, E.S., Wei, Z., Sheehan, P., Houston, B.H.: Wafer-scale reduced graphene oxide films for nanomechanical devices. Nano Lett. **8**(10), 3441–3445 (2008)
60. Whitener, K.E., Jr., Sheehan, P.E.: Graphene synthesis. Diam. Relat. Mater. **46**, 25–34 (2014)
61. Yang, W., Chen, G., Shi, Z., Liu, C., Zhang, L., Xie, G., Cheng, M., Wang, D., Yang, R., Shi, D., Watanabe, K., Taniguchi, T., Yao, Y., Zhang, Y., Zhang, G.: Epitaxial growth of single-domain graphene on hexagonal boron nitride. Nat. Mater. **12**(9), 792–797 (2013)
62. Anders, A.: Cathodic Arcs: From Fractal Spots to Energetic Condensation. Springer, Berlin (2008)
63. Oldfield, D.T., McCulloch, D.G., Huynh, C.P., Sears, K., Hawkins, S.C.: Multilayered graphene films prepared at moderate temperatures using energetic physical vapour deposition. Carbon **94**, 378–385 (2015)
64. Li, X.S., Cai, W.W., Colombo, L., Ruoff, R.S.: Evolution of graphene growth on Ni and Cu by carbon isotope labeling. Nano Lett. **9**, 4268–4272 (2009)
65. Chakrabarti, A., Lu, J., Skrabutenas, J.C., Xu, T., Xiao, Z., Maguire, J.A.: Conversion of carbon dioxide to few-layer graphene. J. Mater. Chem. **21**, 9491 (2011)
66. Peng, Z., Yan, Z., Sun, J., Tour, J.M.: Direct growth of bilayer graphene on SiO_2 substrates by carbon diffusion through nickel. ACS Nano **5**, 8241–8247 (2011)
67. Byun, S.J., Lim, H., Shin, G.Y., Han, T.H., Oh, S.H., Ahn, J.H., Choi, H.C., Lee, T.W.: Graphene's converted from polymers. J. Phys. Chem. Lett. **2**, 493–497 (2011)
68. Hong, N., Yang, W., Bao, C., Jiang, S., Lei, S., Yuan, H.: Facile synthesis of graphene by pyrolysis of poly (methyl methacrylate) on nickel particles in the confined microzones. Mater. Res. Bull. **47**, 4082–4088 (2012)
69. Mazdak, T.: Trends in graphene research. Mater. Today **12**(10), 34–37 (2009)
70. Abbas, A., Mariana, L.T., Phan, A.N.: Biomass-waste derived graphene quantum dots and their applications. Carbon **140**, 77–99 (2018)
71. Kong, X., Zhu, Y., Lei, H., Wang, C., Zhao, Y., Huo, E., Xiaona, L., Zhang, Q., Qian, M., Mateo, W., Zou, R., Fang, Z., Ruan, R.: Synthesis of graphene-like carbon from biomass pyrolysis and its applications. Chem. Eng. J. **399**, 125808 (2020)
72. Li, X.H., Kurasch, S., Kaiser, U., Antonietti, M.: Synthesis of monolayer-patched graphene from glucose. Angew. Chem. Int. Ed. **51**, 9689–9692 (2012)
73. Long, C., Chen, X., Jiang, L., Zhuangjun, F.: Porous layer-stacking carbon derived from in-built template in biomass for high volumetric performance supercapacitors. Nano Energy **12**, 141–151 (2015)
74. Ban, C.L., Xu, Z., Wang, D., Liu, Z., Zhang, H.: Porous layered carbon with interconnected pore structure derived from reed membranes for supercapacitors. ACS Sustain. Chem. Eng. **7**, 10742–10750 (2019)
75. Shams, S.S., Zhang, L.S., Hu, R., Zhang, R., Zhu, J.: Synthesis of graphene from biomass: a green chemistry approach. Mater. Lett. **161**, 476–479 (2015)
76. Long Zhang, L., Zhang, F., Yang, X., Long, G., Wu, Y., Zhang, T., Leng, K., Huang, Y., Yanfeng, M., Ao, Y., Yongsheng, C.: Porous 3D graphene-based bulk materials with exceptional high surface area and excellent conductivity for supercapacitors. Sci. Rep. (2013). https://doi.org/10.1038/srep01408
77. Ruan, G., Sun, Z., Peng, Z., Tour, J.M.: Growth of graphene from food, insects, and waste. ACS Nano **5**(9), 7601–7607 (2011)
78. Wang, Z., Shoji, M., Baba, K., Ito, T., Ogata, H.: Microwave plasma-assisted regeneration of carbon nanosheets with bi- and trilayer of graphene and their application to photovoltaic cells. Carbon **67**, 326–335 (2014)
79. Wang, Z., Ogata, H., Morimoto, S., Fujishige, M., Takeuchi, K., Hashimoto, Y., Endo, M.: Synthesis of carbon nanosheets from Kapton polyimide by microwave plasma treatment. Carbon **72**, 421–424 (2014)
80. Wang, Z., Shoji, M., Shingo, M., Josue, O.M., Masatsugu, M., Kenji, T., Hiroyuki, M., Takuya, H., Mauricio, T., Yoshio, H., Morinobu, E.: Nanocarbons from rice husk by microwave plasma irradiation: from graphene and carbon nanotubes to graphenated carbon nanotube hybrids. Carbon **94**(2015), 479–484 (2015)
81. Feng, C., Juan., Y., Bai, T., Long, B., Zhou, X. : Facile synthesis of few-layer graphene from biomass waste and its application in lithium ion batteries. J. Electroanal. Chem. **768**, 18–26 (2016)
82. Jacob, M.V., Rawat, R.S., Ouyang, B., Bazaka, K., Kumar, D.S., Taguchi, D., Iwamoto, M., Neupane, R., Varghese, O.K.: Catalyst-free plasma enhanced growth of graphene from sustainable sources. Nano Lett. **15**, 5702–5708 (2015)
83. Ding, Z., Yuan, T., Wen, J., Cao, X., Sun, S., Xiao, L.P., Quentian, S., Xiluan, X., Runcang, S.: Green synthesis of chemical converted graphene sheets derived from pulping black liquor. Carbon **158**, 690–697 (2020)
84. Taniya, P., Guneet, S., Mandeep, S., Dinesh, K., Sundar, R.: Large area few-layer graphene with scalable preparation from waste biomass for high-performance supercapacitor. Sci. Rep. **7**, 15239–15314 (2017)

85. Purkait, T., Singh, G., Singh, M., Kumar, D., Dey, R.: Large area few-layer graphene with scalable preparation from waste biomass for high-performance supercapacitor. Sci. Rep. **7**, 15239–15314 (2017)
86. Fahmi, F., Dewayanti, N.A.A., Widiyastuti, W., Setyawan, H., Arellano-Garcia, H.: From coconut shell to porous graphene-like nanosheets for high-power supercapacitors. Cogent Eng. **7**(1748962), 1–9 (2020)
87. Zhou, H., Zhang, J., Amiinu, I.S., Shang, C., Liu, X., Tu, W., Pan, M.: Shichun: Transforming waste biomass with an intrinsically porous network structure into porous nitrogen-doped graphene for highly efficient oxygen reduction. Phys. Chem. Chem. Phys. **18**(15), 10392–10399 (2016)
88. Nirala, N.R., Khandelwal, G., Kumar, B., Vinita, P.R., Kumar, V.: One step electro-oxidative preparation of graphene quantum dots from wood charcoal as a peroxidase mimetic. Talanta **173**, 36–43 (2017)
89. Fang, B., Bonakdarpour, A., Kim, M.S., Kim, J.H., Wilkinson, D.P., Yu, J.S.: Multimodal porous carbon as a highly efficient electrode material in an electric double layer capacitor. Microporous Mesoporous Mater. **182**, 1–7 (2013)
90. Zu, D., Xie, Y., Song, Y.J., Deng, W.Q.: A green and facile method toward synthesis of wastepaper-derived 3D functional porous graphene via in situ activation of cobalt (II). J. Mater. Chem. A **3**(31), 16072–16078 (2015)
91. Keränen, A., Leiviskä, T., Gao, B.Y., Hormi, O., Tanskanen, J.: Preparation of novel anion exchangers from pine sawdust and bark, spruce bark, birch bark and peat for the removal of nitrate. Chem. Eng. Sci. **98**, 59–68 (2013)
92. Sun, Z., Zheng, M., Hu, H., Dong, H., Liang, Y., Xiao, Y., Lei, B., Liu, Y.: From biomass wastes to vertically aligned graphene nanosheet arrays-a catalyst-free synthetic strategy towards high-quality graphene for electrochemical energy storage. Chem. Eng. J. **336**, 550–561 (2018)
93. Suryawanshi, A., Biswal, M., Mdhmane, D., Gokhale, R., Patil, S., Guin, D., Ogale, S.: Large scale synthesis of graphene quantum dots (GQDs) from waste biomass and their use as an efficient and selective photoluminescence on-off- on probe for Ag+ ions. Nanoscale **6**(20), 11664–11670 (2014)
94. Wang, Z., Yu, J., Zhang, X., Li, N., Liu, B., Li, Y., Wang, Y., Wang, W., Li, Y., Zhang, L., Dissanayke, S., Suib, S., Sun, L.: Large-scale and controllable synthesis of graphene quantum dots from rice husk biomass: a comprehensive utilization strategy. ACS Appl. Mater. Interfaces. **8**(2), 1434–1439 (2016)
95. Wang, L., Li, W., Wu, B., Li, Z., Wang, S., Liu, Y., Pan, D., Wu, M.: Facile synthesis of fluorescent graphene quantum dots from coffee grounds for bioimaging and sensing. Chem. Eng. J. **300**, 75–82 (2016)
96. Roy, P., Periasamy, A.P., Chuang, C., Liou, Y.R., Chen, Y.F., Joly, J., Liang, C.T., Chang, H.T.: Plant leaf-derived graphene quantum dots and applications for white LEDs. New J. Chem. **38**(10), 4946–4951 (2014)
97. Mahesh, S., Lekshmi, C.L., Renuka, K.D., Joseph, K.: Simple and cost-effective synthesis of fluorescent graphene quantum dots from honey: application as stable security ink and white-light emission. Part. Part. Syst. Charact. **33**, 70–74 (2016)
98. Kalita, H., Mohapatra, J., Pradhan, L., Mitra, A., Bahadur, D., Aslam, M.: Efficient synthesis of rice-based graphene quantum dots and their fluorescent properties. RSC Adv. **1**, 23518–23524 (2016)
99. Bae, S., Kim, S.J., Shin, D., Ahn, J.H., Hong, B.H.: Towards industrial applications of graphene electrodes. Phys. Scra. **146**, 14024 (2012)
100. Paredes, J.I., Villar-Rodil, S., Solís-Fernández, P., Martínez-Alonso, A., Tascón, J.M.: Atomic force and scanning tunneling microscopy imaging of graphene nanosheets derived from graphite oxide. Langmuir **25**(10), 5957–5968 (2009)
101. Park, J.S., Reina, A., Saito, R., Kong, J., Dresselhaus, G., Dresselhaus, M.S.: G’ band Raman spectra of single, double and triple layer graphene. Carbon **47**, 1303–1310 (2009)
102. Singh, V., Joung, D., Zhai, L., Das, S., Khondaker, S., Seal, S.: Graphene based materials past, present and future. Prog. Mater Sci. **56**(8), 1178–1271 (2011)
103. Ferrari, A.C., Meyer, J.C., Scardaci, V., Casiraghi, C., Lazzeri, M., Mauri, F., Piscanec, S., Jiang, D., Novoselov, K.S., Roth, S., Geim, A.K.: Raman spectrum of graphene and graphene layers. Phys. Rev. Lett. **97**, 187401–187405 (2006)
104. Suryawanshi, A., Biswal, M., Mhamane, D., Gokhale, R., Patil, S., Guin, D., Ogale, S.: Large scale synthesis of graphene quantum dots (GQDs) from waste biomass and their use as an efficient and selective photoluminescence on–off–on probe for Ag + ions. Nanoscale **6**, 11664–11670 (2014)
105. Sun, Z., Zheng, M., Hu, H., Dong, H., Liang, Y., Xiao, Y., Lei, B., Liu, Y.: From biomass wastes to vertically aligned graphene nanosheet arrays: A catalyst-free synthetic strategy towards high-quality graphene for electrochemical energy storage. Chem. Eng. J. **336**, 550–561 (2018)
106. Zhang, H.B., Zheng, W.G., Yan, Q., Yang, Y., Wang, J.W., Lu, Z.H., Ji, G.Y., Yu, Z.Z.: Electrically conductive polyethylene terephthalate/graphene nanocomposites prepared by melt compounding. Polymer **51**(2), 1191–1196 (2010)
107. Naebe, M., Wang, J., Amini, A., Khayyam, H., Hameed, N., Li, L.H., Chen, Y., Fox, B.: Mechanical property and structure of covalent functionalised graphene/epoxy nanocomposites. Sci. Rep. **4**, 4375 (2014)
108. Nelson, F.J., Kamineni, V.K., Zhang, T., Comfort, E.S., Lee, J.U., Diebold, A.C.: Optical-properties-of-large-area-polycrystalline-chemical-vapor-deposited-graphene-by-spectroscopic-ellipsometry. Appl. Phys. Lett. **97**, 253110–253113 (2010)
109. Kravets, V.G., Grigorenko, A.N., Nair, R.R., Blake, P., Anissimova, S., Novoselov, K.S., Geim, A.K.: Spectroscopic ellipsometry of graphene and an exciton-shifted van Hove peak in absorption. Phys. Rev. B. **81**, 155413 (2010)
110. Weber, J.W., Calado, V.E., Van De Sanden, M.C.M.: Optical constants of graphene measured by spectroscopic ellipsometry. Appl. Phys. Lett. **97**, 91904 (2010)
111. Katsournaros, A., Cole, M.T., Tuncer, H.M., Milne, W.I., Hao, Y.: Near-field characterization of chemical vapor deposition graphene in the microwave regime. Appl. Phys. Lett. **102**, 233104 (2013)
112. Amin, E., Saha, J.K., Karmakar, N.C.: Smart sensing materials for low-cost chipless RFID sensor. IEEE Sens. Mater. Integr. Sens. Spl. Issue. **14**(7), 2198–2207 (2014)
113. Karmakar, N.C., Amin, E., Saha, J.K.: Chipless RFID Sensors. Wiley, New Jersey (2016)
114. Stoller, M.D., Park, S., Zhu, Y., An, J., Ruoff, R.S.: Graphene-based ultracapacitors. Nano Lett. **8**(10), 3498–3502 (2008)
115. Pumera, M.: Electrochemistry of graphene: new horizons for sensing and energy storage. Chem. Rec. **9**, 211–223 (2009)
116. Yoo, E.J., Kim, J., Hosono, E.H., Zhou, H.S., Kudo, T., Itaru, H.: Large reversible Li storage of graphene nanosheet families for use in rechargeable lithium ion batteries. Nano Lett. **8**, 2277–2282 (2008)
117. Chung, C., Kim, Y.K., Shin, D., Ryoo, S.R., Hong, B.H., Min, D.H.: Biomedical applications of graphene and graphene oxide. Acc. Chem. Res. **46**(10), 2211–2224 (2013)
118. Shen, H., Zhang, L., Liu, M., Zhang, Z.: Biomedical applications of graphene. Theranostics. **2**(3), 283–294 (2012)
119. Zhang, B., Wang, Y., Zhai, G.: Biomedical applications of the graphene-based materials. Mater. Sci. Eng. C **61**, 953–964 (2016)

120. Zhang, Y., Nayak, T.K., Hong, H.: Graphene: a versatile nanoplatform for biomedical applications. Nanoscale **4**(13), 3833–3842 (2012)
121. Pumera, M.: Electrochemistry of graphene new horizons for sensing and energy storage. Chem. Rec. **9**(4), 211–223 (2009)
122. Hu, S.H., Chen, Y.W., Hung, W.T., Chen, I.W., Chen, S.Y.: Quantum-dot-tagged reduced graphene oxide nanocomposites for bright fluorescence bioimaging and photothermal therapy monitored in situ. Adv. Mater. Commun. (2012). https://doi.org/10.1002/adma.201104070
123. Shang, S., Zhang, G., Sun, X., Lee, S.T., Liu, Z.: Graphene in mice: ultrahigh in vivo tumor uptake and efficient photothermal therapy. Nano Lett. **10**(9), 3318–3323 (2010)
124. Yang, Y., Asiri, A.M., Tang, Z., Du, D., Lin, Y.: Graphene based materials for biomedical applications. Mater. Today. **16**(10), 365–373 (2013)
125. Tang, Z., Wu, H., Cort, J.R., Buchko, G.W., Zhang, Y., Shao, Y., Shao, Y., Aksay, I.A., Liu, J., Lin, Y.: Constraint of DNA on functionalized graphene improves its biostability and specificity. Small **6**(11), 1205–1209 (2010). https://doi.org/10.1002/smll.201000024
126. Cui, S., Mao, S., Lu, G., Chen, J.: Graphene coupled with nanocrystals: opportunities and challenges for energy and sensing applications. J. Phys. Chem. Lett. **4**(15), 2441–2454 (2013)
127. Mao, S., Yu, K., Chang, J., Steeber, D.A., Ocola, L.E., Chen, J.: Direct growth of vertically oriented graphene for field effect transistor biosensor. Sci. Rep. **3**(1), 1696 (2013)
128. Hill, E.W., Vijayaragahvan, A., Novoselov, K.: Graphene sensors. IEEE Sens. J. **11**(12), 3161–3170 (2011)
129. Mittal, G., Dhand, V.K.Y., Rhee, S.J., Park, W.R.: Rapid detection of COVID-19 causative virus (SARS-CoV-2) in human nasopharyngeal swab specimens using field-effect transistor-based biosensor. ACS Nano **14**(4), 5135–5142 (2020)
130. Palmieri, V., Pap, M.: Can graphene take part in the fight against COVID-19? Nano Today **33**, 100883 (2020)
131. Zhang, Z., Zhang, J., Chen, N., Qu, L.: Graphene quantum dots: an emerging material for energy-related applications and beyond. Energy Environ. Sci. **5**(10), 8869–8890 (2012)
132. Wang, G., Guo, Q., Chen, D., Liu, Z., Zheng, X., Xu, A., Yang, S., Ding, G.: Facile and highly effective synthesis of controllable lattice sulfur-doped graphene quantum dots via hydrothermal treatment of durian. ACS Appl. Mater. Interfaces. **10**(6), 5750–5759 (2018)
133. Liu, W.W., Feng, Y.Q., Yan, X.B., Xue, Q.J.: Superior micro-supercapacitors based on graphene quantum dots. Adv. Funct. Mater. **23**, 4111–4122 (2013)
134. Gao, P., Ding, K., Wang, Y., Ruan, K., Diao, S., Zhang, Q., Sun, B., Jie, J.: Crystalline Si/graphene quantum dots heterojunction solar cells. J. Phys. Chem. C **118**(10), 5164–5171 (2013)
135. Tavakoli, M.M., Hossein, A., Simchi, A., Kalytchuk, S., Fan, Z.: Quasi core/shell lead sulfide/graphene quantum dots for bulk heterojunction solar cells. J. Phys. Chem. C **119**(33), 18886–18895 (2015)
136. Zhao, J., Tang, L., Xiang, J., Ji, R., Hu, Y., Yuan, J., Zhao, J., Tai, Y., Cai, Y.: Fabrication and properties of a high-performance chlorine doped graphene quantum dot based photovoltaic detector. RSC Adv. **5**, 29222–29229 (2015)
137. Kim, J.K., Kim, S.J., Park, M.J., Bae, S., Cho, S.P., Du, Q.G., Wang, D.H., Park, J.H., Hong, B.H.: Surface-engineered graphene quantum dots incorporated into polymer layers for high performance organic photovoltaics. Sci. Rep. **5**(1), 14276 (2015)
138. Zhu, Z., Ma, J., Wang, Z., Mu, C., Fan, Z., Du, L., Bai, Y., Fan, L., Yan, H., Phillips, D.L., Yang, S.: Efficiency enhancement of perovskite solar cells through fast electron extraction: the role of graphene quantum dots. J. Am. Chem. Soc. **136**, 3760–3763 (2014)
139. Novoselov, K.S., Jiang, D., Schedin, F., Booth, T.J., Khotkevich, V.V., Morozov, S.V., Geim, A.K.: Two-dimensional atomic crystals. Proc Natl Acad Sci USA **102**(30), 10451–10453 (2005)
140. Randir, E.P., Brownson, D.A.C., Banks, C.E.: A decade of graphene research: production, applications, and outlook. Mater. Today **17**(9), 426–432 (2014)
141. Bae, S., Kim, H., Lee, Y., Xu, X., Park, J.S., Zheng, Y., Balakrishnan, J., Lei, T., Ri, K.H., Song, Y., Kim, Y.J., Kim, K.S., Özyilmaz, B., Ahn, J.H., Hong, B.H., Iijima, S.: Roll-to-roll production of 30-inch graphene films for transparent electrodes. Nat. Nanotechnol. **5**(8), 574–578 (2010)
142. Ismail, M.S., Yusof, N., Yusop, M.Z.M., Ismail, M.F., Jaafar, J., Aziz, F., Karim, Z.A.: Synthesis and characterization of graphene derived from rice husks. Malay. J. Fundam. Appl. Sci. **15**(4), 516–521 (2019)
143. Jixin Zhu, J., Yang, D., Yin, Z., Yan, Q., Zhang, H.: Graphene and graphene-based materials for energy storage applications. Small **10**(17), 3480–3498 (2014)
144. Wang, X., Zhi, L., Mullen, K.: Transparent, conductive graphene electrodes for dye-sensitized solar cells. Nano Lett. **8**(1), 323–330 (2008)